JUNE 2017 M.Sc. in Civil Engineering AHMED ABBAS ABU ALTEMEN

UNIVERSITY OF GAZIANTEP

GRADUATE SCHOOL OF

NATURAL & APPLIED SCIENCES

INVESTIGATION OF RESIDUAL SHEAR STRENGTH OF TWO-WAY SLAB PANELS EXPOSED TO HIGH TEMPERATURES

M. Sc. THESIS

in

CIVIL ENGINEERING

BY

AHMED ABBAS GHALI ABU ALTEMEN

JUNE 2017

Investigation of Residual Shear Strength of Two-way Slab Panels Exposed to High Temperatures

M. Sc. Thesis

in

Civil Engineering

University of Gaziantep

Supervisor

Prof. Dr. Mustafa ÖZAKÇA

by

Ahmed Abbas Ghali ABU ALTEMEN

JUNE 2017

REPUBLIC OF TURKEY
UNIVERSITY OF GAZİANTEP
GRADUATE SCHOOL OF NATURAL & APPLIED SCIENCES
CIVIL ENGINEERING DEPARTMENT

Name of the thesis: Investigation of Residual Shear Strength of Two-way Slab Panels Exposed to High Temperatures

Name of the student: Ahmed Abbas Ghali ABU ALTEMEN

Exam date: June 21, 2017

Approval of the Graduate School of Natural and Applied Sciences

Prof. Dr. Ahmet Necmeddin YAZICI
Director

I certify that this thesis satisfies all the requirements as a thesis for the degree of Master of Science.

Prof. Dr. Abdulkadir ÇEVİK
Head of Department

This is to certify that we have read this thesis and that in our concerns opinion it is fully adequate, in scope and quality, as a thesis for the degree of Master of Science.

Prof. Dr. Mustafa ÖZAKÇA
Supervisor

Examining Committee Members	Signature
Prof. Dr. Mustafa ÖZAKÇA	....
Doç. Dr. Nildem TAYŞİ	....
Yrd. Doç Dr. Derya BAKBAK	....

I hereby declare that all information in this document has been obtained and presented in accordance with academic rules and ethical conduct. I also declare that, as required by these rules and conduct, I have fully cited and referenced all material and results that are not original to this work.

Ahmed Abbas Ghali ABU ALTEMEN

ABSTRACT

INVESTIGATION OF RESIDUAL SHEAR STRENGTH OF TWO-WAY SLAB PANELS EXPOSED TO HIGH TEMPERATURES

ABU ALTEMEN, AHMED ABBAS GHALI
M.Sc. in Civil Engineering
Supervisor: Prof. Dr. Mustafa ÖZAKÇA
June 2017
99 pages

Steel fiber reinforced concrete is an old concept, where first appearance of it was around a 100 years ago, although it's a successful material in improving the behavior of concrete especially when it combines with the conventional steel reinforcement, there's an absence of codes and standard that predict and estimate the real punching capacity of the panels containing steel fiber especially particularly when it is exposed to fire. The current work in this thesis is a twenty slab panels that is casted and tested to obtain the residual punching shear strength after exposing to different temperatures and comparing the results with slab panels in ambient condition, also it is compared with ACI (American concrete institute) predicted results. The recent research results indicate that the steel fiber has a significant improvement on the behavior of concrete in groups under the same conditions, also in general the residual punching shear strength improved after exposing to 150 °C and 300 °C when it compared to the panels containing the same mixture in ambient condition.

Keywords: Steel fiber reinforced concrete, residual punching shear strength, conventional steel reinforcement.

ÖZET

YÜKSEK SICAKLIĞA MARUZ KALMIŞ İKİ YÖNLÜ DÖŞEME PANELLERDEKİ ARTIK (REZİDÜAL) KAYMA DAYANIMININ İNCELENMESİ

ABU ALTEMEN, AHMED ABBAS GHALİ

Yüksek Lisans, İnşaat Mühendisliği Bölümü

Tez Yöneticisi: Prof. Dr. Mustafa ÖZAKÇA

Haziaran 2017

99 Sayfa

Çelik elyaf takviyeli beton eski bir konsept olup ilk uygulamalar yaklaşık 100 yıl öncesine dayanmaktadır. Bununla birlikte özellikle geleneksel çelik takviye ile birleştirildiğinde betonun davranışının iyileştirilmesinde başarılı bir malzeme olmasına rağmen, özellikle ateşe maruz kaldıklarında, çelik tel içeren panellerin gerçek delme kapasitesini tahmin eden ilgili standartlar yoktur. Bu tez çalışmasında, yirmi döşeme levhası döküldü ve farklı sıcaklıklara maruz bırakıldıktan sonra artık zımbalama kesme mukavemetini elde etmek için test edildi. Sonuçlar oda sıcaklığına maruz döşeme levhaları ile karşılaştırıldı ve aynı zamanda ACI (Amerikan Beton Enstitüsü) tarafından öngörülen sonuçlarla karşılaştırıldı. Mevcut çalışma sonuçları, çelik lifin, aynı koşullar altındaki döşeme levhaları karşılaştırıldığında betonun davranışında belirgin bir iyileşme sağladığı ve ayrıca 150 °C'ye ve 300 °C'ye maruz bırakılan çelik lifli döşeme levhalarında, artık zımbalama kesme mukavemetinin artığını ortaya görülmüştür.

Anahtar Kelimeler: Çelik lif takviyeli beton, artık zımbalama kesme mukavemeti, konvansiyonel çelik donatı.

Dedication

To

The greatness of a father,

The generosity of a mother,

The togetherness of a family,

and to

The love of a wife.

ACKNOWLEDGEMENTS

Praise and glory be to Allah who guided me in every step to finish my thesis project. My deep gratitude goes to my supervisor Prof. Dr. Mustafa ÖZAKÇA who gave me the golden opportunity to do this wonderful project which also helped me in doing a lot of research and I came to know about so many new things.

I also like to express my sincere gratitude to all my teachers who poured me with knowledge and that I will keep learning for the rest of my life.

All my words cannot express my thanks for the Ph.D. Students Farid and Hayder.

My final thanks go to my family, my wife and friends who helped me a lot and support me in finalizing this project within the limited time frame.

TABLE OF CONTENTS

Page

LIST OF FIGURES

Page

LIST OF TABLES

Page

LIST OF SYMBOLS /ABREVIATIONS

Scalars

RC	Reinforced Concrete
FRC	Fiber reinforced concrete
ACI	American Concrete Institute
ASTM	American Society for Testing and Materials
BS	British standards code
A	Area
d	Effective depth
E_C	Modulus of elasticity for concrete
a/d	Shear span over effective depth
a/h	Shear span ratio
l_s/d_s	Aspect ratio of steel fiber
f_c'	compressive strength of concrete
v_u	Ultimate Shear force
v_f	Fiber volume fraction
V_R	Punching shear nominal strength
W_{wet}	Wet panel weight
W_{dry}	Dry panel weight

f_{ct}, f_{sp}	Tensile strength for concrete
f_{st}	Splitting tensile strength for concrete
f_y	Yield stress of steel
h	Slab thickness
D_p	Diameter of punching
d_{agg}	Maximum aggregate size
L	Slab length
b	Slab width
B	Perimeter of the slab supported on one column
b_o	Perimeter of critical shear crack
C_{eq}	Equivalent side dimension of the column
c	Column dimension
δ	Displacement
δ_1	Displacement at the center of the panel
δ_2	Displacement at a distance 10 cm from the center of the panel
δu	Deflection at ultimate
δy	Deflection at yielding
δcr	Deflection at first crack
Py	Yield load
P_u	Ultimate load
P_{flex}	Flexural capacity
ρ	Reinforcement ratio
Σ_c	Perimeter of column
GFRC	Glass Fiber reinforced concrete

HSC	High strength concrete
NSC	Normal strength concrete
FR	Fiber Reinforcement
NFRC	Natural Fiber reinforced concrete
SF	Steel fiber
SNFRC	Synthetic fiber reinforced concrete
SFRC	Steel fiber reinforced concrete
LWC	Light weight concrete
LVDT	Linear variable displacement transducers
R	Radius of column
E_T	The strain hardening modulus
ASTM	American Society for Testing and Materials
C °	Temperature in Celsius

CHAPTER ONE

INTRODUCTION

1.1 General

Structural fire research has focused more on steel and steel-concrete composites than on concrete, due to concrete's beneficial properties of low thermal conductivity and non-combustibility. The shear behaviour of reinforced-concrete in fire is poorly understood when compared to its flexural response, and the Gretzenbach car park failure in Switzerland in 2004 (smith, 2016) prompted concerns over the lack of understanding of punching shear response of reinforced-concrete in fire. Punching shear in reinforced-concrete at elevated temperature is dependent upon the effects of: steel and concrete properties with elevated temperature, differential material thermal expansion effects, combined with the whole structural effects of: in-plane actions that result from restrained thermal expansion, and large deflection load carrying mechanisms.

1.2 Slab Column Connection Structural Behavior

According to the American Concrete Institute (American Concrete Institute 318-14, 2014) terminology, the flat plate can be defined as a slab supported by columns without columns' capital and drop panels. Experimental studies developed a concrete that could reach a compressive strength up to 250 MPa, however, a compressive strength like that causes an increase in brittle behavior of concrete. In fact, this might result in increasing the brittle behavior of concrete and make it worse, this brittleness behavior cannot be overlooked and a solution must be found at once to improve the ductility of concrete.

One of the dangerous and catastrophic failures in building construction due to the brittleness of concrete is punching failure. The two-way shear failure in a flat plate positioned at column vicinity, or at specified distance from column face, that lead to total collapsing in the whole structure, as shown in Figure 1.1, (Piper's Row Car Park, UK) and (Tropicana Casino parking garage).

Figure 1.1 An example of punching shear.

Many methods have been proposed, in order to prevent punching shear failure. Among these methods are using reinforcement bars normal to the cracks direction, which can be produced in deferent ways, such as shear reinforcement, corrugated studs system, cages of continuous stirrups system and hidden beams as shown in Figure 1.2a, b. In recent years the trends were to improve the behavior of concrete by including fibers, keeping a low amount of conventional reinforcement ratio. Combining with the danger of punching shear a greater danger could accrue due to exposing building to fire corresponding with punching shear that could accelerate the failing in elements of a concrete building. In case of accidental fire the problems of concrete brittleness are aggravated as shown in Figure 1.3.

Figure 1.2 Building collapsing due to fire (Westgate mall)

(a)

(b)

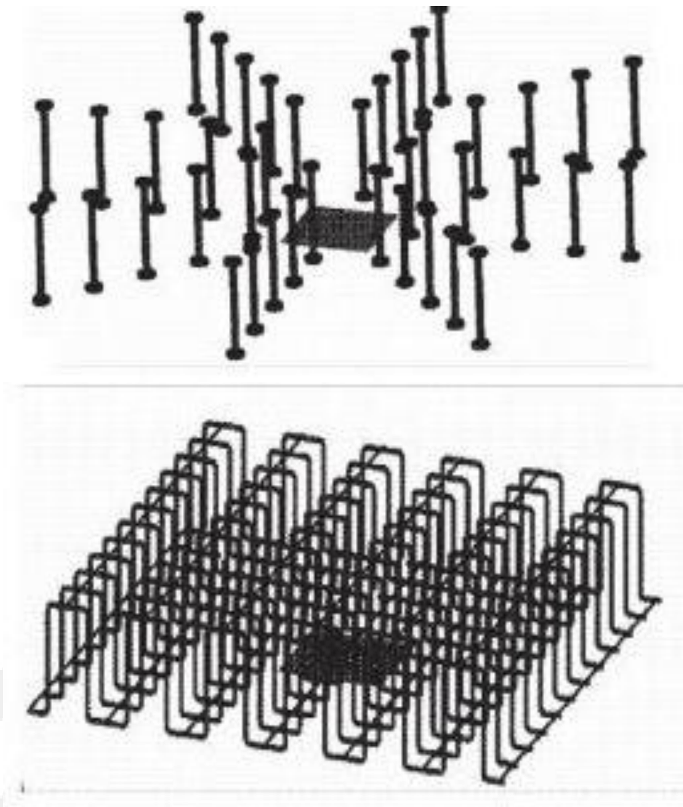

Figure 1.3 Methods used to prevent punching shear, (a) corrugated stud's system, (b) Cages of continuous stirrups system.

1.3 Steel Fiber Reinforced Concrete

Fiber Reinforced Concrete (FRC) is mostly a cement, gravel and sand aggregates, various types of fibers and water. In addition to fiber, steel fiber is considered one of the fibers that come from artificial resources, Steel Fiber Reinforced concrete (SFRC) is the concrete obtained from mixing steel finer with concrete.

SFRC is widely used in concrete structures that is purposed to increase the tensile strength of the concrete. Also using steel fiber increases the cohesion between the aggregate particles and forbid them from separation, also the addition of steel fiber prevents the formation of micro openings that form micro cracks, that led to lower stress at the end of the cracks due to the transportation of tensile forces in steel fiber, which means to minimize crack growth and help the concrete sample to endure loads even after visible crack occurred. One of the most important advantages of the steel fiber, is that the fiber reinforcement consider as an enhancement to the bond between concrete and conventional steel reinforcement in SFRC.

Experimental researchers and studies proved that SFRC have a plastic behavior with a higher tensile strength and a resistance for crack formation, also prevent the particles separation throw enhancing the cohesion, which as a result reduce the brittle behavior that comes in form of shear (Chen, 2004), (Narayanan & Darwish, I.Y.S., 1987), (Ashour, 1992), (Sharma, A. K., 1986)). The inclusion steel fibers in concrete enhances the mechanical properties like tensile strength, flexural strength, ductility, cracks and impact resistance (Orange, 1999)) moreover, earlier researches showed the benefit of using steel fiber in improving the shear failure and the concrete performance in general.

(Kwak, 2002), replaced the conventional stirrups by different amount of steel fiber added to high strength concrete. They found that the addition of steel fiber decreased the space and size of the crack with an increase of deformation capacity, also the behavior was altered from brittle to ductile. On the other side steel fiber cannot be considered as a full replacement to longitudinal reinforced bars in a Reinforced Concrete (RC) or a prestressed concrete (PC) members because the percentage used is often not greater than 2% in SFRC, that's why a conventional steel reinforcements are still needed to endure tensile ‹shear or compressive loads (Chanh, 2005).

Despite of the large numbers of researches and studies the conducted on beams, columns, slabs and footing using SFRC, which proved the efficiency of steel fiber in improving the concrete properties. There are a lot of applications and benefits not applied practically or conducted in laboratories, that's because most codes of practice does not yet produced full agreement on the effects of steel fiber in the concrete properties, still there's a large argument about the way of applying steel fiber to the concrete or how the benefits can be concluded and applied in the design of SFRC, therefore; more studies are in need to meet the growing demand of using steel fiber in various applications in concrete and also to study it's behavior under different types of loading.

As mentioned earlier there are a few researches on the effect of high temperature on two-way shear behavior ("can count on the hand fingers"); this number will be less for SFRC. Present research aimed to investigate, the residual strength of two-way panels of SFRC under high temperature, and the degradation of concrete mechanical properties (compressive and tensile strength) under the same condition. The main parameters will be the effect of different steady state high temperature exposing, and the volume fraction of steel fibers. Total of twenty specimens are suggested to investigate; fifteen of them are of SFRC, which will compare with five control panels of normal concrete under high temperature and three of SFRC at ambient condition. The mechanical properties and its degradation will be investigated by using standard specimens under ASTM provisions.

1.4 ACI Provisions

(American Concrete Institute 318-14, 2014) adopted a minimum nominal punching shear strength of normal concrete weight, the slab minimum strength is the least of the Equations 1.1 sub-numbering. This stress act on a specified perimeter distanced d/2 from the column face, the details of the critical shear crack is showing in Figure 1.4, where the code permit to use right angle corners.

ACI nominal shear strength is the smallest value of the three following sub-numbering equations:

$$V_c = 0.33\ \sqrt{f'_c}\, b_o\, d \qquad \text{Equation 1.1a}$$

$$v_c = 0.17\ \left(1 + \frac{2}{\beta}\right)\sqrt{f'_c}\, b_o\, d \qquad \text{Equation 1.1b}$$

$$v_c = 0.083\ \left(2 + \frac{\alpha_s d}{b_o}\right)\sqrt{f'_c}\, b_o\, d \qquad \text{Equation 1.1c}$$

where f'_c is the concrete compressive strength, b_o is the perimeter of critical shear crack, d is the effective depth, β is a ratio of long to short side of column, α_s equal to 40 for interior column.

Equation 1.1a was derived from semi-empirical analysis method based on experimental results and the analysis basis on Column yield criterion.

Equation 1.1c considered the size effect, however, Bazant, et al., (1987) (Bazant & Cao, 1987) believe that this equation didn't take into consideration the size effect, because it is basis on plastic limit analysis not on fracture mechanics, which is not justified for specimens of short horizontal yielding plateau.

Although ACI is easy in application and calculation for obtaining the punching shear capacity but it didn't take into consideration the effect of steel reinforcement ratio.

Therefore, the critical perimeter with straight sides can be calculated as follows:

$b_o = 4c + 2\pi\ d/2 \rightarrow 4c + \pi d$

Where:

f'_c concrete compressive strength.

b_o perimeter of critical shear crack.

d effective depth.

c side dimension of the column.

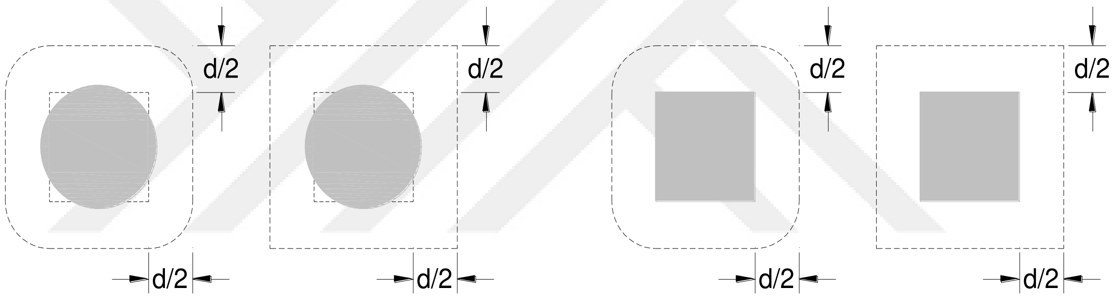

Figure 1.4 Critical section perimeter according to (American Concrete Institute 318-14, 2014).

For circular or polygon-shaped column, the code is suggested to assuming equivalent area of square column and then following the aforementioned provision for square column, as follows,

Area of circle = Area of equivalent square

$R^2\ \pi = c^2_{\ eq}$

$c_{\ eq} = R\sqrt{\pi}$

Where:

R radius of the column, C_{eq} equivalent side dimension of the column.

1.5 Problem Statements

Concrete slab supported directly by columns are subjected to two type of shear force (one and two-way shear) in addition to the flexural forces, these forces are Interfere with each other so that; it will be hard to recognizing between them. The main two problems resulting from these loads are, high deflection, and brittle, sudden and catastrophic two-way shear failure. This is may be occur due to structural behavior (concentration of shear force) or due to the brittleness properties of concrete. There are a huge number of researches have been addressed in this subject, many mechanical model have been proposed, and many code equations have been introduced, but still many problems are set on the table, such as, how to increase the concrete strength and ductility in the same time. Many methods have been suggested to increasing the ductility, and resisting the two-way shear action of partially loaded panels. Using shear reinforcements and steel stud are widely used nowadays, but using fibrous concrete (mostly using SFRC) shows good improvement.

Accidental fire may aggravate the two-way shear problem. There are a few researches on the effect of fire on normal concrete panels, let alone the SFRC.

1.6 Objectives and Scopes

Based on the aforementioned, the effect of steel fiber on the residual strength of the flat plate is experimented. In order to achieve this objective, SFRC flat plate are exposed to different temperature levels that are studied through the:

- A comparison between the residual punching shear behaviour of SFRC slab due to exposing to high temperature and punching shear behaviour of SFRC slab at ambient condition.
- Investigation of the effect of steel fiber volume fraction on punching shear capacity.
- Characterizing the post cracking and cracks pattern at failure stage.

Figure 1.5 shows the study program diagram.

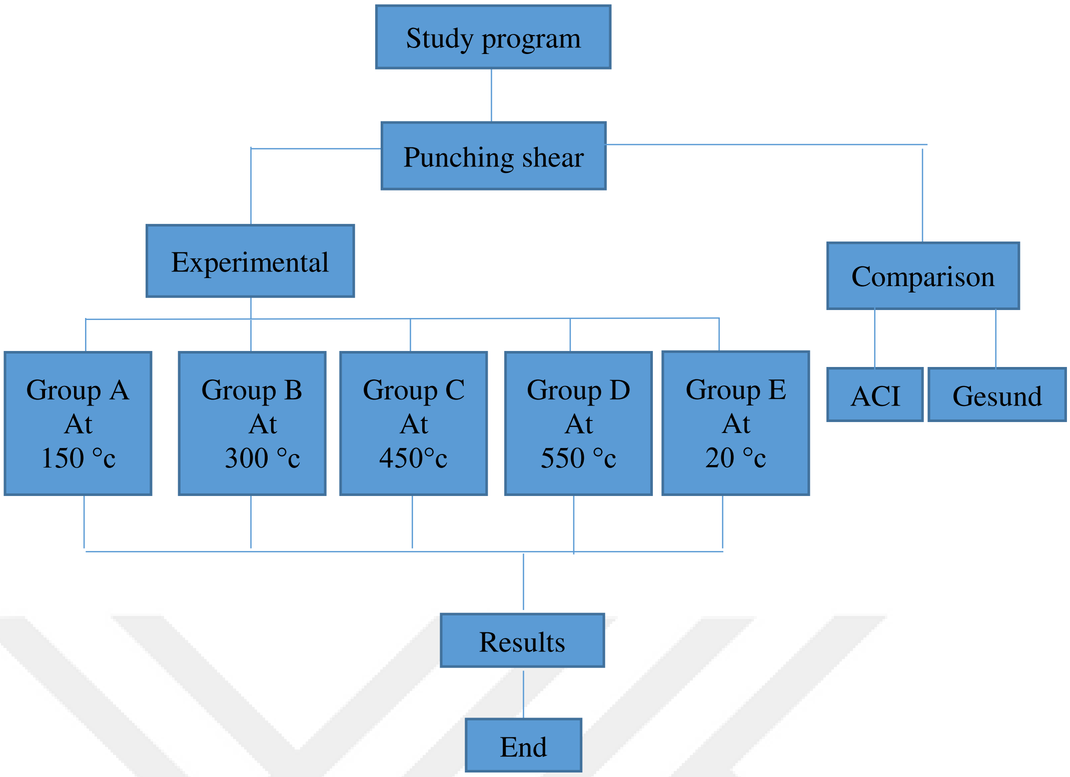

Figure 1.5 Study program diagram.

1.7 Organization of the Thesis

This thesis has five chapters. Chapter one includes an introduction to flat plate behavior under punching shear strength and the effect of fire and steel fiber on the behavior.

Chapter two presents a general view of steel fibers as well as the burning effects on concrete behaviour in different studies collected from vary researches. By other meaning a comparison between earlier similar works.

The experimental program, including the studied parameters, the work methodology, and testing of SFRC flat plates specimens, are presented in Chapter three .

Chapter four discuss the result and the calculation of the work. Finally Chapter five is the conclusion.

CHAPTER TWO

LITERATURE REVIEW

2.1 General

Concrete slab panels are a common structural element of modern building at the same time, the wide diversity of materials and factors that directly affect the behavior of slabs is also varied, therefore; an intensively studies on the factors and characteristics that effect it and how to improve it are always conducted such as adding steel fiber to the mix and the behavior after applying high temperature to the structure.

When cement was introduced in the early ages, also steel fiber was mixed with cement based matrix whether it was short discrete steel fibers or continuous long steel. The concrete material obtained from reinforcing concrete with steel fiber is called SFRC which means SFRC. It is considered a major breakthrough in engineering industry where it gradually becoming a new horizon in composite material in construction project.

FRC is a concrete mixed with fibrous materials of a diverse types to improve the properties of concrete. Given that the concrete is a brittle material that tolerate compression but a weak endurance to shear and tensile forces which mostly would crack and fail by lots of ways, therefore adding fibers would enhance the concrete properties and strengthens its ability to resist failures to a certain point, Figure 2.1.

The purpose of using fiber reinforcement is to create a whole new building material with a new properties better than the properties of concrete alone which could save a lot of lives when building collapse because fibers reinforced concrete structures will fall a few millimeters or centimeters before completely fall down, (Tepfers, 2010).

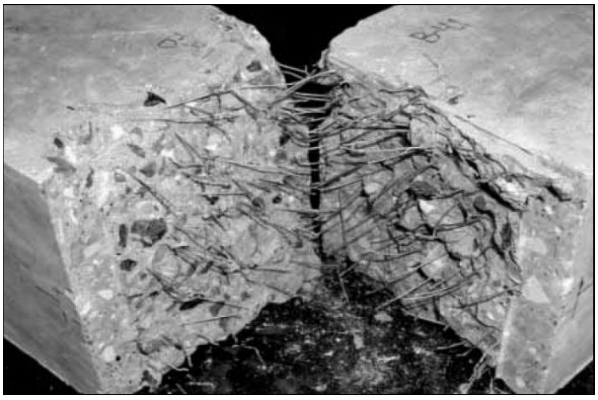

Figure 2.1 Steel fiber reinforcement (Löfgren, 2005).

There are about 19 different kinds of fiber used as reinforcement, as shown in Table 2.1. According to ACI 544 there are four FRC based on fiber material type:

- Steel fiber reinforced concrete SFRC.
- Glass Fiber reinforced concrete GFRC.
- Natural Fiber reinforced concrete NFRC.
- Synthetic fiber reinforced concrete SNFRC.

The most common in use as a reinforcement is steel fiber, almost fifty percent or more of fibers used in reinforcement is steel fiber, the polypropylene is the next higher percentage in use, twenty percent for synthetic fibers and five percent for glass fibers use. The remaining twenty five percent is distributed between the other kinds of fibers (Banthia, 2008). The current study investigates only steel fibers as reinforced concrete.

Table 2.1 Types of fiber.

Fiber type
Steel
E glass
AR glass
Acrylic (PAN)
Aramid
Carbon
Nylon
Polyester
Polyethylene
Polypropylene
Polyvinyl acetate
Cellulose (Wood)
Coconut
Bamboo
Jute
Asbestos
Wollastonite

One of the hazard that could endanger concrete structures is fire in which a lot of precaution ways are taking place to decrease the risks that come from concrete structure fail to endure fires, which leads to loss of lives.

The behaviour of a concrete structural element exposing to fire depends on thermal, mechanical, and deformation properties of the concrete of which the member is consist of. Like any other materials the thermo physical ‹mechanical, and deformation properties of concrete change automatically within the temperature range associated with the type of fire that building endures.

The properties mentioned diverge as a function of temperature and rely on what the concrete composition and characteristics. Concrete strength has important influence on its properties at the room temperature and high temperatures.

High strength concrete properties vary in different ways with temperature than the normal strength concrete. This variation is more stated for mechanical properties, which can be affected by strength, moisture content، density, heating rate, amount of silica fume, and porosity.

2.2 Historical background

Historically, humans began to use fibrous material as a reinforcement for brittle material like mud bricks or with mortars before more than 3500 years ago as found in ancient city of Aqar Quf near Baghdad (Hannant, 2000). Later, a varied uses for fibrous material like using straw or horsehair as a reinforcement in a lot of structure in that time (Sanyal, 2009).

According to (Singh, 2003) Feret in 1906 tests on early stage fatigue behaviour of concrete, a lot of researchers conducted fatigue tests in order to evaluate fatigue behaviour of concrete including steel fiber. But most of the studies were scarce when it comes to the determination of flexural fatigue endurance limit for the type of steel fiber, volume fraction (V_f) and aspect ratio (l_s/d_s) of steel fibers added (Batson, 1972), (Ramakrishnan V. O., 1987), (Tatro, 1987), (Ramakrishnan V. , 1989), (Ramakrishnan V. W., 1989) and (Johnston C. &., 1991).The history of SFRC begins in 1874, when A. Bernard, from California ،find out an idea for enhancing the concrete strength by adding steel splinters and steel leftovers.

(Katzer, 2006) states that in the year of 1918, H. Alfsen from France find out a solution to enhance the properties of concrete by using long steel fibers, long wooden fibers, and other kinds of fibers. Also Alfsen was one of the first researchers that mentioned that the roughness of steel fiber surface could affect the concrete mix, also he insisted on the importance of adding steel fiber to the concrete mix. Thirty six years later Porter mentioned the possibility of applying short wire to concrete to improve the concrete. Researchers still developing the uses of the current fiber and searching for new ones to enhance the building materials properties.

2.3 Steel Fiber Reinforced Concrete

SFRC is a composite material made of concrete mixed with steel fibers that are accommodate the cement-matrix. The matrix, also sometimes of silica fume, fly ash or any other materials are added to the concrete mixture.

Firstly the steel fibers and concrete are bonded together homogenously .After casting and using in building or any other construction it behaved differently during the increasing of loads, when concrete start to crack, steel fiber will still carry out the load, Thereafter; the mechanism depends only on the steel fibers shape and properties. Fibers may fracture and others may split out, that depends on properties and length of steel fiber also concrete strength.

A lot of steel fibers with different sizes, shapes and properties are available including normal steel and high tensile steel, also stainless steel fibers are available. The steel manufacturing is a series of hot and cold working methods. Sometimes the steel is obtained from chopping wires and in other cases it's obtained from cutting steel sheets or milled from ingots, also steel fibers might be produced from hot melt extract (Shah, march, 1981).

There are two main categories of steel fibers, smooth and deformed. They come in various shapes like circular, rectangular, hook shaped etc, as shown in Figure 2.2. And mechanically deformed in ways to improve the bonding strength between the steel and the concrete. According to engineering view, the deformed steel fibers are more efficient because of the increasing in surface area which increases the cement-matrix bond that result in improving the pull out resistance (Hughes, 1976).

The straight fibers (not deformed) type on the other hand are only bond with the concrete by friction and chemical adhesion. Steel fiber lengths are in range from 10 to 65 mm with diameters ranges between 0.5 and 1.2 mm.

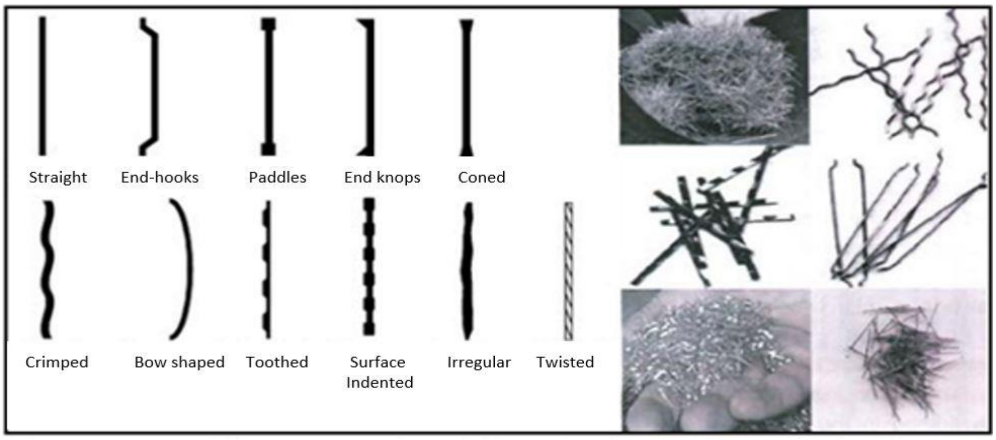

Figure 2.2 Different shapes of steel fibers (Löfgren, 2005).

2.3.1 Fiber and concrete matrix interaction

The yield or the ultimate strain of steel fiber is greater than the tensile cracking strain of cement matrix, so when SFRC is under load, the matrix will crack long before the fibers can be break. When the first crack happens, the element continues to endure the increasing tensile stress because of the steel fibers.

The stress peak and the strain peak of SFRC are much more than the stress peak and the strain peak of the matrix alone. Also, during the inelastic phase between first cracking and the peak, multiple cracking of matrix will take place like shown in the Figure 2.3. Finally, the element fail when the fibers being pull out and separate from the matrix.

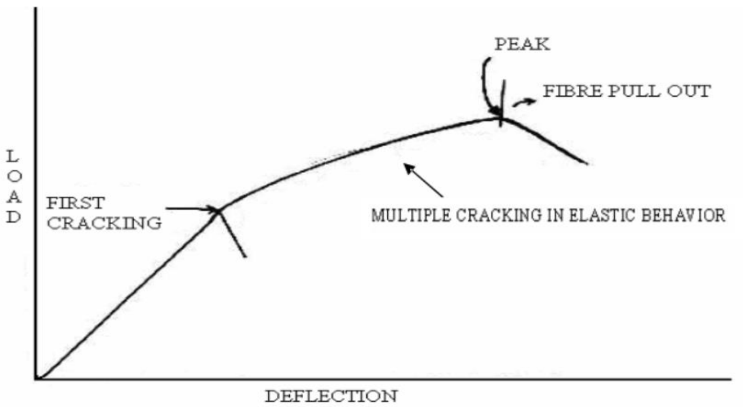

Figure 2.3 Steel fiber mechanisms (Nataraja, 1999).

2.3.2 Bridging action

Steel fibers pullout resistance (dowel action or anchorage) is highly significant in the mean of efficiency. Pull out strength of steel fibers remarkably enhance the concrete post-cracking tensile strength. When SFRC is subjected to load, steel fibers will bridge the cracks, as shown in Figure 2.4. Bridging action like that supply the SFRC with higher ultimate tensile strength, more toughness, and an improvement in energy absorption.

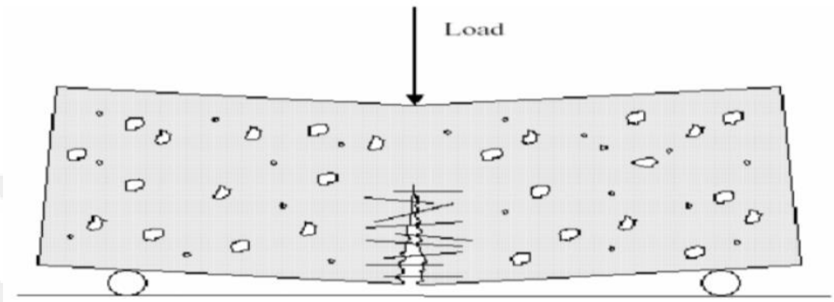

Figure 2.4 Fiber pull-out (Bayasi, 2001).

Basically, a substantial advantage of this steel fiber behaviour is the material damage tolerance. According to (Bayasi, 2001), they conducted a study stating that damage tolerance factor can be defined as the ratio of flexural resistance at 2 mm maximum crack width to ultimate flexural capacity. As a result, at volume friction (V_f) equal to 2% ‹damage tolerance factor was found to be 93%.

2.3.3 Mechanical properties

The mechanical properties imply the reactions of SFRC, deflect either in elastic or plastic, on account of the applied stress. The mechanical properties contain compressive strength, tensile strength, flexural strength, shear strength ‹punching shear resistance, ductility, and crack pattern. The mentioned mechanical properties appear to be affected by parameter of V_f (%), l_s/d_s as aspect ratio, shear span ratio, thickness (h), and also concrete strength (fcu).

2.3.3.1 Compressive strength

(Yazıcı, 2007) carry out series of experiments on compressive strength of SFRC. They report that the 28-day compressive strength values of SFRCs are written in Table 2.2 .

The Compressive strength of control concrete (plain concrete) was found to be 49.1 MPa.

Table 2.2 Compressive properties of concrete mixture (Yazıcı, 2007).

Mixture code	l_s/d_s ratio	V_f (%)	f_c^a(MPa)	Relative f_c(%)
CC	-	-	49.1	100
SFRC1	45	0.5	50.8	104
SFRC2	45	1	53.7	109
SFRC3	45	1.5	57.7	117
SFRC4	65	0.5	53.5	109
SFRC5	65	1	58.3	119
SFRC6	65	1.5	56.4	115
SFRC7	80	0.5	56	114
SFRC8	80	1	58.3	119
SFRC9	80	1.5	52.1	106

The values granted in Table 2.2, for aspect ratio of 45 (SFRC1–3), 65 (SFRC4–6), and 80 (SFRC7–9), the minimum compressive strength concluded in this study was 50.8 MPa, 53.5MPa, and 52.1MPa, respectively. Furthermore, the maximum compressive strength calculated was 57.7MPa, 58.3MPa, and 58.3MPa respectively. As a conclusion from the results, the compressive strengths of SFRCs are higher by percentage range 4%–19% than the control mixture which was a plain concrete. Also, compressive strengths of SFRCs together with 45 aspect ratio (SFRC1–3) were increased with the increasing of V_f. On the other hand for 65 and 80 aspect ratios, the compressive strength of SFRCs (SFRC4–5 & 7–8) were only increased up to 1% V_f. but, for SFRCs with V_f of 1.5%, 1.0%, and 1.0% had highest compressive strength for aspect ratio of 45, 65, and 80, in sequent (Yazıcı, 2007).

Figure 2.5 referring that fibers did enhance the compressive strength of concrete, with increasing in strength ranging from basically 0% to almost 25% also, adding steel fibers increases the post-cracking ductility, or energy absorption of the concrete. We can conclude from the figure that the increasing of V_f led to the increasing of compressive strength of concrete (Johnston C. D., 1991).

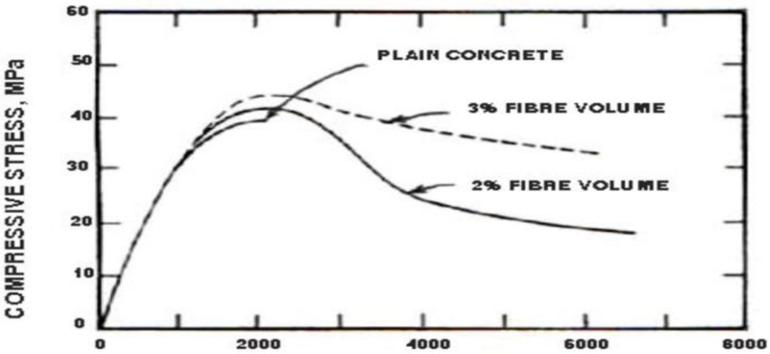

Figure 2.5 Stress – strain curves in compression for SFRC (Johnston C. D., 1991).

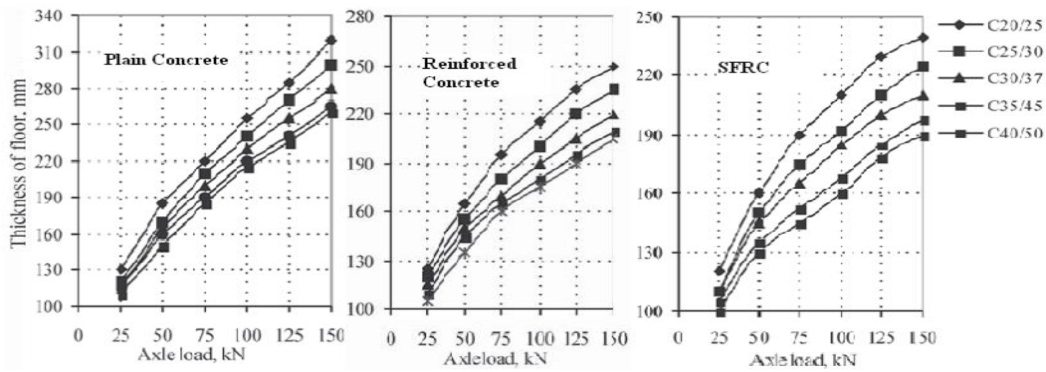

Figure 2.6 Thickness of slab dependent on axil load and concrete class (Žiogas, 2005).

According to Figure 2.6 above, the decreasing of concrete strength for the plain concrete, reinforced concrete, and SFRC; the thickness must be increased in order to obtain the same value of axle load. For example, for concrete strength ranged 20 MPa to 25MPa (C20/25), in order to reserve 100kN, the plain concrete, reinforced concrete, and SFRC needs slab must be at thickness of 253mm, 218mm, and 209mm respectively. This shows that the compressive strength is increased also. It can be shown by other perspective, that the concrete strength role is a very important role in affecting compressive strength. For example, for plain concrete at 150 kN, from C20/25 to C40/50, the slab thickness is decreases by 65mm (20.3%); for reinforced concrete, the slab thickness is decreases by 45mm (18%); and for SFRC, the slab thickness is decreases by 45mm (19.1%).

As shown in Figure 2.7 curves, the highest effect on load capacity is shown at shear span ratio a/h equal to one. This refers to that the principal stresses were very affected by shear stresses. After increasing fiber volume from 1% to 2% when a/h is equal to one, load capacity expand from 1.62 to 1.89 times. At higher values of a/h ratio, the increase of load capacity is not so significant. For example ‹when a/h = 1.5 and a/h =2, the increase from 1.26 to 1.56 and 1.14 to 1.54 times ‹respectively, was observed.

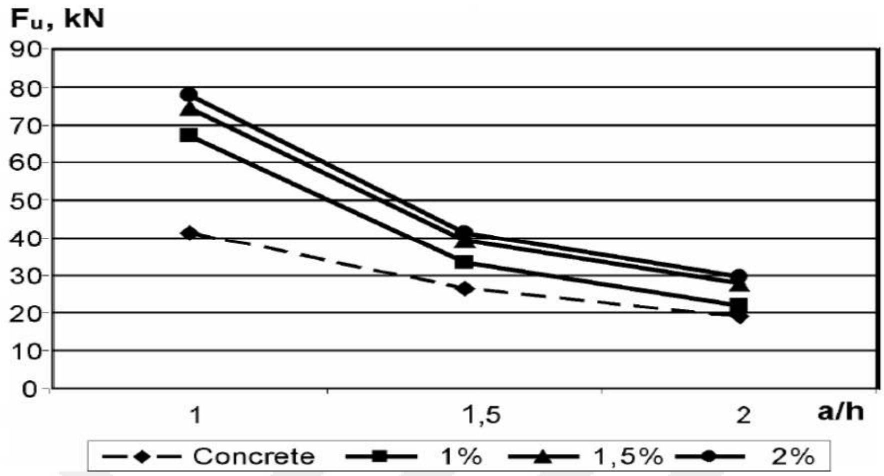

Figure 2.7 Influence of V_f and a/h ratio on load capacity of tested beam (Šalna, 2007).

2.3.3.2 Tensile strength

As shown in Table 2.3, the split tensile strength of control concrete was 4.1 MPa. For l/d ratio of 45 (SFRC1–3), 65 (SFRC4–6), and 80 (SFRC7–9), the minimum tensile strength calculated was 4.50MPa, 4.51MPa, and 4.58MPa ‹respectively.

Table 2.3 Split tensile properties of concrete mixture (Yazıcı, 2007).

Mixture code	l_s/d_s ratio	V_f (%)	f_{st}(MPa)	Relative f_{st}(%)
CC	-	-	4.01	100
SFRC1	45	0.5	4.5	111
SFRC2	45	1	4.69	116
SFRC3	45	1.5	5.69	140
SFRC4	65	0.5	4.51	111
SFRC5	65	1	4.77	117
SFRC6	65	1.5	6.26	154
SFRC7	80	0.5	4.58	113
SFRC8	80	1	5.18	128
SFRC9	80	1.5	5.9	145

The maximum tensile strength obtained was 5.69 MPa, 6.26 MPa, and 5.90 MPa in sequence. The results shows that, the tensile strengths of SFRCs were more by about 11%–54% than control mixture which was a plain concrete.

Tensile strength of SFRC increased when l/d ratio increased; especially with the employment of 1.5% fiber volumes more efficient on the tensile strength .In a similar way, tensile strengths were also raised with the raising of V_f.

Fibers aligned in the same direction of the tensile stress may be result higher raise in direct tensile strength, reaches up to 133% for 5% V_f of smooth, straight steel fibers. On the other hand, the random distribution of steel fiber, may not increase the strength a bit, or increase it in some examples nearly 60%, as many investigations indicating intermediate values, as shown in Figure 2.8 (Johnston C. D., 1974).

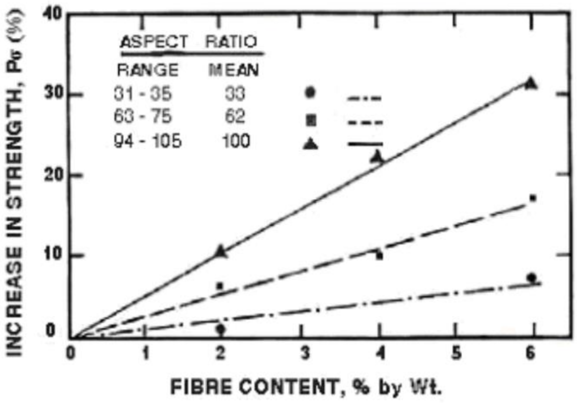

Figure 2.8 Influence of Fiber Content on Tensile Strength (Johnston C. D., 1974).

Splitting-tension test of SFRC also shows comparable result .Thus, the addition of fibers is simply to increase the direct tensile strength is probably worthless. However, as a compression, steel fibers is grated for the increases in the post-cracking behaviour or composites toughness.

2.3.3.3 Flexural strength

(Žiogas, 2005), studied the flexural strength of SFRC, they carried out series of tests and reported the results, Figure 2.9 shows that by increasing steel fiber dosage from 20 kg/m3 to 40kg/m3, the flexural concrete strength will increase nearly 12% in the concrete class. At the meantime, in the concrete class, the flexural strength varies from 9.5% to 11%. Sometimes, steel fiber dosage also may refer in term of V_f.

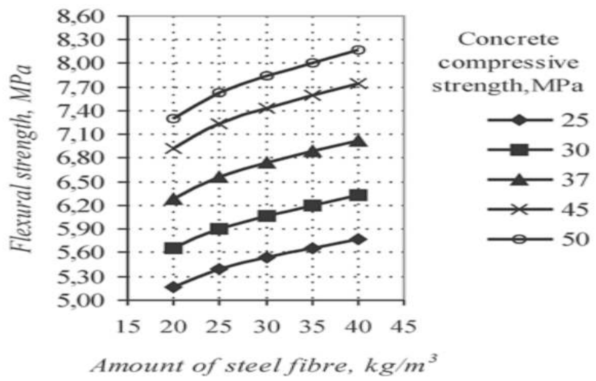

Figure 2.9 Flexural strength dependence on the amount of steel fiber (Žiogas, 2005).

According to Table 2.4, the flexural strength of control concrete was 5.94 MPa. For l/d ratio of 45 (SFRC1–3), 65 (SFRC4–6), and 80 (SFRC7–9), the minimum flexural strength obtained is 6.14MPa, 6.24MPa, and 6.42MPa, respectively.

Table 2.4 Flexural properties of concrete mixture (Yazıcı, 2007).

Mixture code	l_s/d_s ratio	V_f (%)	f_{st}(MPa)	Relative f_{st}(%)
CC	-	-	5.94	100
SFRC1	45	0.5	6.14	103
SFRC2	45	1	6.32	106
SFRC3	45	1.5	7.75	130
SFRC4	65	0.5	6.24	105
SFRC5	65	1	8.08	136
SFRC6	65	1.5	9.33	157
SFRC7	80	0.5	6.42	108
SFRC8	80	1	9.74	164
SFRC9	80	1.5	10.76	181

On the other hand, the maximum flexural strength registered was 7.75 MPa ،9.33 MPa, and 10.76 MPa in sequence. It can also be seen from the results that, the flexural strengths of SFRCs were higher nearly about 3% - 81% than control mixture which is a plain concrete.

Clearly, steel fibers significantly improved the flexural strength of concrete as compared to compressive and split tensile strength. Also, flexural strength of SFRC is significantly improved with the increasing of l_s/d_s ratio and V_f.

2.3.3.4 Shear resistance

(Kwak, 2002) studied the shear resistance behaviour of SFRC. According to the Figure 2.10 shown above, the shear stress at failure consistently decreased with the increasing of shear span ratio (a/d). The differences obtained from capacity between beams with a/d= 2 and a/d = 3 was significantly higher than the differences between beams with a/d= 3 and a/d = 4. In fact, such behaviour also expected due to the increased of a/d ratio that causes the curving action and dowel action become less effective.

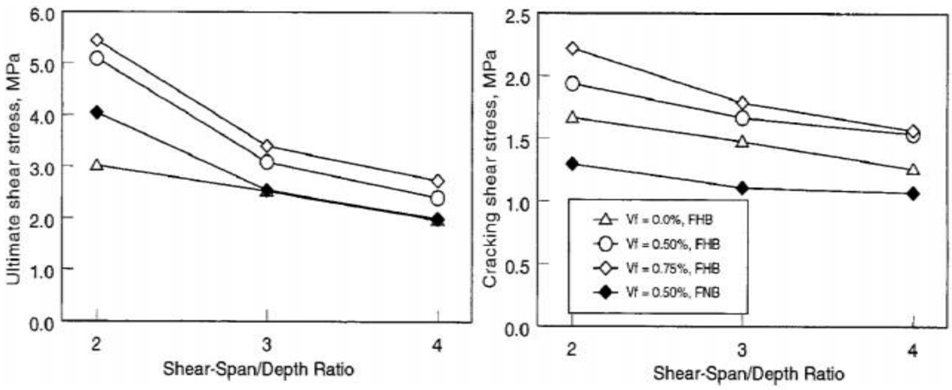

Figure 2.10 Influence of shear span ratio on shear resistance (Kwak, 2002).

In addition, similar orientation also expected for beam failing in flexure. If the flexural capacity of beam controls the maximum shear, then the ultimate shear would be proportional to 1/a. The effects of V_f on shear strength of SFRC are explained in Figure 2.11.

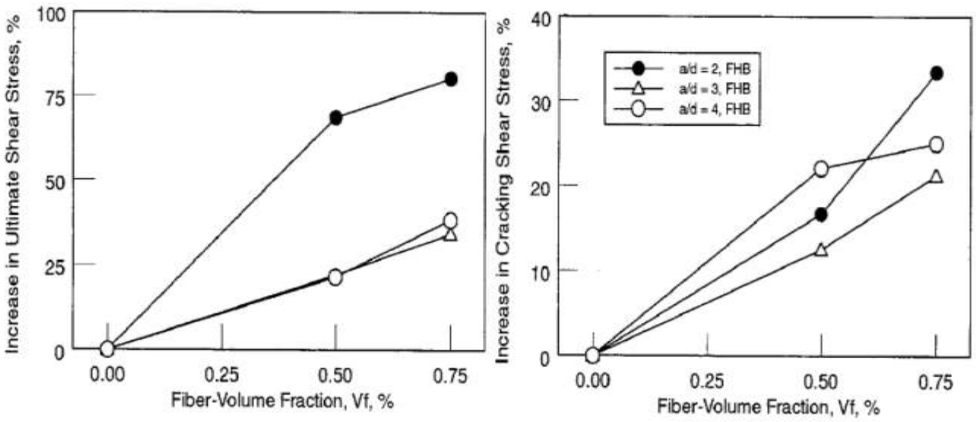

Figure 2.11 Influence of volume friction on shear strength (Kwak, 2002).

The strength of SFRC beams ranged from 122% to 180% of the strength of the plain concrete beams. The increase of strength was particularly large with the range of 69%

to 80% for the beams with low a/d ratio, which is a/d = 2 as shown in figure that will probably fail in combination of shear and flexure. For larger a/d ratios, which is a common thing in engineering, the increase in strength ranged from 22% to 38%. These beams will definitely fail in flexure; so, the applied load at failure is not equal to the shear strength. In fact, this load will only provide a lower bound on the shear strength. On the other hand, concrete strength also plays a role in affecting the shear strength. As the concrete strength was approximately doubled from 31Mpa to 65MPa, the shear strength increased by 21% to 26% for a given V_f and a/d ratio (Kwak, 2002).

2.3.3.5 Punching shear resistance

(Chen YM, 1979), studied the punching shear resistance. According to Table 2.5, the maximum punching shear load increased when the glass fiber layer increased. To be exact, the layers number of glass fiber can be assumed to be equivalent to the V_f of steel fiber. Hence, the increased in V_f will lead to the increase of punching shear load too.

Table 2.5 Influence of glass fiber layer on punching shear (Chen YM, 1979).

Slab no.	Maximum punching load (KN)	Percent increased* (%)	Mode of failure
SR1-C1	103.9	-	Flexure
SR1-C1-F1LT	148	42.44	Punching
SR1-C1-F2LT	202.1	94.51	Punching
SR1-C2	123.8	-	Flexure
SR1-C2-F1LT	180	45.40	Punching
SR1-C2-F2LT	218.8	76.74	Punching
SR2-C1	146.1	-	Punching
SR2-C1-F1LT	189.6	29.77	Punching
SR2-C1-F2LT	224.2	53.46	Punching
SR2-C2	225.7	-	Punching
SR1-C1-F2LT	263.9	16.93	Punching
SR2-C2-F1LT	289.4	28.22	Punching
*The percent increased indicated the increasing of the punching load compared to that of the corresponding control specimen without GFRP reinforcement.			

Figure 2.12 indicates that by increasing the slab thickness (h), it will result in a higher cracking load, yield load, and ultimate load .On the other hand, the ductility defined by $\delta u/\delta y$ where δu is the deflection at ultimate and δy is the deflection at yielding, also tends to increase with the increase of slab thickness (h).

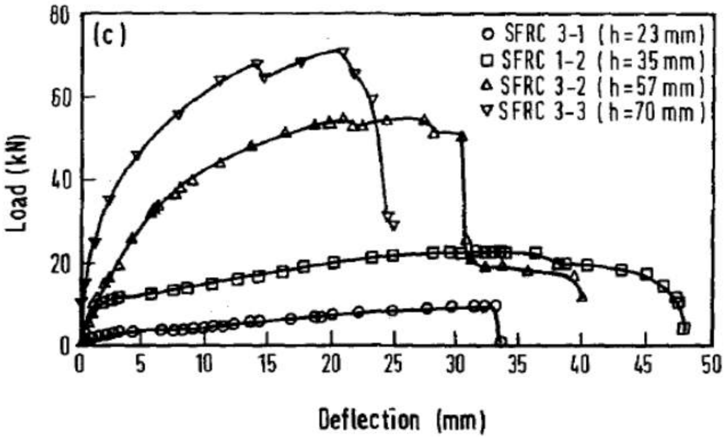

Figure 2.12 Load-deflection characteristic of SFRC influenced by thickness under punching shear (Tan, 1994).

2.3.3.6 Ductility

(Tan, 1994), studied the ductility, according to Figure 2.13, the region in load-deflection curve that defines the deflection at first crack (δcr), deflection at yielding (δy), and also deflection at ultimate (δu) corresponding to the cracking load (P_{cr}), yield load (Py) ‹and ultimate load (P_u) for slabs tested.

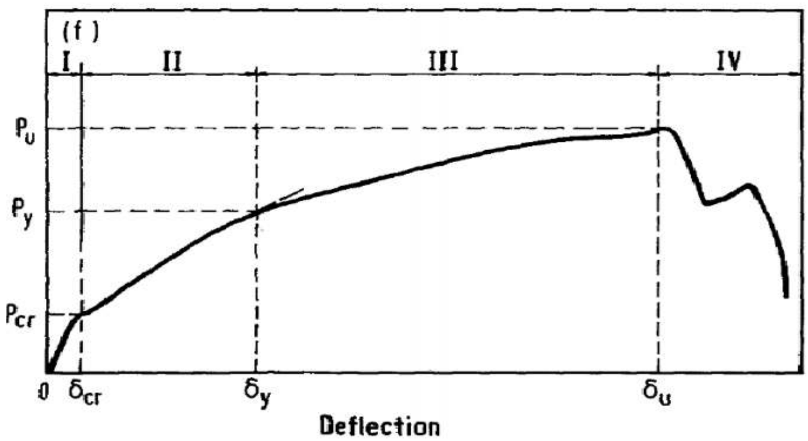

Figure 2.13 Load-deflections under punching shear (Tan, 1994).

In fact, the cracking load was determined from the load-deflection curve and confirmed by steel-strain reading. The yield load (Py) was obtained from the intersection of linear portions of regions II and III as shown in Figure 2.13. The same procedure is applied when getting the ultimate load (P_u) which was obtained from the intersection of region III and IV.

Also, the Table 2.6 gives the values of P_{cr}, P_y and P_u for all slabs tested. Moreover, the value of $\delta u/\delta y$, which represents the ability of the slabs to sustain further deflection after first yield of steel reinforcement without any reduction in load-carrying capacity.

Table 2.6 Experiment result of SFRC slab under punching shear (Tan, 1994).

Mixture code	a/d	P_f (%)	h (mm)	f_{cu}^{a} (MPa)	r (mm)	P_{cr} (kN)	P_y (kN)	P_u (kN)	δy (mm)	δu (mm)	δu $/\delta y$
SFRC1-1	27.2	0.31	35	50	100	6.7	19.4	19.4	14.1	23.2	1.65
SFRC1-2	40.9	0.31	35	50	100	5.5	20	22.6	19.4	30.7	1.58
SFRC1-3	54.5	0.31	35	50	100	5.3	14.1	18.9	32.4	53.3	1.65
SFRC2-1	40.9	0.5	35	50	100	6.6	18.7	20.9	19.5	29.3	1.5
SFRC2-2	40.9	1	35	50	100	5.1	21.3	23.7	23	31.4	1.37
SFRC2-3	40.9	1.5	35	50	100	4.5	20	24.6	21	35	1.67
SFRC2-4	40.9	2	35	50	100	9.1	23.3	27.4	21.3	35	1.64
SFRC3-1	65.2	0.31	22	50	100	3.1	7.3	9.4	17.6	32.7	1.86
SFRC3-2	25.1	0.31	57	50	100	15.5	36.7	54.9	6.8	21.3	3.13
SFRC3-3	20.5	0.31	70	50	100	23.9	43.3	70.5	3	20	6.67
SFRC4-1	40.9	0.31	35	35	100	5.5	14.3	19	18.2	32.5	1.79
SFRC4-2	40.9	0.31	35	65	100	7	15.3	20	17.8	36	2.02
SFRC5-1	40.9	0.31	35	50	200	6.2	22.2	26.1	23.1	37.5	1.62
SFRC5-2	40.9	0.31	35	50	150	5.3	15.6	18.7	20	32.5	1.63

As a result, these values can be considered a measurement of slabs ductility. From the table also, it indicates that with the increase of slab thickness (h), the ductility also increased as compare to other parameter such as the concrete strength f_{cu} , loaded area (r), and volume fraction (V_f) that give a low ductility result (Tan, 1994).

2.3.4 Crack pattern

(Kwak, 2002), studied the crack pattern in beams. According to Figure 2.14, the presence of steel fibers in concrete is highly affect the observed cracking patterns for beam with a/d ratio of 2. In this figure, the three beams are identical except for the addition of steel fibers.

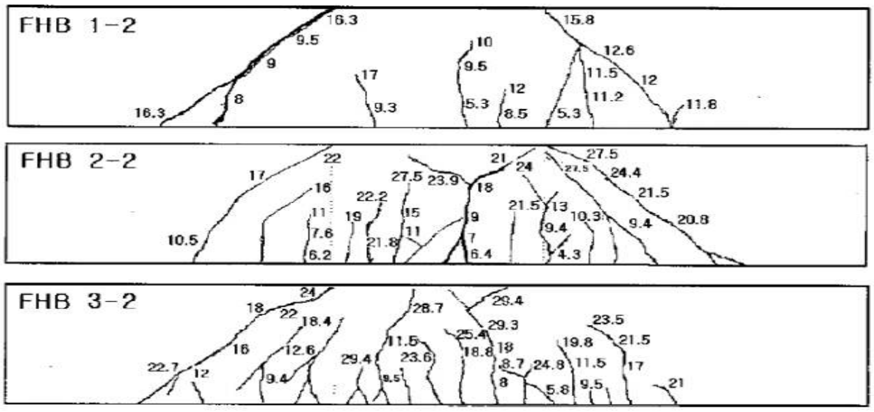

Figure 2.14 Typical crack patterns (a/d = 2), (Kwak, 2002).

The results beside to the cracks refers to the load, which is the first observation of the cracks. Specimen FHB 1-2, that had no steel fibers addition, the flexural cracks formed firstly within the constant moment region, usually near the middle of the span. After that, two shear cracks happened near each quarter span point within the areas of constant shear. Therefore; beam failed suddenly along a single shear crack.

Moreover, as shown in Table 2.7, the V_f increased to 0.50% and 0.75 %for FHB 2-2 and FHB 3-2, in sequent; the failure mode is changed from shear to a collection of shear and flexure. In similar failures, significant diagonal shear cracks and vertical flexural cracks are both happened, which might interacted to produce the failure. The flexural and shear cracks were distanced nearly as the V_f increased. As an example, in concrete beams that has no fibers, the crack spacing was typically 90mm to 170mm ، while this spacing decreased to 70mm to 90mm in the addition of steel fibers (Kwak, 2002).

Table 2.7 Failure mode of concrete beam influence by Vf (Kwak, 2002).

Beam designation	Fiber volume fraction V_f (%)	Shear span/depth ratio l/d	Concrete compressive strength f_c' (MPa)	Average shear stress		Ultimate displacement mm	Failure mode
				V_{cr} MPa	V_u MPa		
FHB1-2	0.00	2.0	62.6	1.67	3.02	6.080	Shear
FHB2-2	0.50	2.0	63.8	1.94	5.09	16.50	Shear-flexure
FHB3-2	0.75	2.0	68.6	2.22	5.44	34.35	Shear-flexure
FHB1-3	0.00	3.0	62.6	1.48	2.53	9.680	Shear
FHB2-3	0.50	3.0	63.8	1.67	3.09	18.20	Flexure
FHB3-3	0.75	3.0	68.6	1.80	3.40	33.59	Flexure
FHB1-4	0.00	4.0	62.6	1.26	1.98	13.86	Shear
FHB2-4	0.50	4.0	63.8	1.54	2.41	28.49	Flexure
FHB3-4	0.75	4.0	68.6	1.57	2.74	43.87	Flexure
FNB2-2	0.00	2.0	30.8	1.30	4.04	8.930	Shear
FNB2-3	0.50	3.0	30.8	1.11	2.55	10.81	Shear
FNB2-4	0.75	2.0	30.8	1.07	2.00	41.07	Flexure

2.4 Residual Punching Strength of Various Types of Concrete Panels Exposed to High Temperatures

According to (Muhammed, 2012), research on residual punching strength of NSC (normal strength concrete), HSC (high strength concrete) and LWC (light weight concrete) panels are exposed to high temperatures, that studied eleven slabs divided into three groups, the first group contains four plates of NSC, one plate under ambient condition and the other three subjected to three different temperatures (320, 450 and 700 °C), the second group contains four plates of HSC, one plate under ambient condition and the other three subjected to three different temperatures (320, 450 and 700 °C), the durations of heating were 1hr, 2hrs and 4hrs for both groups and the third group contains three plates of LWC, one plate under ambient condition and the other two subjected to two different temperatures 320 °C and 700 °C, the durations of heating 1hr and 4hrs. The mentioned work was aiming to study the post heating behavior of (NSC) ،(HSC) and (LWC) plates and analyzing the residual punching shear strength of two-way flat plate specimens. The work results of the work are shown in Table 2.8 to 2.10.

Table 2.8 Test results of slab specimens of NSC (Muhammed, 2012).

Specimen	Temperature C°	Compressive strength MPa	Residual ultimate load kN	Residual load %	Maximum failure	Failure mode
N1C	Room temperature	50	18	100	2.77	Punching
N11	320	352.1	21	116.67	5.45	Punching
N12	450	36.52	11	61.11	2.82	Punching
N14	700	25.2	6	33.33	7.23	Flexural

Table 2.9 Test results of slab specimens of HSC (Muhammed, 2012).

Specimen	Temperature C°	Compressive strength MPa	Residual ultimate load kN	Residua l load %	Maximum failure	Failure mode
H1C	Room temperature	93.67	26	100	7.74	Punching
H11	320	91.83	24.5	94.23	11.72	Punching
H12	450	62.63	18	69.23	4.91	Punching
H14	700	36.20	14	53.84	2	Flexural

Table 2.10 Test result of slab specimens of LWC (Muhammed, 2012).

Specimen	Temperature C°	Compressive strength MPa	Residual ultimate load kN	Residual load %	Maximum failure	Failure mode
L1C	Room temperature	36.67	13	100	3.66	Punching
L11	320	31	11	84.61	3.58	Punching
L12	450	23.2	9	69.23	6.39	Punching

The experimental work recorded residual punching shear capacity, load deflection, crack patterns and the effect of different temperature exposure. The results of residual punching strength decreased from the ambient control plates at maximum temperature exposure by percentages 33.3%, 53.8% and 69.2% for NSC, HSC and LWC plates in sequent as shown in Figure 2.15 (Muhammed, 2012).

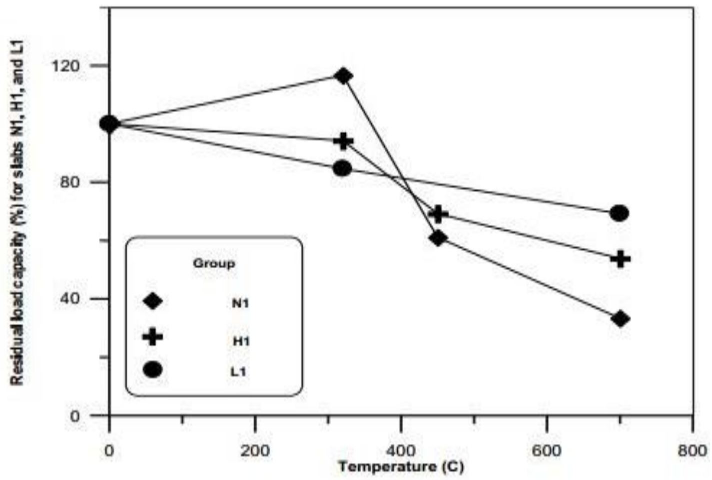

Figure 2.15 Effect of high temperature on the residual load capacity for the punching groups of slab specimens (Muhammed, 2012).

At the maximum point of burning (700 °C), the type of failure changes from what was expected as punching shear failure to a flexural failure in the specimens of NSC and HSC, on the other hand the LWC plate specimen, failure type stays punching shear at the same temperature.

Concrete compressive strengths for NSC, HSC and LWC were reduced after they were exposed to burning, the results of the test showed that for NSC which was heated to 450 °C and 700 °C were reduced to 26.96% and 49.6% in sequent from the ambient condition, for HSC, which was heated to 320 °C, 450 °C and 700 °C were reduced to 1.97% , 33.14% and 61.36% in sequent from the ambient condition and for LWC which was heated to 320 °C and 700 °C were reduced to 15.47% and 36.74% in sequent from the ambient condition.

The size of the punching shear failure zones for the specimens subjected to heat was found larger than that in ambient condition. The punching failure pyramid angle was increased when the slab strength increases, the least results were for LWC slabs and the highest results were for HSC slabs. Also hair cracks can be seen when the specimens were heated at high temperature more than 500 °C (Muhammed, 2012).

2.5 Ultimate Load Proposed Equations

Punching shear is introduced decades ago, therefore; it was taken in consider by lots of cods that gives designs and calculation provisions for punching shear capacity, such as:

• ACI 318-83 and CSA A23.3 84M: Punching perimeter in ACI 318-83 and CSA A23.3 84M is located at a distance d/2 from the column face, both calculate the shear strength from the root of concrete strength (American Concrete Institute 318-14, 2014), (CSA, 1984).

$$V_u = 0.33 \times b_o\, d\, (f'c)^{1/2}$$

Where b_o is the perimeter $d/2$ from the column face.

d effective depth.

• Regan 1981: (Regan, 1981) in a contract with the Construction Industries Research and Information Association, Regan developed an equation for punching shear capacity calculation. Regan suggested that the shear perimeter is rounded rectangular located 1.25d form the face of rectangular columns and a circular shear perimeter located 1.25 from the face of circular columns.

$$V_u = K_a K_{SC} K_S\, (p \times f'c)^{1/3} \times d(\Sigma_c + 7.85d\,)$$

Where:

V_u ultimate Shear force.

K_a 0.13 for concrete of normal density.

K_{SC} $1.15 \times (4\pi x\ column\ area\ /\ (column\ perimeter)^2)^{1/2}$

K_S size effect term $(300/d)^{1/4}$ (SI units).

p steel ratio.

$f'c$ compressive strength.

d effective depth of slab in mm.

Σ_c the perimeter of column.

• British standard BS8110:1985: The standards proposed by the British standard BS8110:1985 are comparable to what Regan proposed. (part1, 1985)

$$V_c = const \times (p \times f'c)^{1/3} \times (400/d)^{1/4} \text{ (SI units)}$$

Where:

d is the effective depth of slab in mm.

But it can be seen in British standard BS8110:1985 that the critical shear perimeter are rectangular located 1.5d form the face of the column, regardless of the column shape if it was circular or rectangular.

• Bazant and Cao: (Bazant & Cao, 1987) Bazant and Cao focused on the size effects, also a formula was suggested for calculating the punching shear.

$$v_u = \frac{V_u}{D_p h}$$

$$v_c = const \times f'c \, \frac{(1 + 0.6 \, {}^{D_p}/_{h})}{(1 + {}^{h}/_{25 d_{agg}})^{1/2}}$$

Where:

D_p diameter of punching.

h slab thickness.

d_{agg} maximum aggregate size.

CHAPTER THREE

EXPERIMENTAL WORK

3.1 Introduction

In this study an experimental work using a model of SFRC panels was carried out to study the residual strength of two-way panels of SFRC under high temperature, and the degradation of concrete mechanical properties (compressive and tensile strength) Flat slabs experienced a high stress at the connection with column, and it's rather fail because of punching shear than in bending especially when a high reinforcement ratio is used in the slabs. The experimental work was conducted at the Structural and Materials Laboratories at the University of Gaziantep. The experimental program can be described as follows: the main parameters are the effect of high temperature, and the volume fraction of steel fibers. A total of twenty specimens are suggested for investigation; fifteen of them are of SFRC, which will be compared with five control panels of normal concrete that were marked as groups: (A, B, C, D and E) in which each group contains one panel without steel fiber and three panels of different percentages of steel fiber panels, Group E was at ambient conditions and the other four groups were subjected to heat exposure in furnace at a temperature (150, 300, 450 and 550 °C), like follow in Table 3.1.

Table 3.1 Study groups.

Group	Exposed temperature °C	Vf = 0%	Vf = 0.75%	Vf = 1%	Vf = 1.25%
A	150	A1	A2	A3	A4
B	300	B1	B2	B3	B4
C	450	C1	C2	C3	C4
D	550	D1	D2	D3	D4
E	Ambient condition	E1	E2	E3	E4
Where Vf is the volume fraction.					

3.2 Specimens Geometry

The specimens are selected as a model with dimensions of 500 × 500 × 60 mm, which was supported with column steel plate of dimension 55 ×55 mm, this steel plate was used as loading through, where the slabs are supported by special made support.

The support are of 8 points of half steel balls, distributed with 22.5 degree central angles, with a total loading radius of 400 mm as shown in Figure 3.1 This half balls are used so that the frictions would be as minimum as possible, in this case the axial forces induced from this friction are prevented.

All specimens were designed to fail in punching ($V_R < P_{flex}$) where V_R is the punching shear nominal strength according to ACI318, P_{flex} is the flexural capacity which is obtained from yield line analysis. Overall, the slabs were reinforced orthogonally by the same reinforcing ratio (ρ), a ten deformed bars of 5.3 mm diameter were used in each direction with an ultimate and yield strength of 476 MPa and 400 MPa respectively as shown in Figure 3.2. These reinforcement were placed orthogonally at tension face as a single reinforcement layer with clear cover of 15 mm and equally spaced in each horizontal directions $Sx = Sy = 46.6$ mm center-to-center (with reinforcement ratio equal to 1.2%). All bars were bended with 90 deg., all free bends were tied together by additional one bar in each side of compression face.

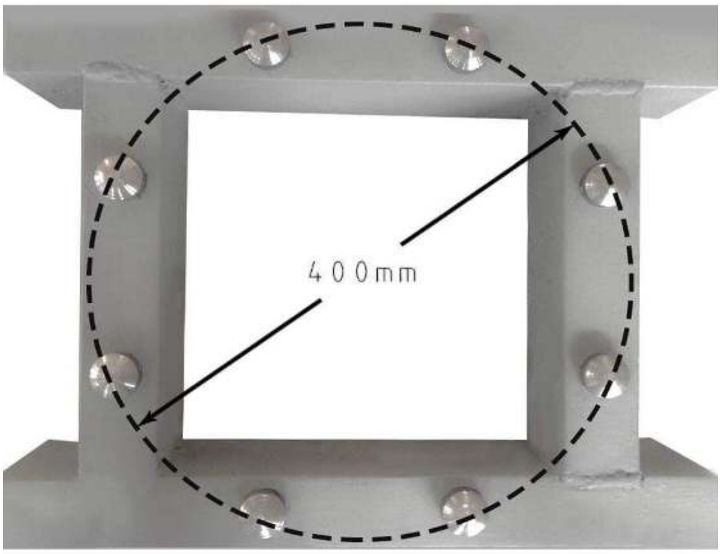

Figure 3.1 Test support model.

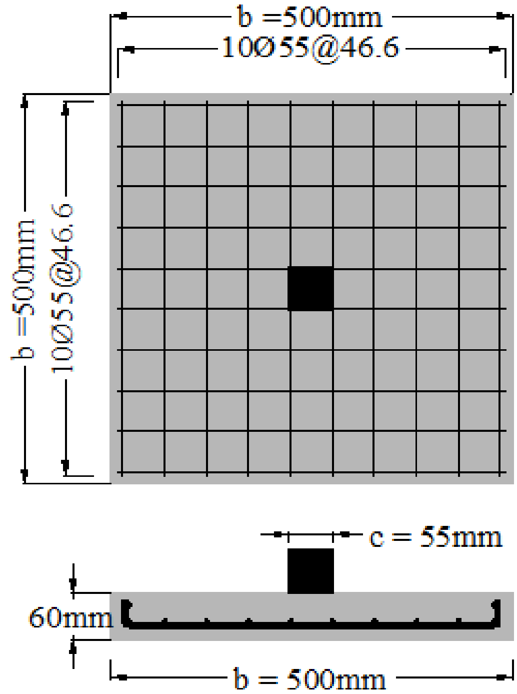

Figure 3.2 Slab geometry and reinforcement details.

In order to construct a slabs with uniform dimensions that can sustain the vibrating forces, and with right angle faces, the mold sides shutter are made from angle iron of 5 mm that are fixed perpendicularly to the plywood as shown in Figure 3.3.

Figure 3.3 Casting mold.

3.3 Mix Design and Materials Properties

3.3.1 Mixture

According to earlier researches and studies fibers are more active with a mixture with fine aggregate, therefore; the plan was introducing a mixture with 63.24 % of fine aggregate and 36.75% of the total mix percentage as shown in the Table 3.2.

Table 3.2 Mix design.

Mix code	V_f %	Cement (kg)	Sand (kg)	Gravel (kg)	Super plasticizer (kg)	Steel fiber (kg)	Water (kg)	Silica fume (kg)
S0	0	10.5	26.5	17	0.15	0.0	3.5	0.8
S0.75	0.75	10.5	26.5	17	0.15	1.3	3.5	0.8
S1	1	10.5	26.5	17	0.15	1.75	3.5	0.8
S1.25	1.25	10.5	26.5	17	0.15	2.2	3.5	0.8

3.3.2 Material Properties:

• Cement: The type of cement used in this study was cem II / A-LL 42.5 R. It is obtained from Limak Gaziantep cement factory.

• Superplasticizer: due to the high percentage fine aggregate, the workability of the designed mixture are too lows, therefore, a high water reducer are used in constant percentage for all mixture. A superplasticizer under traditional name Glenium 51 are used, which is complies with ASTM C 494 Types A.

• Fine aggregate: a graded river sand brought from local source. The size of particles are ranging from 0.075 mm to 4.75 mm was used. The sieve analysis of the used fine aggregate is shown in Table 3.3 and Figure 3.4.

Table 3.3 Grading of fine (river sand) aggregate.

Sieve opening (mm)	Retained weight (gm.)	Passing %
12.5	0	100
9.5	0	100
4.75	104.7	93
2	554	63
1.18	816.5	45
0.6	1048.7	29
0.3	1255.4	16
0.15	1407.4	5
0.075	1431	4

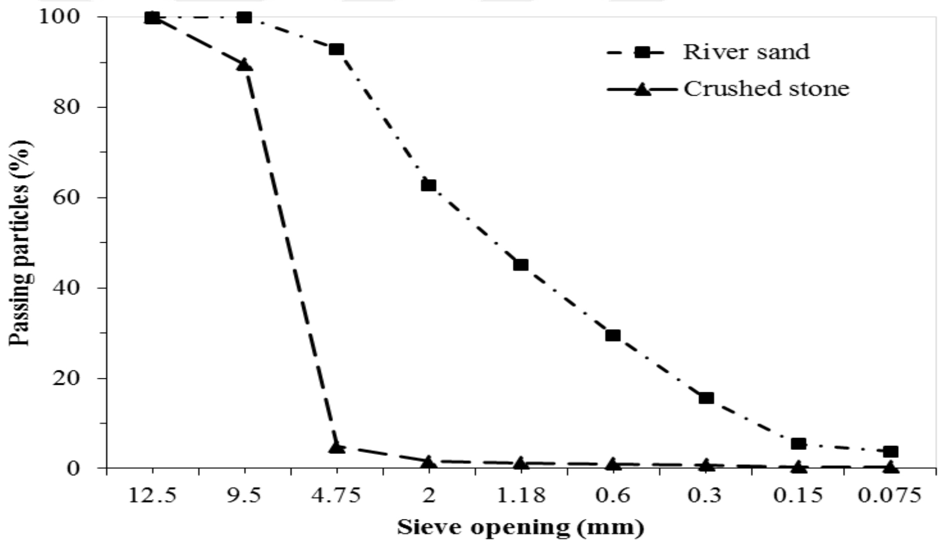

Figure 3.4 Sieve analysis.

• Coarse aggregate: a crashed stone with a gap graded of crashed stone are used. The maximum size of the particles was 9.5 mm. As seen in Table 3.4 it is shown that there are a gap between particles of 4.75 mm and 9.5 mm, this means that even the coarse aggregate has higher fine aggregate.

Table 3.4 Grading of coarse (crashed stone) aggregate.

Sieve opening (mm)	Retained weight (gm.)	Passing %
12.5	0	100
9.5	186.6	89
4.75	1690.8	5
2	1749.7	2
1.18	1754.9	1
0.6	1758.5	1
0.3	1763.8	1
0.15	1770	0
0.075	1770	0

• Steel fiber: a 3 cm hooked at their ends steel fiber with a diameter of 0.75 mm and aspect ratio 40 was used in this study. It's manufactured by Dramix Company and collected into bundles by dissolvable glue as shown in Figure 3.5.

Figure 3.5 Steel fiber.

• Silica fume: is an amorphous (non-crystalline) polymorph of silicon dioxide, silica. It is an ultrafine powder collected as a by-product of the silicon and ferrosilicon alloy production and consists of spherical particles with an average particle diameter of 150 nm.

• Steel reinforcement: deformed steel bars of 5.3 mm in diameter were used as reinforcement placed in the tension face of the slab. The yield strength was determined from tensile test. The average yield strength was 400 MPa.

• Water: tap water was used throughout this work for both mixing and curing of concrete.

3.3.3 Mixing

As a first step, the dry materials (sand, gravel, cement and silica fume) was mixed in vertical rotations mixer that has four paddles for blending the materials as shown Figure 3.6. The dried materials were mixed for almost five minutes to get homogeneous mixture before adding water. The water is added slowly to the mixture also in slow rotations for almost five minutes, then super plasticizer is added and rotate the mixer on the maximum speed before adding the steel fiber which is added slowly soon after adding the steel fiber the mixture will be ready for casting. The mold was oiled well to prevent the concrete attaching the mold and make it easy to extract the sample.

Figure 3.6 Mixer.

When the mix is ready it was moved to the mold for casting the panel by using vibrator in this operation, exterior vibration for the panels. Also a standard cylinder, 100 mm in diameter and 200 mm long was casted, exterior vibration for the cylinder containing steel fiber however: the cylinder containing normal concrete was casted as three layers, each layer flattened with a rod carefully. The vibration process continued until the air bubble escaped from the surface of the specimen. These mentioned cylinders are used to determine the compressive strength f_c', the modulus of elasticity E and the tensile strength f_{ct}, casting three cylinders to get an accurate test reading.

After pouring the concrete in the mold, surface of the concrete was leveled and smoothed using a trowel. It can easily be noticed that the concrete mix without steel fiber is so ease when it comes to finishing using trowel and a lot more workable than the mix containing steel fiber.

Then the mold was taken to a place where the temperature is kept constant (room temperature) because of the cold weather and it stays there for 24 hours as shown in Figure 3.7.

Figure 3.7 A place where the temperature is kept constant (room temperature).

3.3.4 Slump test

Concrete slump test is used to determine the consistency of concrete fresh mixture. It is used to measure the workability of concrete. The slump test result of the work were as shown in Table 3.5, which shows that there is a direct relation between the slump result and the increasing percentage of steel fiber. Also it shows that there is an inverse relation between the workability and the percentage of steel fiber.

Table 3.5 Slump test results.	
Specimen	Slump test result (mm)
S0	97
S0.75	68
S1	62
S1.25	58

3.4 Curing process

When 24 hours is past the mold was opened and the sample was taken to a water tank with heater to begin the curing process with an average temperature of 25 °C and it remains there for 28 days as shown in Figure 3.8.

Figure 3.8 Curing tank.

3.5 Drying process

After curing is finished, the samples surfaces are wiped with piece of cloth to make it saturated surface dry and weight it before going to the furnace and dry it for 24 hours at a temperature of 105 °C as shown in Figure 3.9.

Figure 3.9 Drying process.

3.6 Weighting

After the drying process, the samples were weighted again with a balance the give a degree of accuracy up to three digits in grams as shown in Figure 3.10.

Figure 3.10 Weighting the specimens.

Using the two times weighting of each sample allows to calculate the moisture content (is the quantity of water contained in a material, such as soil (called soil moisture), rock, ceramics, or wood. Water content is used in a wide range of scientific and technical areas, and it is expressed as a ratio, which can range from 0 (completely dry) to the value of the materials' porosity' at saturation. Moisture content can be calculated by this equation $(W\ wet - \frac{W\ dry}{W\ dry} +) * 100$, as follows in table 3.6.

Table 3.6 Moisture content.

Group	Exposed temperature °C	Mix code	Weight		Moisture content
			W_{wet}	W_{dry}	
A	150	S0	40.195	39.885	0.78
		S0.75	38.555	38.04	1.35
		S1	40.235	39.87	0.92
		S1.25	40.66	40.07	1.47
B	300	S0	39.525	38.95	1.48
		S0.75	39.135	38.485	1.69
		S1	39.855	39.56	0.75
		S1.25	41.37	40.945	1.04
C	450	S0	39.085	38.725	0.93
		S0.75	39.375	38.97	1.04
		S1	38.92	38.495	1.10
		S1.25	39.57	39.175	1.01
D	550	S0	38.885	38.6	0.74
		S0.75	40.625	40.325	0.74
		S1	38.81	38.445	0.95
		S1.25	41.005	40.5	1.25

It can easily been noticed in Table 3.6 the results that the flat plates has a low moisture content, that's due to the using of fine materials in the mix which has a large surface area that led to a higher reaction with water.

3.7 Heat Exposure Details

After weighting and calculating the moisture content the Samples were taken to furnace to start the burning process in different temperature according to which group was taken.

Group (A) was heated to the temperature of 150 °C in the furnace , at first it was heated gradually to 150 °C in 20 minutes then for three hours under a constant temperature of 150 °C after that it was cooled down from 150 °C to 50 °C in 2 hours.

Group (B) was heated to the temperature of 300°C in the furnace, at first it was heated gradually until it reached 300°C in 30 minutes then for three hours under a constant temperature of 300°C after that it was cooled down from 300°C to 66 °C in 40 minutes.

Group (C) was heated to the temperature of 450°C in the furnace, at first it was heated gradually until it reached 450° C in 30 minutes then for three hours under a constant temperature of 450°c after that it was cooled down from 450°C to 50°C in 70 minutes.

Group (D) was heated to the temperature of 550°C in the furnace, at first it was heated gradually until it reached 550° C in 1 hours then for three hours under a constant temperature of 550° c after that it was cooled down from 550° C to 105° C in 100 minutes.

3.7.1 Furnace

The furnace dimensions is 130×130×80 with a sliding base, it has four sides heaters and an opening in the upper side which work as ventilation.

The furnace can be programed seven different programs, each program can conclude more than 5 steps, and the furnace temperature could reach up to 1300° c.

Also there's thermocouple placed in the rare side of the furnace to measure the temperature as shown in Figure 3.11.

The increasing and the decreasing of temperature in time and the burning profile curves for each group are shown in Figure 3.12.

Figure 3.11 Furnace.

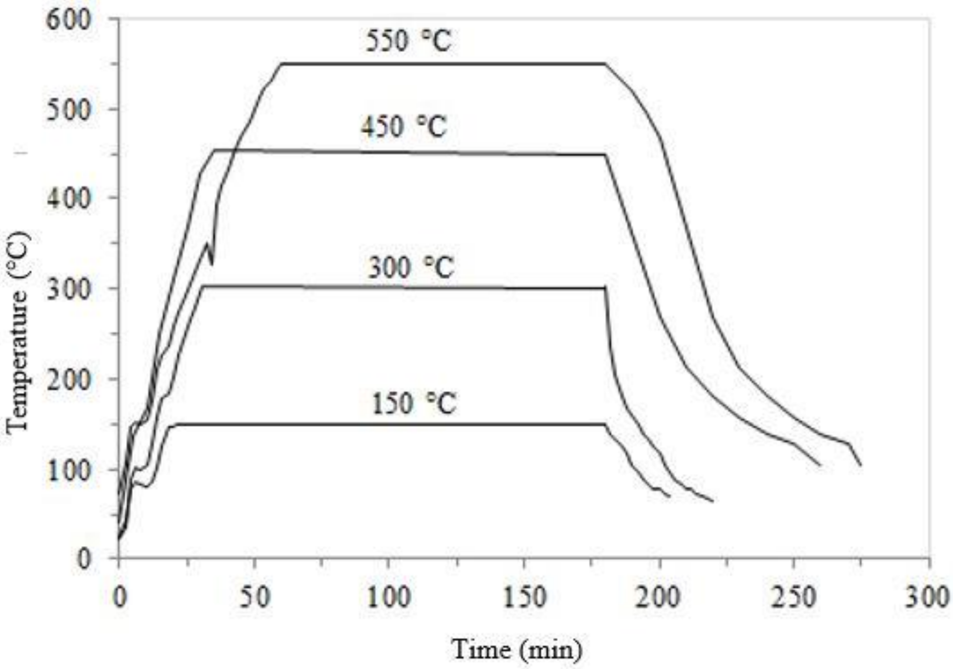

Figure 3.12 Burning profile curves for each group.

3.8 Concrete mechanical properties

Cylinders tests were carried out on the same day as the corresponding slab test.

3.8.1 Compressive strength

(ASTM C39, 1997) describes the procedure of calculating the compressive strength of concrete cylinders. After preparing the sample putting it in the center of the machine, a compressive axial load shall be applied till failure occurs, as shown in Figure 3.13.

Figure 3.13 Cylinder compressive test.

3.8.2 Tensile stress

(ASTM C496, 2004) setup the foundation for developing this procedure. A diametric compressive load shall be applied along the specimen length until the failure occurs.

The cylinder shall be positioned vertically in the test frame exactly in the center, two segment of plywood must be placed longitudinally on the upper and lower sides of the cylinder, also a steel bar is used to strict the cylinder in place, The next step would be setting the frame in the center of the compression machine and stating the test as shown in Figure 3.14.

Figure 3.14 Splitting tensile test.

3.8.3 Modulus of elasticity test

(ASTM C469, 2002) describes the procedure of measuring the modulus of elasticity in compression, the concrete cylinders are submitted to a slow increasing longitudinal compressive stress. Longitudinal strains are specified using a bonded or not bonded sensor, which helps measure the average deformation of two locations of quite the contrary. ASTM C469 does not restrict a standard test samples dimensions. However, casted concrete cylinders are usually the same dimensions as the cylinder used for compression resistance measurements.

Firstly the frame is assembled by adjusting the frame rings while the spacers are kept in position, then Keep the longitudinal screws must be tightened to lock the rings before placing the cylinder on a level surface. After placing the cylinder, the horizontal screws must be tightened on the specimen by an equal distance from every side of the ring. When all the adjustments are finished the vertical screws must be removed before the test. The next step would be setting the frame in the center of the compression machine and stating the test as shown in Figure 3.15

Figure 3.15 Modulus of elasticity test.

3.9 Specimen test setup

Two LVDT's (Linear variable differential transformer) shown in Figure 3.16, were placed under the tested specimen, one in the center of the specimen and the other one is located at 11 cm from the center. The LVDT's were attached to the frame of the test machine by magnetic base and connected to data logger.

Figure 3.16 LVDT.

The frame was centralized on the test machine carefully before testing and also LVTDs were adjusted and checked. A steel cubic column of dimensions 55×55 mm was placed in the center of the panel centralize the force.

A testing machine (Instron 5590R) with maximum capacity of 250 kN was used as shown in Figure 3.17, the details of the testing machine and specimen.

Figure 3.17 Testing machine.

The applied loading rate was 0.4 kN/sec. In all tests the machine was stopped after reaching the ultimate load and the machines jack was removed to allow more photographs of the final cracks and failure patterns to be taken.

When the test is finished, the sample was removed from the test machine and the crack lines were marked with red marker as shown in Figure 3.18, also the radius of failure was measured, then the sample was photographed and placed a side and another sample is placed on the test machine.

Figure 3.18 Sample of marking the tested panels.

CHAPTER FOUR

TEST RESULTS AND DISCUSSION

4.1 Introduction

Chapter 4 presents the test results of load-deformation behavior, modes of failure and residual punching shear. The results will be discussed in eight titles, which are load deformation behavior, materials properties, effect of steel fiber percentage on the ultimate slab strength, effect of heating exposure on the ultimate slab strength, effect of steel fiber percentage on slab tensile strength, effect of heating exposure on slab tensile strength, failure mode and ACI Comparison.

As mentioned earlier in a previous chapter the experimental work was divided into five groups (A, B, C, D and E) in which each group contains one panel without steel fiber and three panels of different percentages of steel fiber panels, Group E was at ambient conditions and the other four groups were subjected to heat exposure in furnace at a temperature (150, 300, 450 and 550 °C), the details of the group are shown in Table 4.1.

Table 4.1 Details of the groups.

Specimen	Steel fiber V_f (%)	Exposed Temperature °C	Slump	Density $kg/m3$
E1	0	Ambient condition	97	2.59
E2	0.75		68	2.48
E3	1		62	2.59
E4	1.25		58	2.62
A1	0	150	97	2.57
A2	0.75		68	2.45
A3	1		62	2.57
A4	1.25		58	2.58
B1	0	300	97	2.51
B2	0.75		68	2.48
B3	1		62	2.55
B4	1.25		58	2.64
C1	0	450	97	2.49
C2	0.75		68	2.51
C3	1		62	2.48
C4	1.25		58	2.52
D1	0	550	97	2.49
D2	0.75		68	2.60
D3	1		62	2.48
D4	1.25		58	2.61

4.2 Load-deformation behavior

The load-deflection curves was obtained from the two LVDT's beneath every slab in two positions located at the center and 10 cm from the center as shown in Figure 4.1.

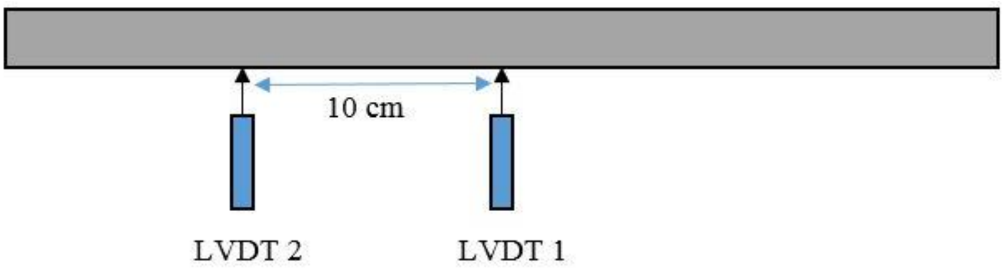

Figure 4.1 Location of the two LVDT's.

The results of the two LVDT's for groups E, A, B, C and D can be shown in Figure 4.2 to 4.11 in sequent for all tested specimens . Also deflection results of each group are presented in Table 4.1 to 4.5 in sequent.

Group E is the control group in ambient conditions, the deflection results can be seen in Table 4.2, Figure 4.2 and 4.3 indicates that when the specimens at ambient conditions, increasing the steel fiber dosages by 0.75% leads to lower deflection values, then by increasing the steel fiber dosages by 1% or 1.25% the deflection remain nearly similar to the specimen without steel fiber for the center LVDT except for specimen E3, for the second LVDT increasing the steel fiber dosages leads to lower deflection values.

Table 4.2 Deflection results of Group E two LVDT's.

Specimen	LVDT at the center $\delta_1^{(1)}$ (mm)	LVDT 10 cm from the center $\delta_2^{(1)}$ (mm)
E1	3.86179	2.80496
E2	3.66709	2.62106
E3	4.764281	2.01652
E4	4.00485	2.75839
δ are the displacement that corresponding to ultimate loads P_u.		

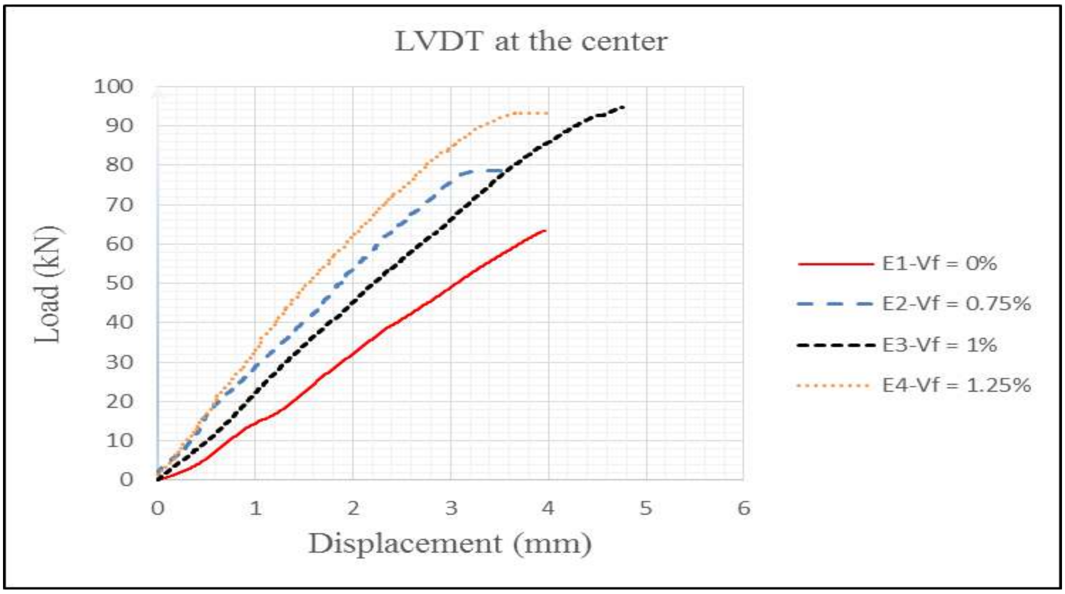

Figure 4.2 Load deflection of Group E, LVDT located at the center.

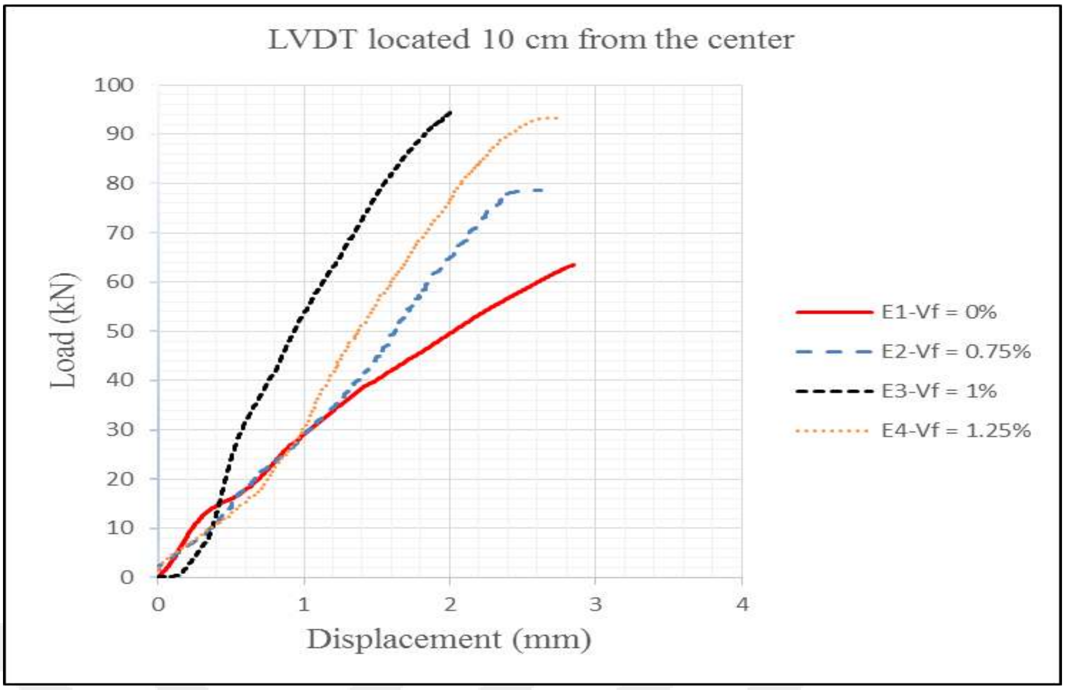

Figure 4.3 Load deflection of Group E, LVDT located 10 cm from the center.

For Group A, the deflection results can be seen in Table 4.3 and Figure 4.4 indicates that when the burning temperature is constant 150 °C, increasing the steel fiber dosages causes lower deflection values as it can be seen in the result of the LVDT located at the center. The same behavior can be seen in second LVDT as shown in Figure 4.5.

Table 4.3 Deflection results of Group A two LVDT's.

Specimen	LVDT at the center δ_1 (mm)	LVDT 10 cm from the center δ_2 (mm)
A1	3.98575	2.82953
A2	3.78688	2.72052
A3	3.52290	2.51071
A4	2.76307	2.03160

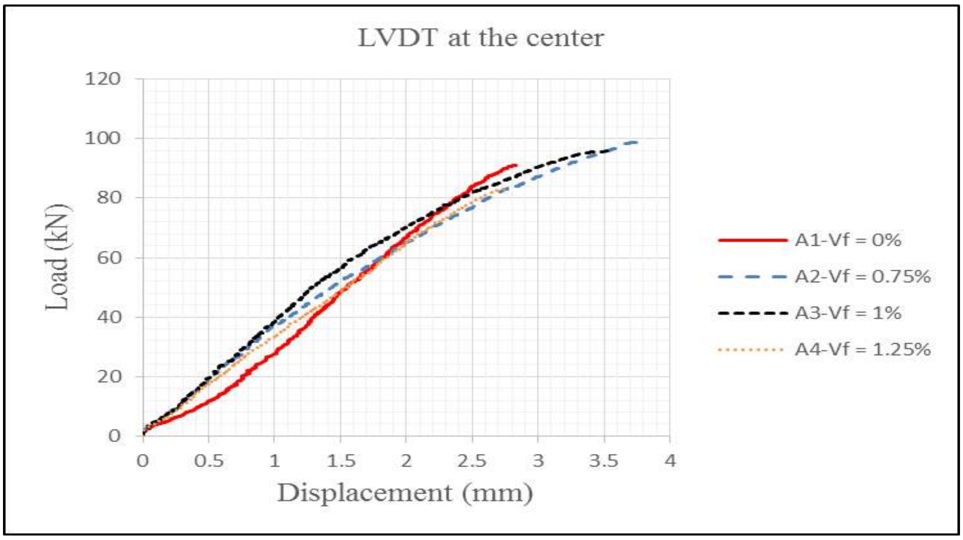

Figure 4.4 Load deflection of Group A, LVDT located at the center.

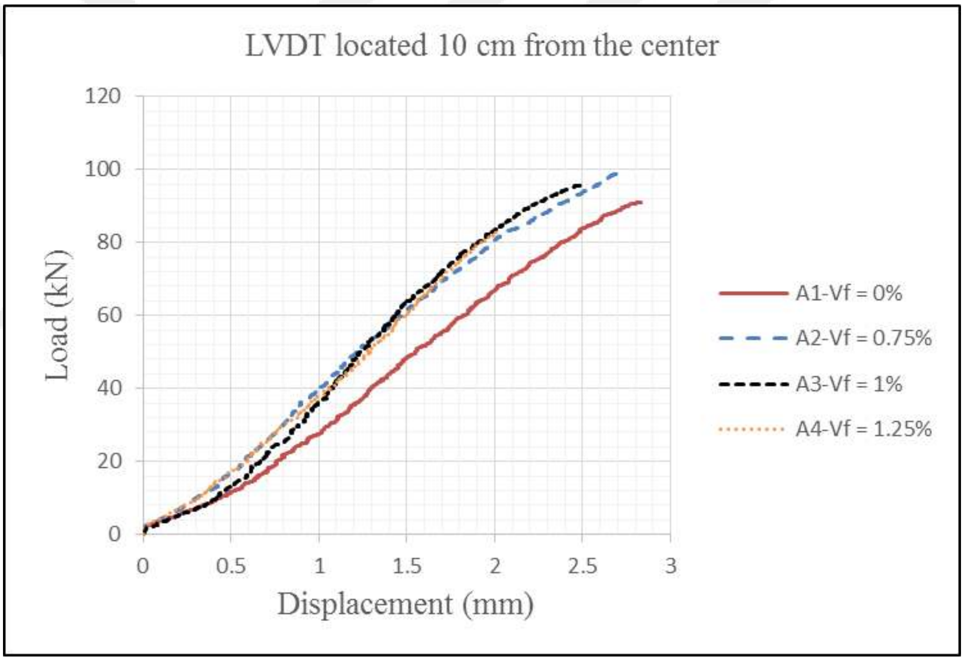

Figure 4.5 Load deflection of Group A, LVDT located 10 cm from the center.

As shown in Figures 4.3 and 4.4 the deflection curve starts similarly in all specimen of group A for the first 15 kN of loading for almost 10 minutes then it diverges giving different results.

For Group B, the deflection results can be seen in Table 4.4, Figure 4.6 shows that when the burning temperature is constant 300 °C, increasing the steel fiber dosages causes higher deflection values, as it can be seen in the result of the LVDT located at the center. The same behavior can be seen for second LVDT as shown in Figure 4.7 except for specimen B2.

Table 4.4 Deflection results of group B two LVDT's.

Specimen	LVDT at the center δ_1 (mm)	LVDT 10 cm from the center δ_2 (mm)
B1	3.80682	3.07520
B2	3.97427	2.97347
B3	4.31717	3.37667
B4	4.78159	3.38602

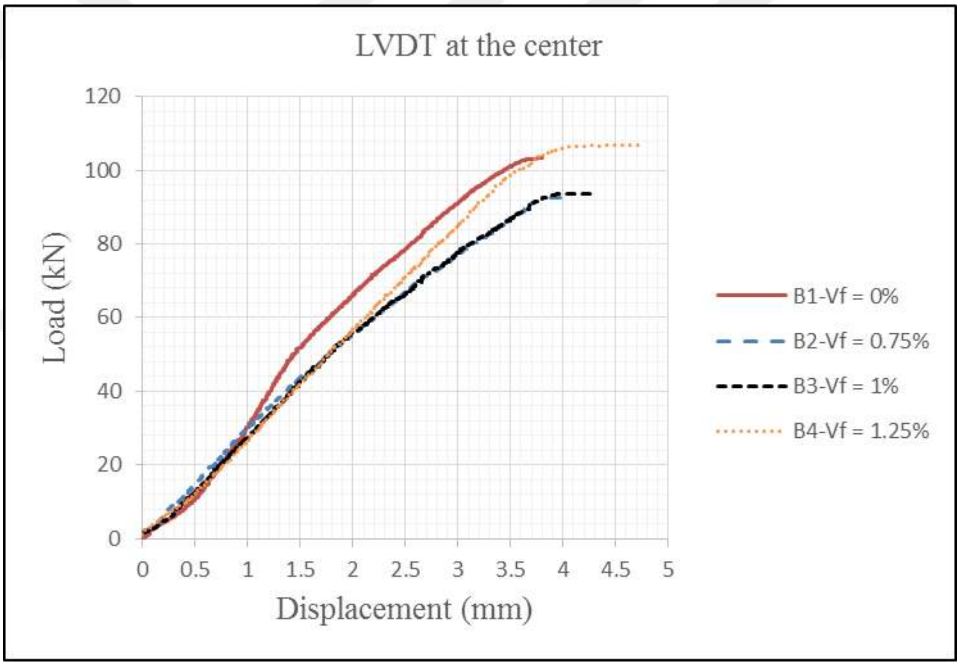

Figure 4.6 Load deflection of Group B, LVDT located at the center.

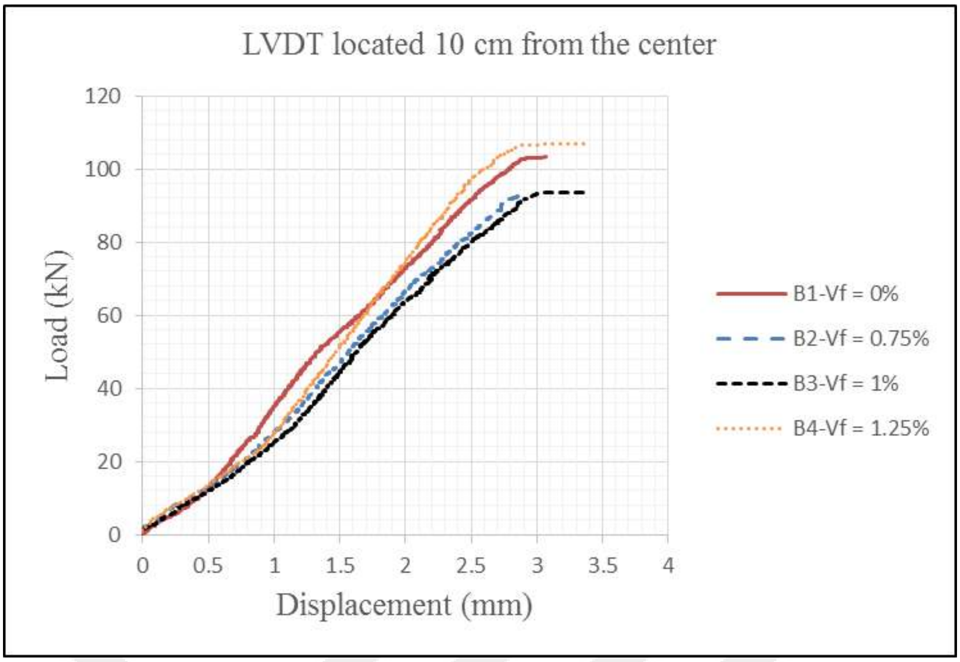

Figure 4.7 Load deflection of Group B, LVDT located 10 cm from the center.

AS shown in Figures 4.6 and 4.7 the deflection curve starts similarly in all specimens of Group B for the first 20 KN of loading for almost 20 minutes then it diverges giving different results.

For Group C, the deflection results can be seen in Table 4.5, Figure 4.8 and 4.9 indicates that when the burning temperature is constant 450 °C, increasing the steel fiber dosages causes slightly lower deflection values, as it can be seen in the result of the two LVDT's

Table 4.5 Deflection results of Group C two LVDT's.

Specimen	LVDT at the center δ_1 (mm)	LVDT 10 cm from the center δ_2 (mm)
C1	5.75679	4.25467
C2	5.93240	4.51580
C3	4.85120	3.62110
C4	5.65550	4.36300

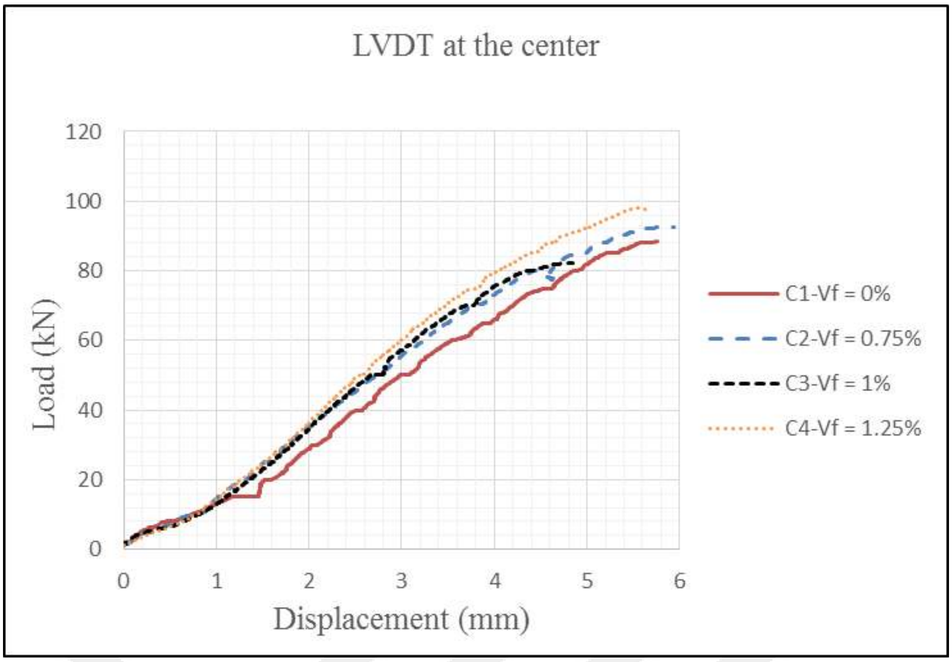

Figure 4.8 Load deflection of Group C, LVDT located at the center.

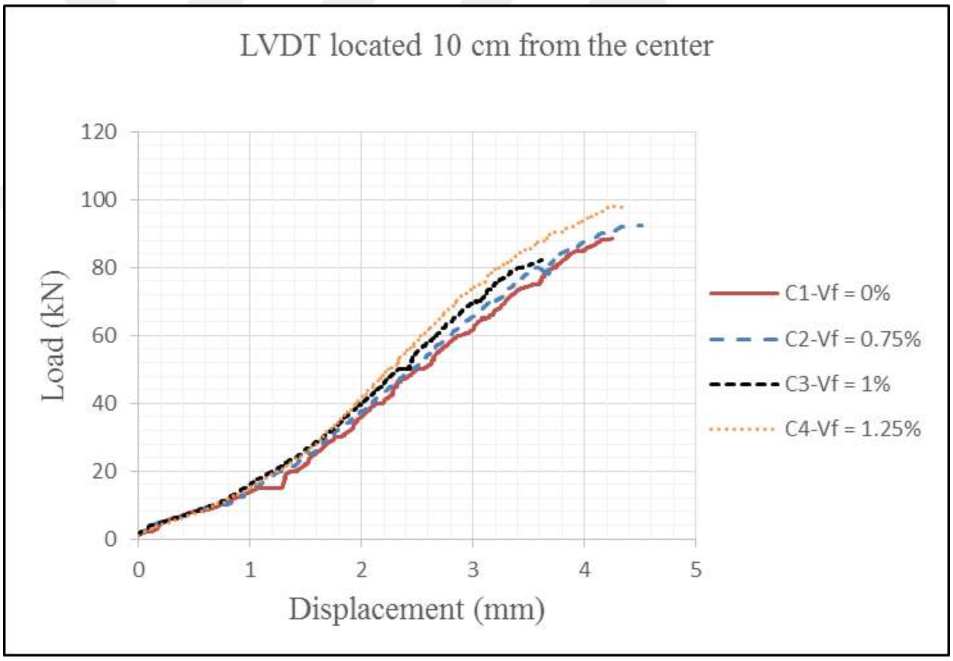

Figure 4.9 Load deflection of Group C, LVDT located 10 cm from the center.

As shown in Figures 4.8 and 4.9 the deflection curve starts similarly in all specimens of Group C for the first 20 kN of loading for almost 12 minutes then it diverge giving different results.

For Group D, the deflection results can be seen in Table 4.6, Figure 4.10 and 4.11 indicates that when the burning temperature is constant 550 °C, adding steel fiber doesn't affect the deflection values by a noticeable amount, as it can be seen in the result of the two LVDT's.

Table 4.6 Deflection results of Group D two LVDT's.

Specimen	LVDT at the center δ_1 (mm)	LVDT 10 cm from the center δ_2 (mm)
D1	4.69890	3.07919
D2	6.15660	4.21760
D3	3.24478	4.50893
D4	4.75944	3.43695

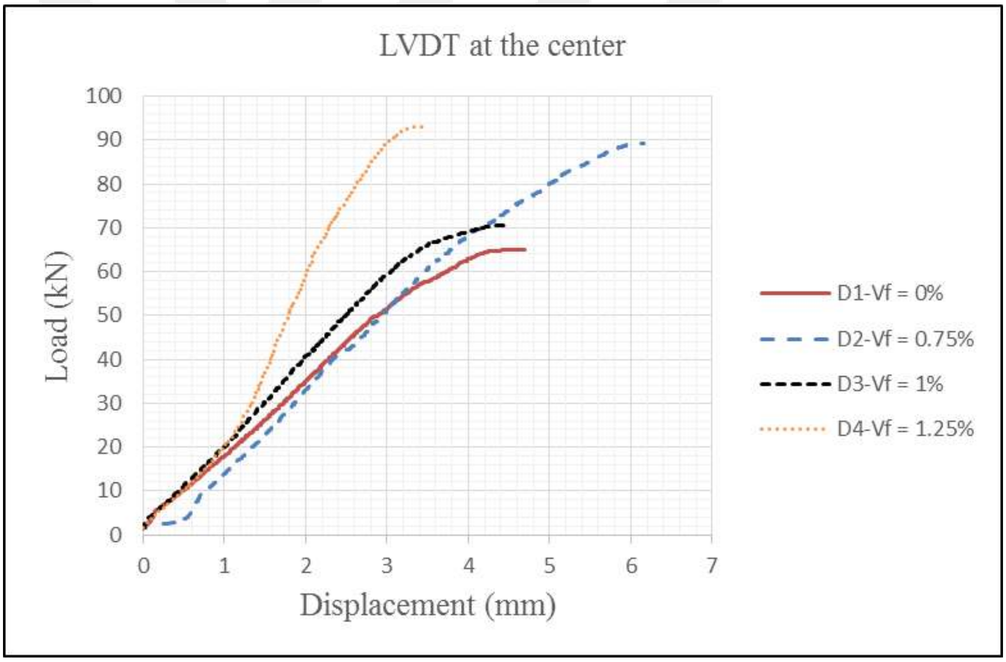

Figure 4.10 Load deflection of Group D, LVDT located at the center.

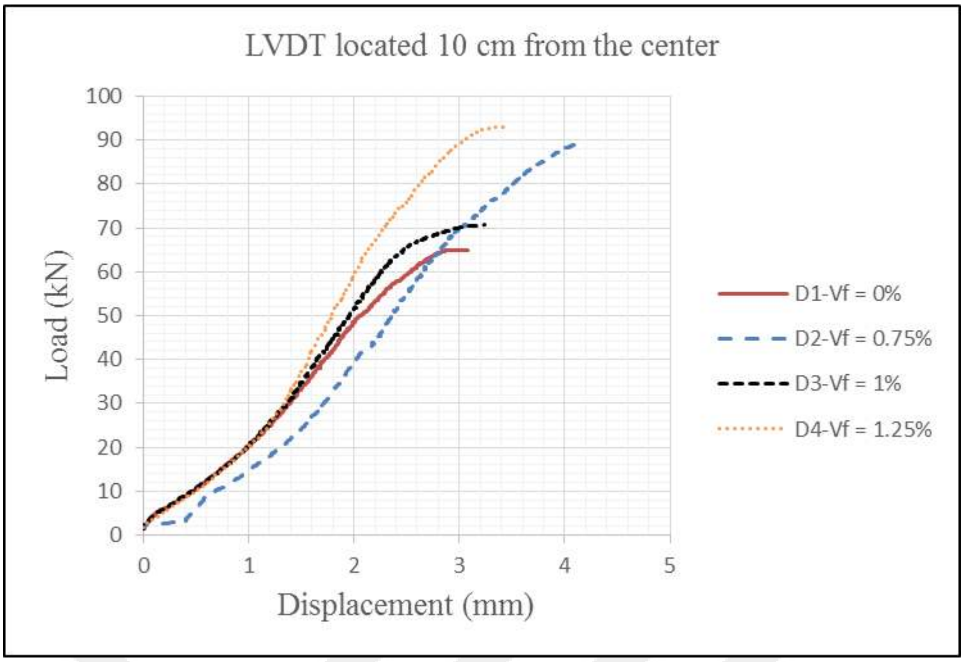

Figure 4.11 Load deflection of Group D, LVDT located 10 cm from the center.

As shown in Figure 4.10 the deflection curve starts similarly in all specimens of Group D for almost the first 32 KN of loading for nearly 15 minutes except specimen D4 which diverge after the 32 kN loading giving different path.

Figure 4.12 shows center LVDT values of deflection comparing with the control specimen for (E1 (control specimen), A1, B1, C1 and D1) which consists of the same mixture (no steel fiber addition) the specimens were at (ambient condition, 150°C, 300°C, 450 °C and 550 °C) respectively. It shows that for 150 °C heat exposure the deflection is slightly increased but almost constant, for 300 °C heat exposure the deflection is slightly decreased but almost constant, for 450 °C and 550 °C heat exposure the deflection values were increased significantly.

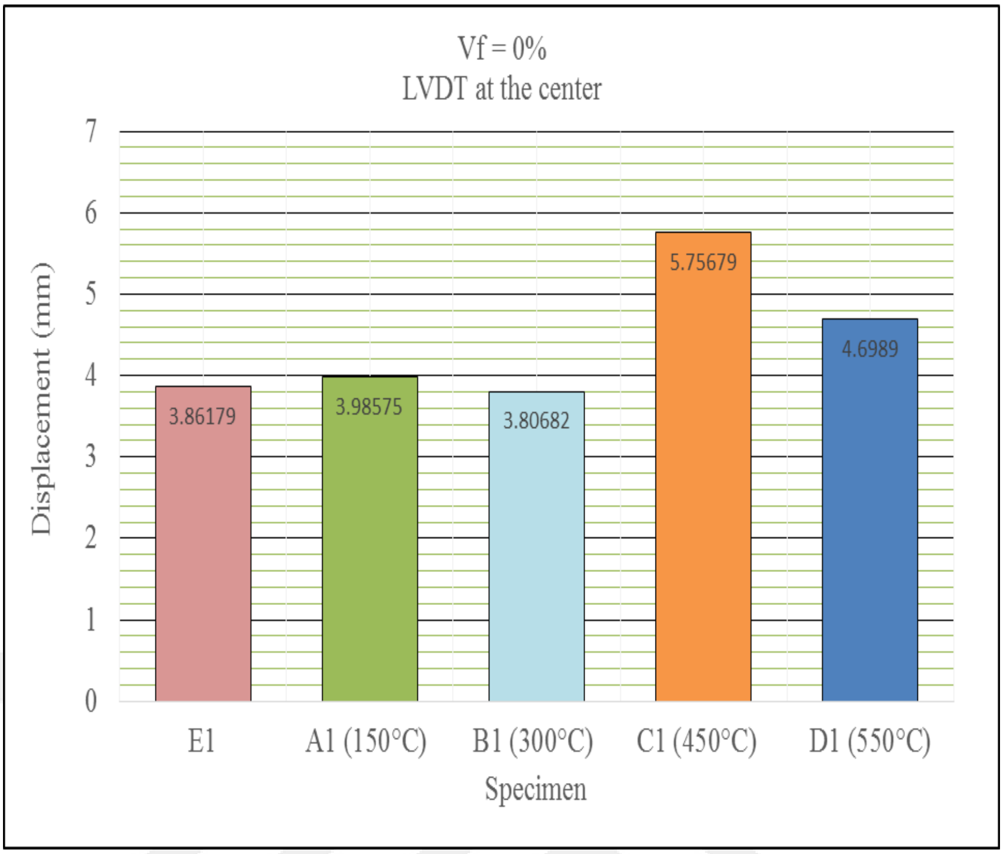

Figure 4.12 Deflection values of LVDT located at the center for the specimens consists of the same mixture (V_f = 0%) at different temperature.

Figure 4.13 shows LVDT located 10 cm from the center values of deflection comparing with the control specimen for (E1 (control specimen), A1, B1, C1 and D1) which consist of the same mixture (no steel fiber addition) the specimens were at (ambient condition, 150 °C, 300 °C, 450 °C and 550 °C) respectively. It shows that for 150 °C, 450 °C and 550 °C heat exposure the deflection is slightly increased but almost constant, for 300 °C heat exposure the deflection was increased significantly.

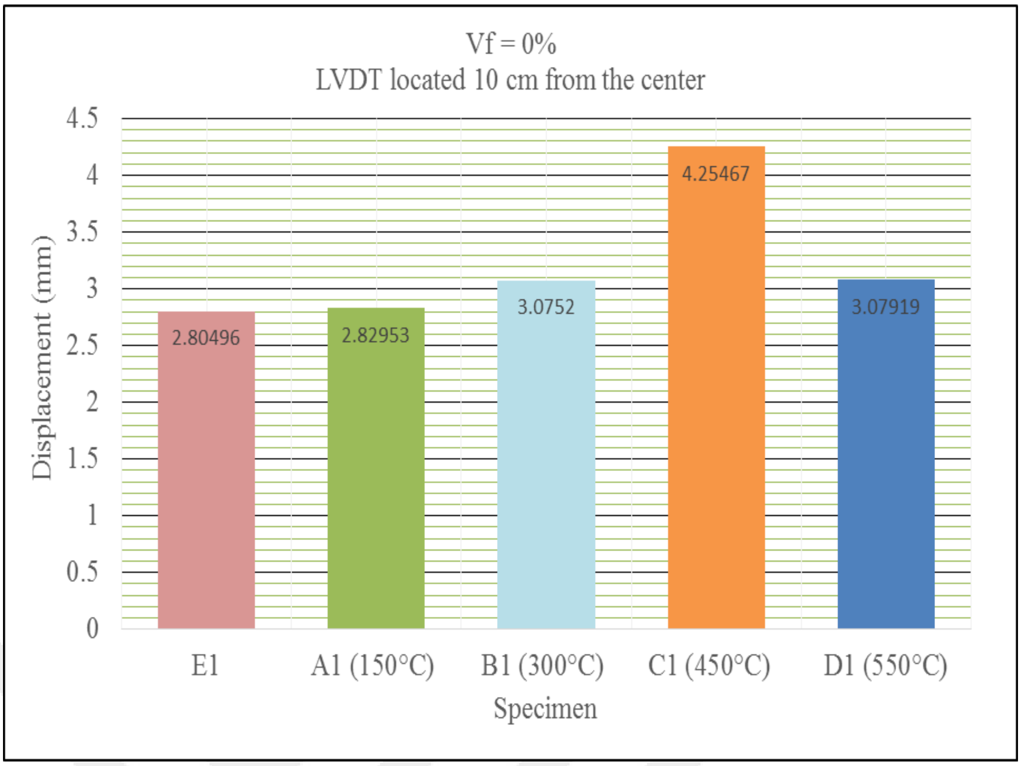

Figure 4.13 Deflection values of LVDT located at 10 cm from the center for the specimens consist of the same mixture ($V_f = 0\%$) at different temperature.

Figure 4.14 shows center LVDT values of deflection comparing with the control specimen for (E2 (control specimen), A2, B2, C2 and D2) which consist of the same mixture (0.75% steel fiber addition) the specimens were at (ambient condition, 150 °C, 300 °C, 450 °C and 550 °C) respectively. It shows that for 150°c and 300 °C heat exposure the deflection is slightly increased but almost constant, for 450 °C and 550 °C heat exposure the deflection values were increased significantly. The same results of Figure 4.14 can be seen in Figure 4.15.

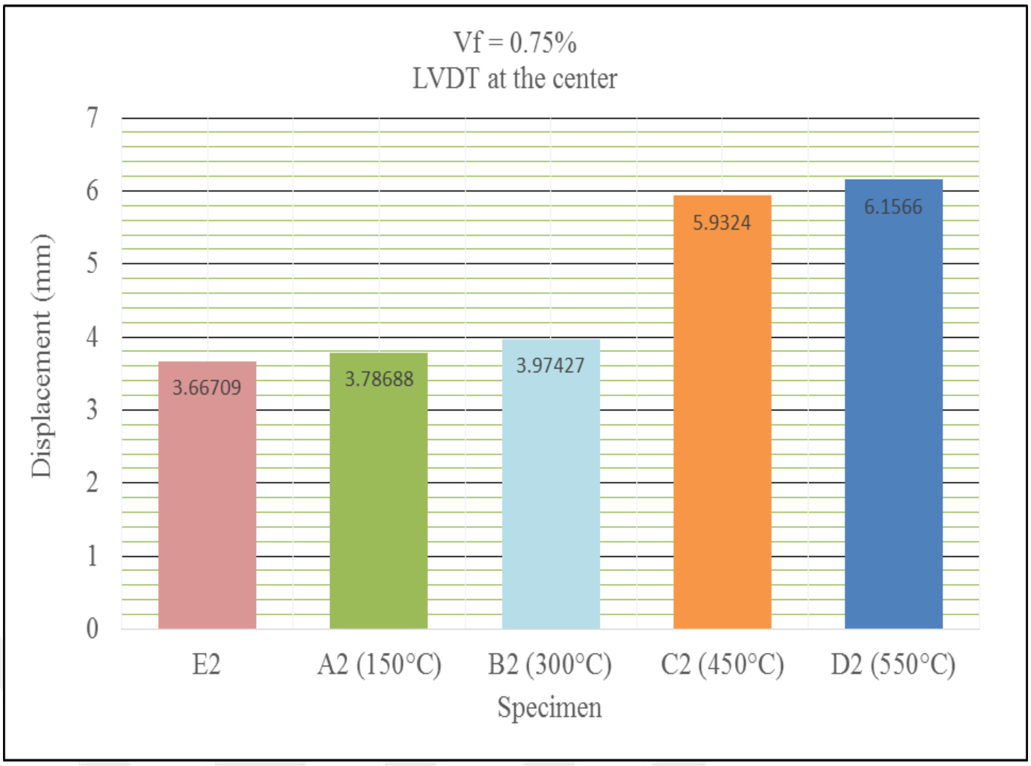

Figure 4.14 Deflection values of LVDT located at the center for the specimens consist of the same mixture (V_f = 0.75%) at different temperature.

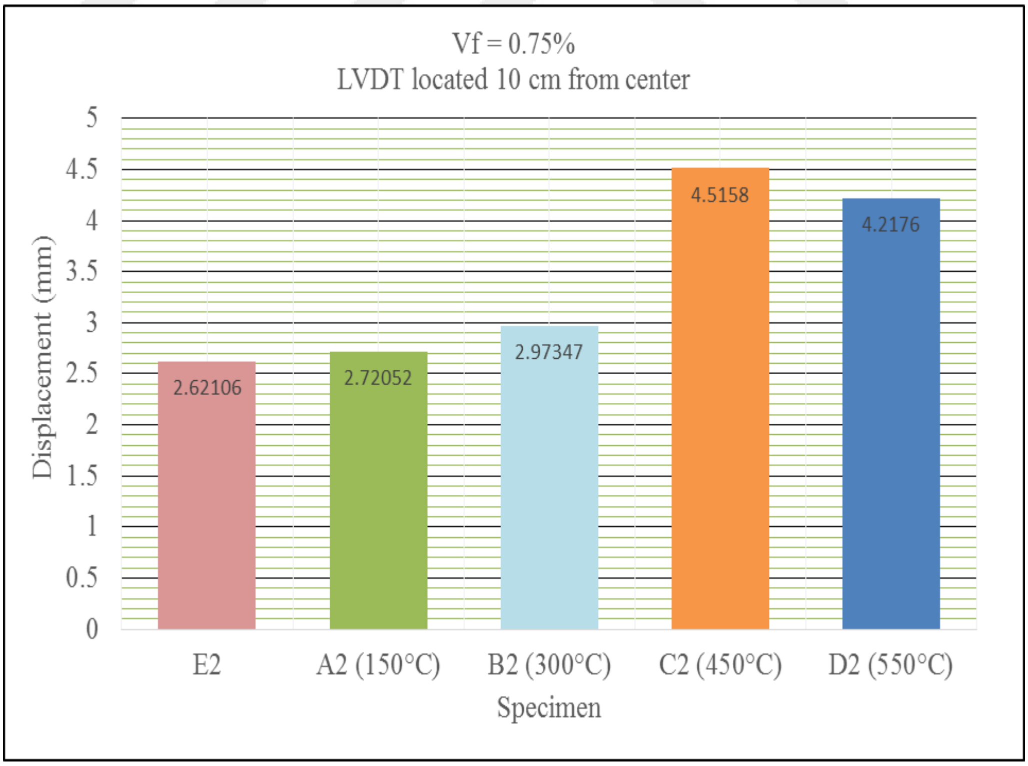

Figure 4.15 Deflection values of LVDT located at 10 cm from the center for the specimens consist of the same mixture (V_f = 0.75%) at different temperature.

Figure 4.16 shows center LVDT values of deflection comparing with the control specimen for (E3 (control specimen), A3, B3, C3 and D3) which consist of the same mixture (1% steel fiber addition) the specimens were at (ambient condition, 150 °C, 300 °C, 450 °C and 550 °C) respectively. It shows that for 150 °C, 300 °C and 450 °C heat exposure the deflection is decreased significantly except at 550 °C, it slightly increased.

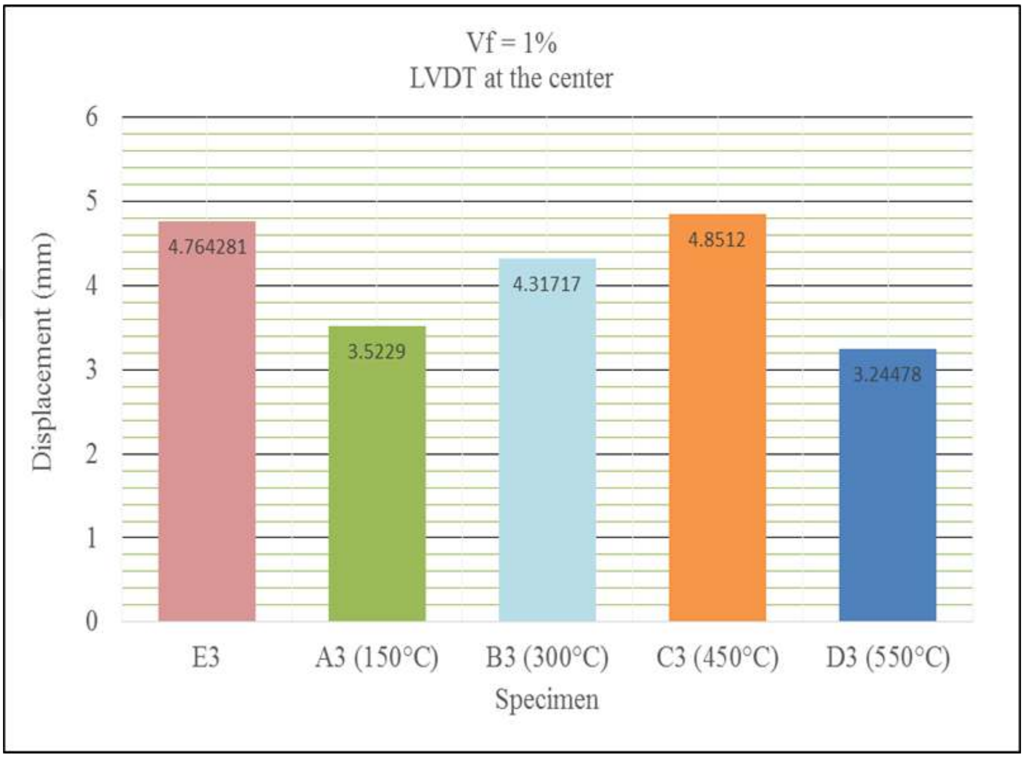

Figure 4.16 Deflection values of LVDT located at the center for the specimens consist of the same mixture (V_f = 1%) at different temperature.

Figure 4.17 shows LVDT located 10 cm from the center values of deflection comparing with the control specimen for E3 (control specimen), A3, B3, C3 and D3) which consist of the same mixture (no steel fiber addition) the specimens were at (ambient condition, 150 °C, 300 °C, 450 °C and 550 °C) respectively. It shows that for 150 °C heat exposure the deflection value is slightly increased but almost constant, for 300 °C, 450 °C and 550 °C heat exposure the deflection was increased significantly.

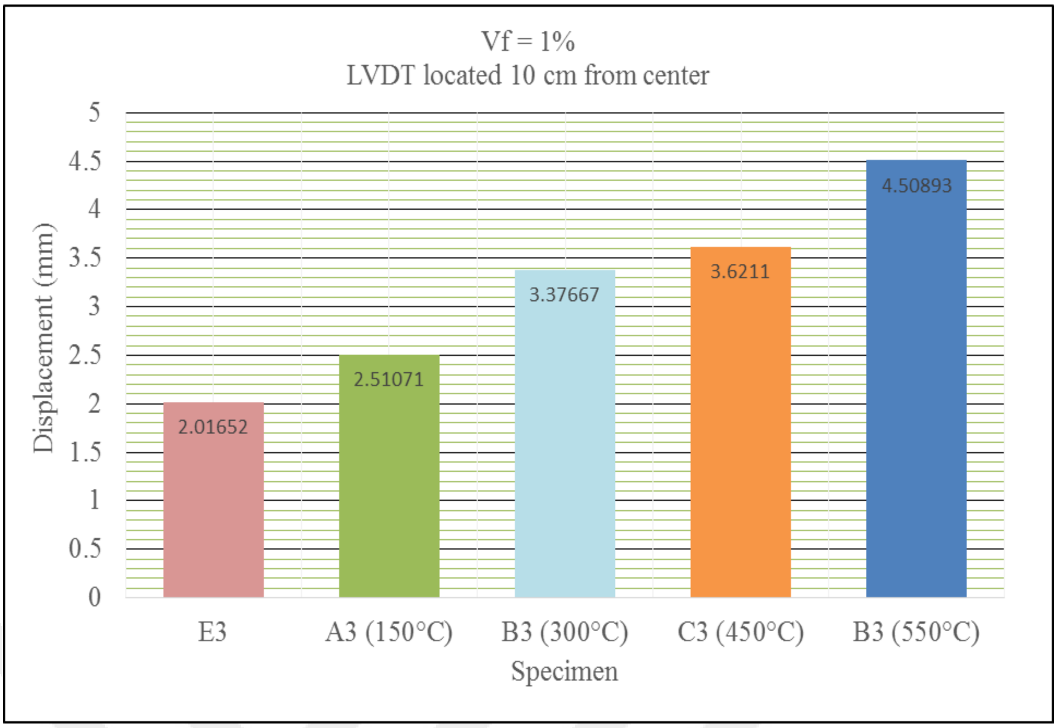

Figure 4.17 Deflection values of LVDT located at 10 cm from the center for the specimens consist of the same mixture (V_f = 1%) at different temperature.

Figure 4.18 shows center LVDT values of deflection comparing with the control specimen for E4 (control specimen), A4, B4, C4 and D4 which consist of the same mixture (1.25% steel fiber addition) the specimens were at (ambient condition, 150 °C, 300 °C, 450 °C and 550 °C) respectively. It shows that for 150 °C heat exposure the deflection is slightly decreased but almost constant, for 300 °C, 450 °C and 550 °C heat exposure the deflection was increased significantly. The same results of Figure 4.18 can be seen in Figure 4.19.

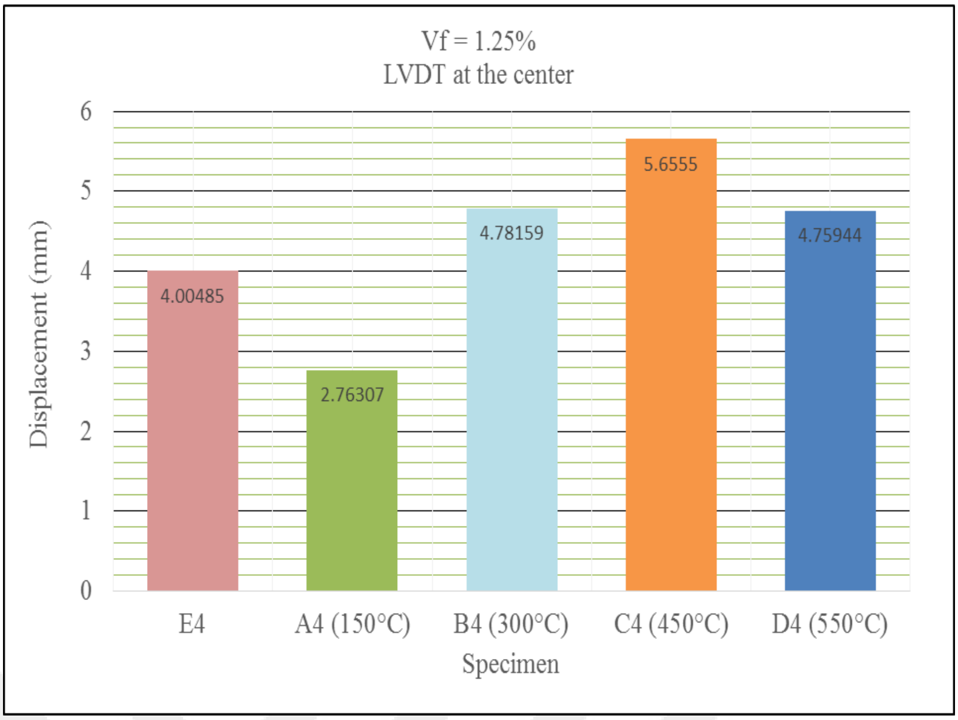

Figure 4.18 Deflection values of LVDT located at the center for the specimens consist of the same mixture (V_f = 1.25%) at different temperature.

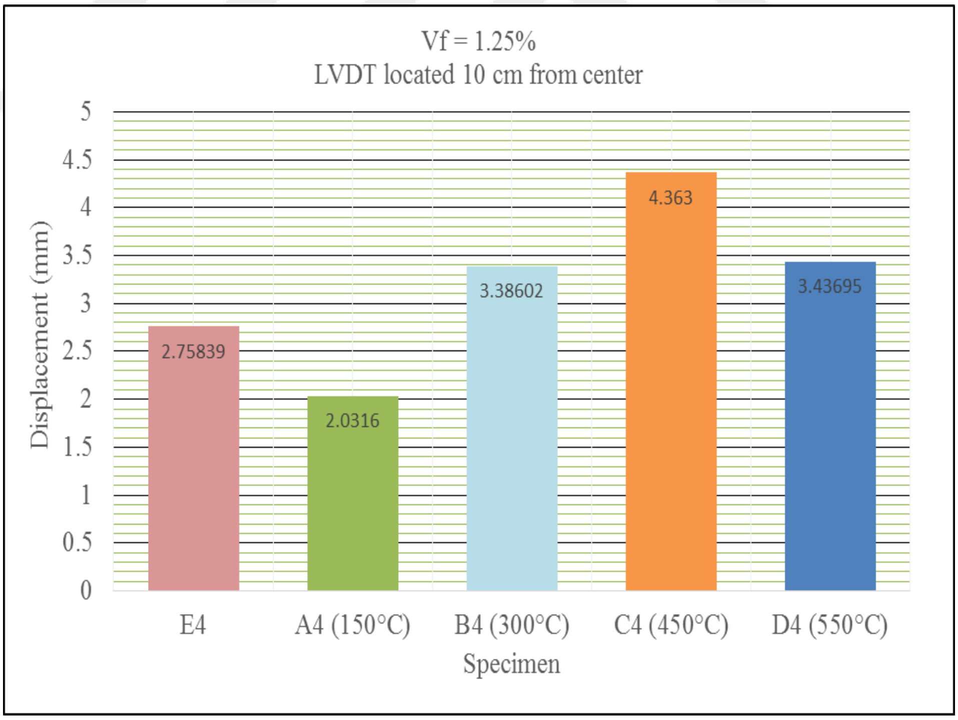

Figure 4.19 Deflection values of LVDT located at 10 cm from the center for the specimens consist of the same mixture (V_f = 1.25%) at different temperature.

4.3 Materials Properties

Table 4.7 shows the results of experimental standard cylinders of the control Group E at ambient conditions and the other four groups A, B, C and D that were tested to calculate the compressive strength (f'_c), according to ASTM C39 (ASTM C39, 1997), splitting tensile strength (f_{sp}) according to ASTM C496 (ASTM C496, 2004), and static Young's modulus according to ASTM C469 (ASTM C469, 2002).

Table 4.7 Concrete mechanical properties.

Spec. No.	Steel fiber V_f (%)	f'_c (MPa)	f_{sp} (MPa)	E_c (GPa)	Exposed temperature °C
E1	0	53	6.17	38.13	ambient condition
E2	0.75	51	6.76	37.27	
E3	1	60	8.61	37.32	
E4	1.25	59	7.00	37.41	
A1	0	63	6.17	33.213	150
A2	0.75	60	9.21	31.221	
A3	1	71	8.61	-	
A4	1.25	65	7.97	38.37	
B1	0	51	5.28	37.82	300
B2	0.75	55	6.55	20.93	
B3	1	64	8.83	21.50	
B4	1.25	61	8.26	23.78	
C1	0	34	3.96	10.73	450
C2	0.75	46	6.87	9.64	
C3	1	47	6.48	9.98	
C4	1.25	49	8.03	10.53	
D1	0	24	2.85	5.39	550
D2	0.75	39	5.02	5.86	
D3	1	32	5.49	4.32	
D4	1.25	30	4.53	4.07	

4.3.1 Compressive strength

It can be noticed that the steel fiber has a significant improving effect on the (f'_c) in Groups E, A, B, C and D that exposed to room temperature, 150 °C, 300, °C 450 °C and 550 °C in sequent.

For Group E the addition of steel fibers in concrete significantly improved the (f'_c) of specimens with 1% and 1.25% by nearly 13% and 11% respectively, however using 0.75 % of steel fiber, didn't improve the (f'_c) as it shown in Figure 4.20.

For Group A the addition of steel fibers in concrete significantly improved the (f'_c) of specimens with 1% and 1.25% by nearly 13% and 3% respectively, however using 0.75 % of steel fiber, didn't improve the (f'_c) as it shown in Figure 4.21.

For Group B the addition of steel fibers in concrete significantly improved the (f'_c) of specimens with 0.75, 1% and 1.25% by nearly 8%, 25% and 20% respectively, as it shown in Figure 4.22.

The compressive strength was improved in Group C using 0.75 %, 1% and 1.25% of steel fiber by nearly 35%, 37% and 44%) respectively, as shown in Figure 4.23.

For Group D the addition of steel fibers in concrete significantly improved (f'_c) of specimen with 0.75%, 1% and 1.25% by nearly 62%, 33% and 25%) respectively as shown in Figure 4.24.

Lots of codes have been relying on the square root of compressive strength (for example ACI 318), which presented good example of punching shear for specimens of reinforcement ratio $\rho > 0.5$, therefore, $\sqrt{f'_c}$ is used here to evaluate the strength of specimens in this work. Furthermore, $\sqrt{f'_c}$ is relating to splitting tensile strength form of $f_{sp}=k\sqrt{f'_c}$, where k is a constant.

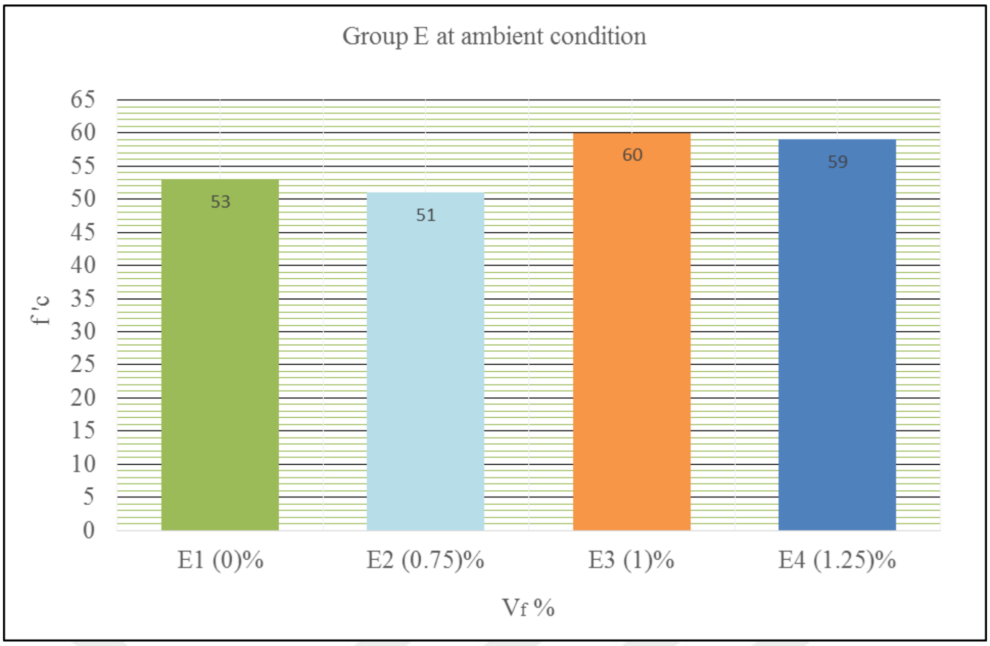

Figure 4.20 The effect of steel fiber dosages on the compressive strength (Group E).

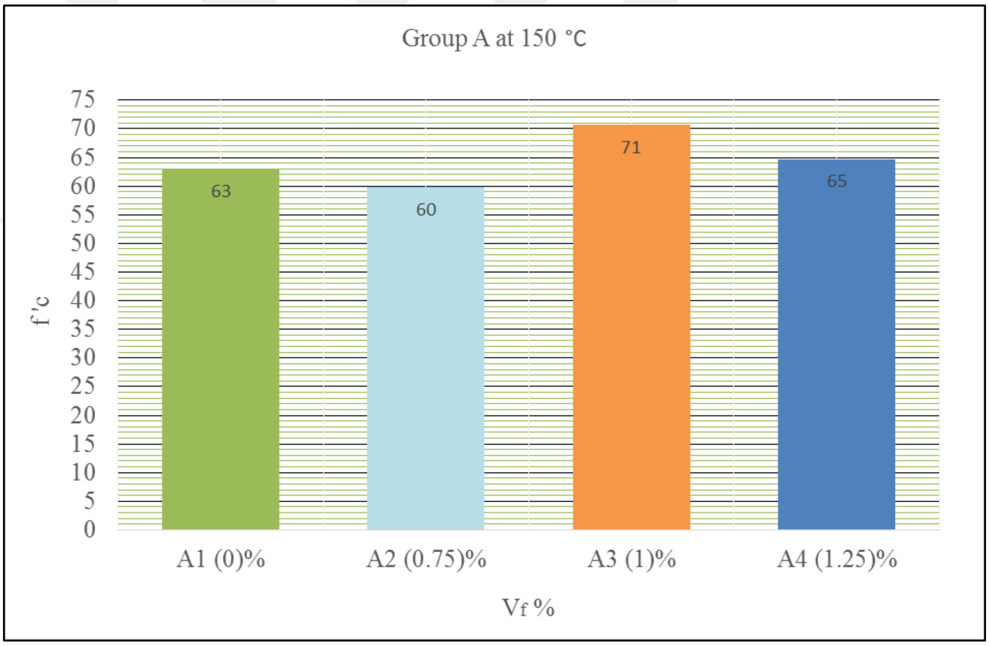

Figure 4.21 The effect of steel fiber dosages on the compressive strength (Group A).

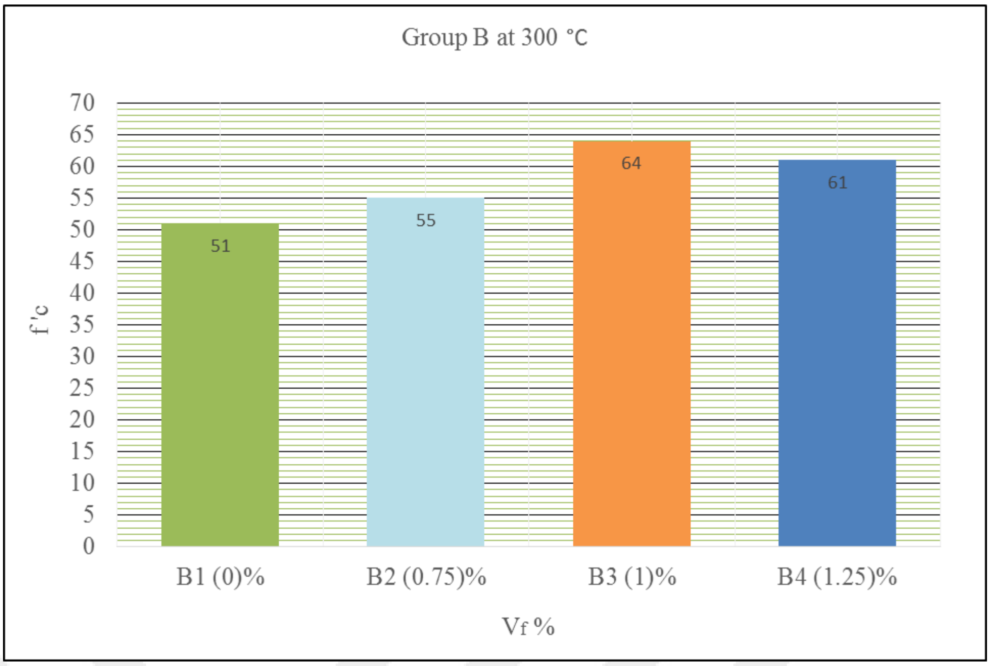

Figure 4.22 The effect of steel fiber dosages on the compressive strength (Group B).

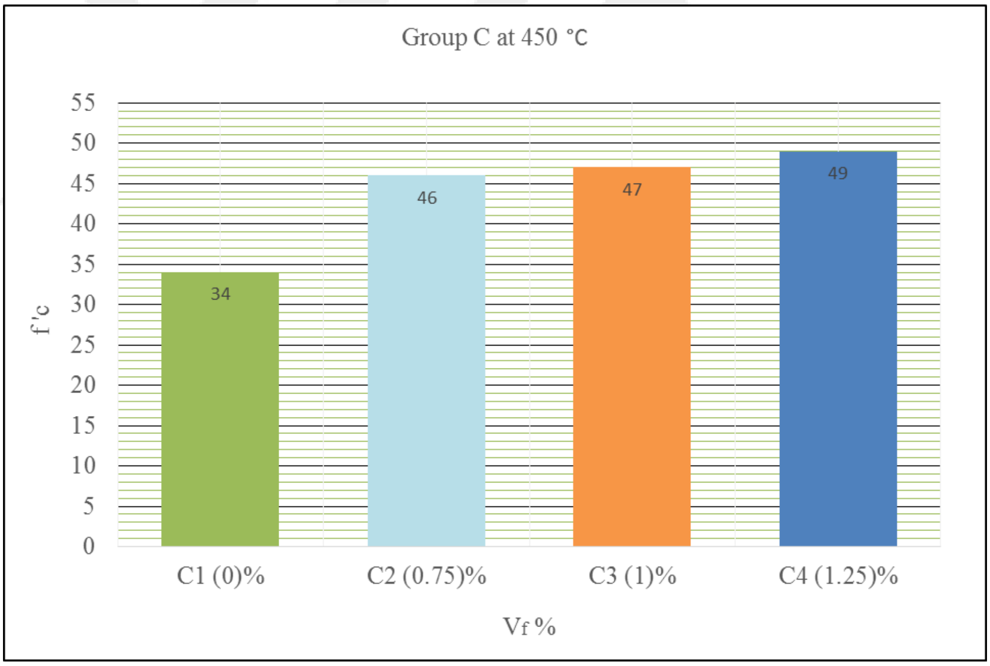

Figure 4.23 The effect of steel fiber dosages on the compressive strength (Group C).

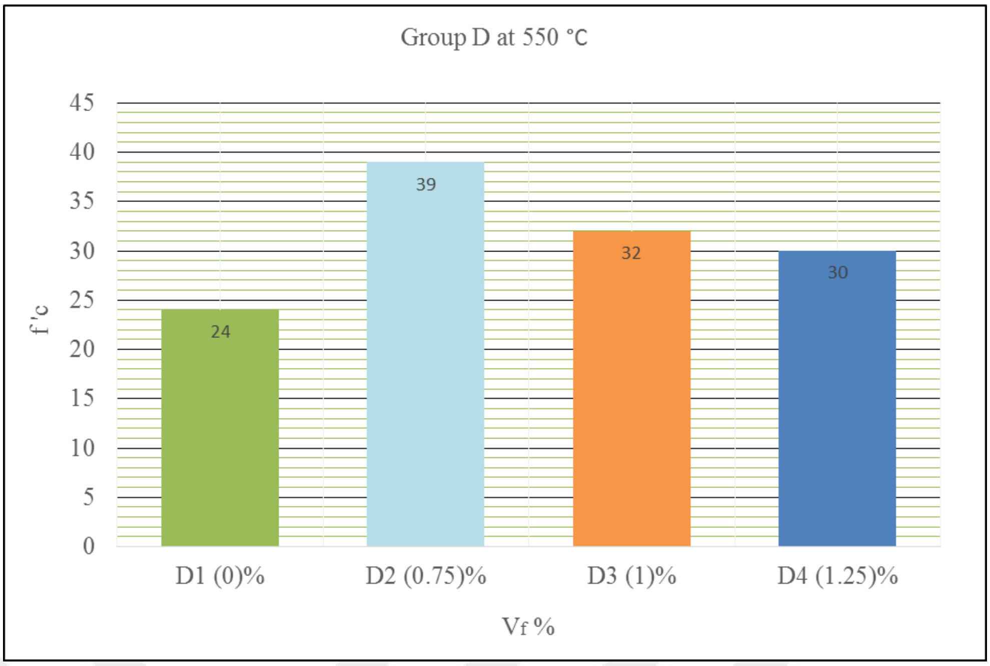

Figure 4.24 The effect of steel fiber dosages on the compressive strength (Group D).

4.3.2 Tensile strength

In general it can be noticed that the steel fiber has a significant improving effect on the tensile strength in groups E, A, B, C and D that exposed to room temperature, 150 °C, 300, °C 450 °C and 550 °C in sequent. Tensile strength will be discussed extensively and separately for each group later in this chapter.

4.3.3 Modulus of elasticity

There's no noticeable improvement on the modulus of elasticity.

4.4 Ultimate slab strength

4.4.1 Effect of steel fiber percentage on the ultimate slab strength

Table 4.8 is a brief of the ultimate slab strength and the failure modes, it is shown for Group E that the addition of 0.75%, 1% and 1.25% steel fibers in concrete significantly improved the ultimate slab strength for all specimens by nearly 24%, 49% and 47% respectively, as shown in Figure 4.25.

Also it shows for Group A that the addition of 0.75% and 1% steel fibers in concrete significantly improved the ultimate slab strength of specimen by nearly 8% and 5% respectively, however using 1.25 % of steel fiber, didn't improve the behavior of the slab as shown in Figure 4.26.

For Group B the addition of steel fibers in concrete significantly improved the ultimate slab strength of specimen with 1.25% (nearly 3%), on the contrary 0.75% and 1% of steel fiber, didn't improve the behavior of the slab as shown in Figure 4.27.

The ultimate slab strength was improved nearly 4.5% and 11% in Group C using 0.75 % and 1.25% of steel fiber respectively, however using 1% of steel fiber, didn't improve the behavior of the slab as shown in Figure 4.28.

For Group D the addition of 0.75%, 1% and 1.25% steel fibers in concrete significantly improved the ultimate slab strength of specimen by nearly 37%, 8.7% and 43%) respectively as shown in Figure 4.29.

Table 4.8 Experimental ultimate slab strength results.

Specimen	Steel fiber V_f (%)	P_u (kN)	Exposed temperature °C
E1	0	63.41	ambient condition
E2	0.75	78.80	
E3	1	94.77	
E4	1.25	93.28	
A1	0	91.09	150
A2	0.75	98.95	
A3	1	95.81	
A4	1.25	82.86	
B1	0	103.23	300
B2	0.75	92.44	
B3	1	93.66	
B4	1.25	106.88	
C1	0	88.49	450
C2	0.75	92.48	
C3	1	82.08	
C4	1.25	98.05	
D1	0	64.98	550
D2	0.75	89.22	
D3	1	70.64	
D4	1.25	93.09	

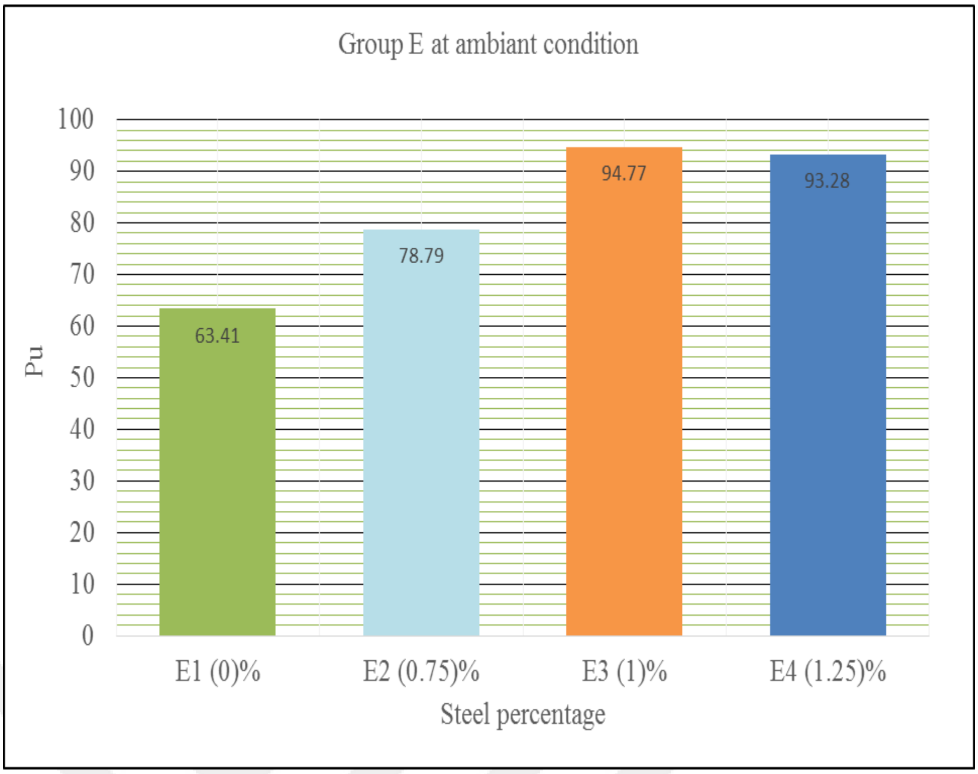

Figure 4.25 The effect of steel fiber dosages on the ultimate slab strength (Group E).

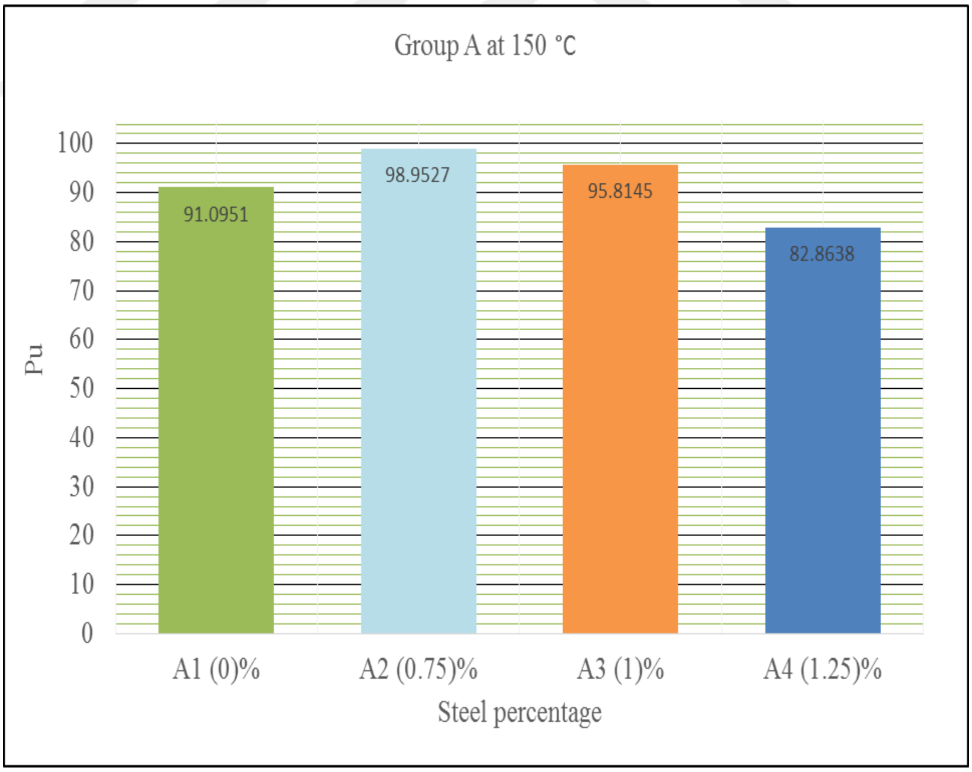

Figure 4.26 The effect of steel fiber dosages on the ultimate slab strength (Group A).

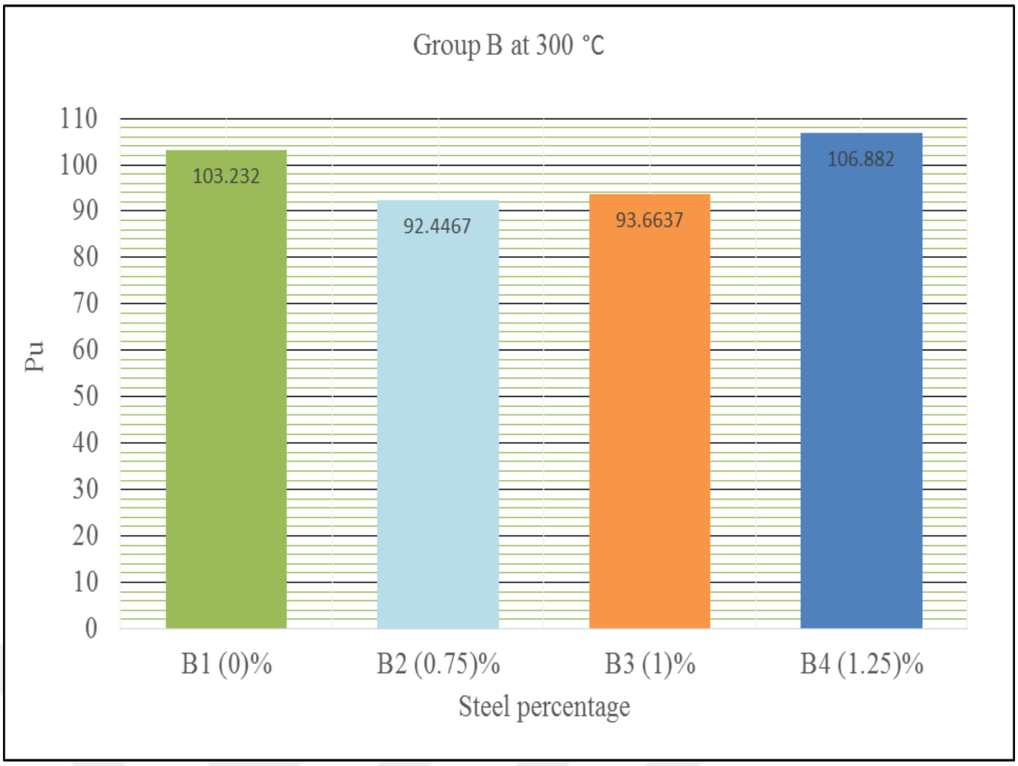

Figure 4.27 The effect of steel fiber dosages on the ultimate slab strength (Group B).

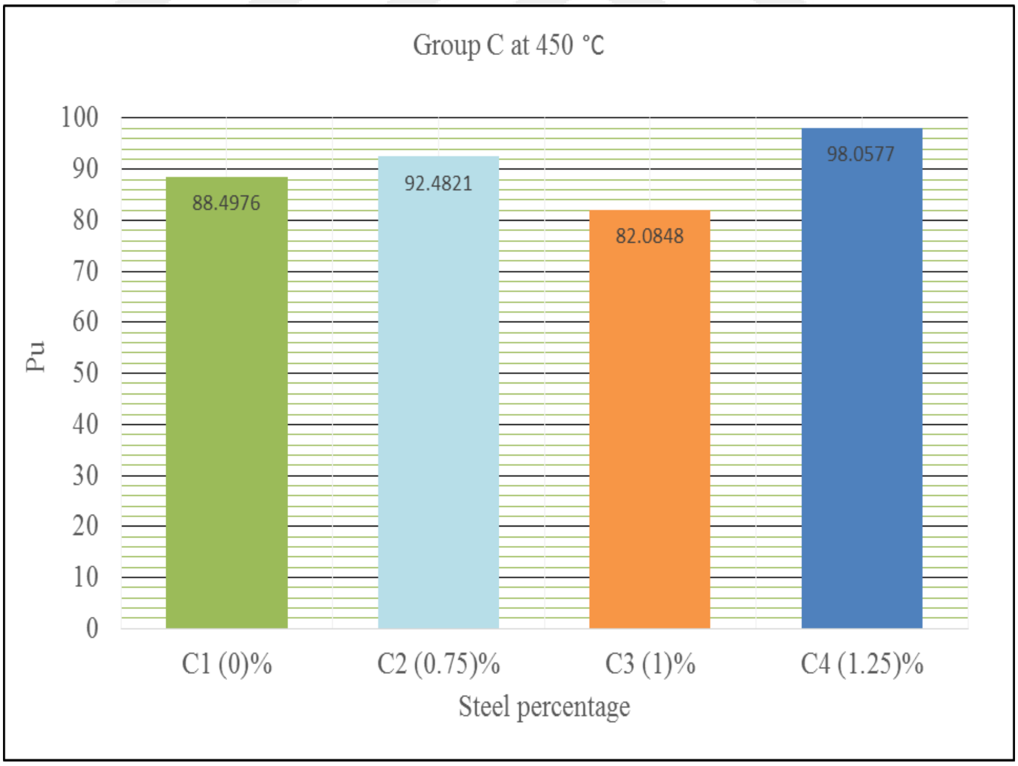

Figure 4.28 The effect of steel fiber dosages on the ultimate slab strength (Group C).

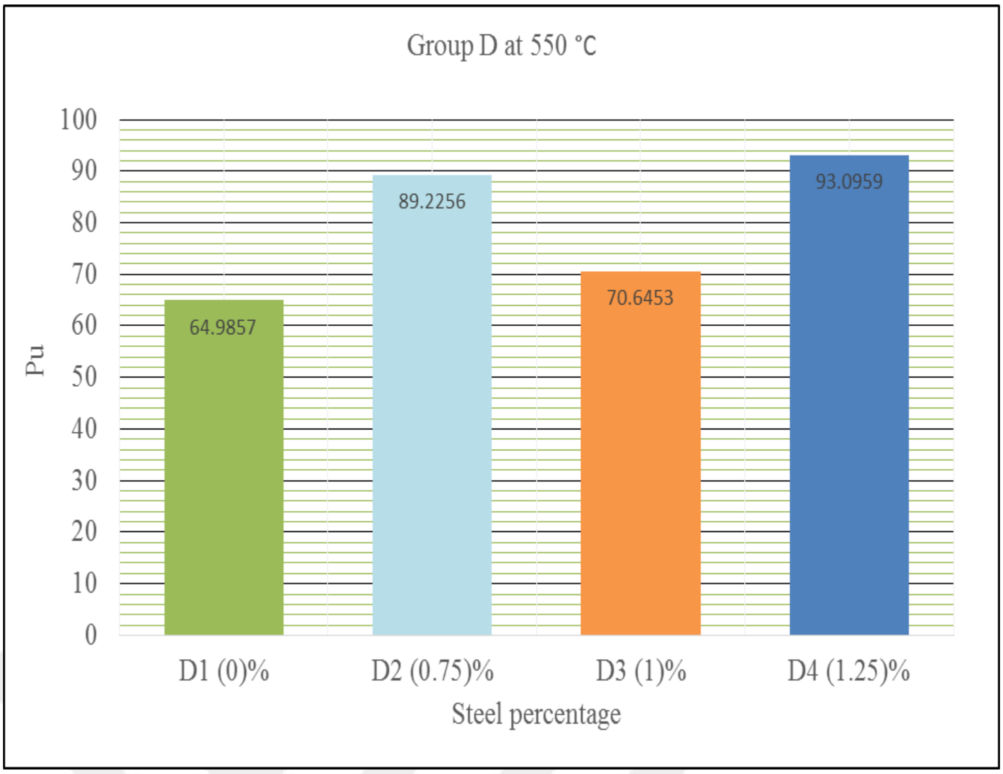

Figure 4.29 The effect of steel fiber dosages on the ultimate slab strength (Group D).

4.4.2 Effect of heating exposure on the ultimate slab strength

Taking in consideration the effect of heat exposure on the ultimate slab strength. The ultimate slab resistance for the similar slabs consists of the same mixture in different temperatures is presented in Table 4.8.

As a comparison between the ambient condition and different temperature, for the slabs without the addition of steel fiber E1, A1, B1, C1 and D1 (ambient condition, 150 °C 300 °C, 450 °C and 550 °C) in sequent, the ultimate strength was improved for A1, B1, C1 and D1 by (nearly 43%, 62% and 39%) respectively, however for D1 it was almost constant with an increase nearly 2% as shown in Figure 4.30 and Figure 4.31.

For the slabs with 0.75% addition of steel fiber E2, A2, B2, C2 and D2 (ambient condition, 150°C 300°C, 450°C and 550°C) in sequent, the ultimate strength was improved for A2, B2, C2 and D2 by (nearly 25.5%, 17%, 17% and 13%) respectively, as shown in Figure 4.32 and Figure 4.33.

For the slabs with 1% addition of steel fiber E3, A3, B3, C3 and D3 (ambient condition, 150°C 300°C, 450°C and 550°C) in sequence, the ultimate strength was slightly improved for A3 by nearly 1% and nearly constant for B3 with slightly decrease by nearly 1%, however for it was decreased significantly for C3 and D3 by nearly 15% and 34% respectively, as shown in Figure 4.34 and Figure 4.35.

For the slabs with 1.25% addition of steel fiber E4, A4, B4, C4 and D4 (ambient condition, 150°C 300°C, 450°C and 550°C) in sequence, the ultimate strength was improved for B4 and C4 by (nearly 14.5% and 5%), however for A4 it was decreased by nearly 12.5%, also for D4 it was nearly constant, as shown in Figure 4.36 and Figure 4.37.

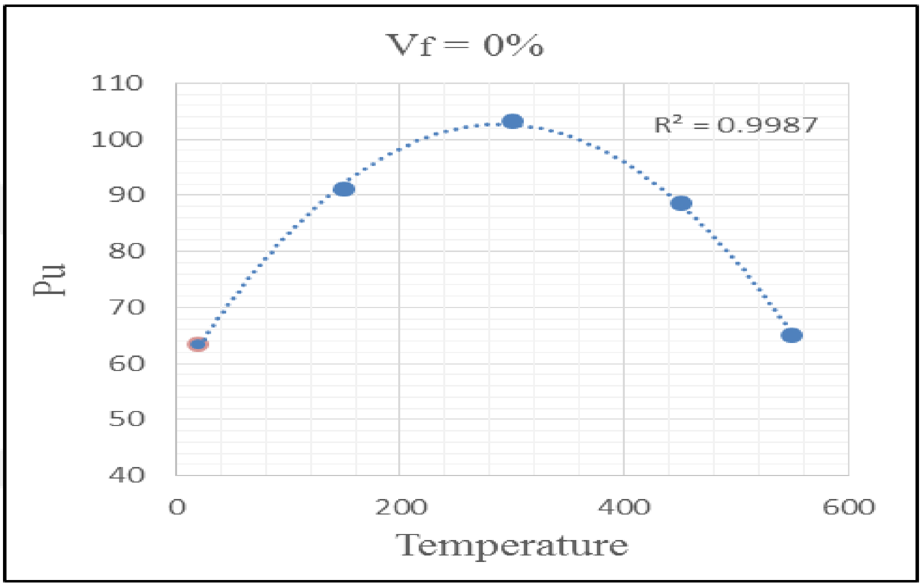

Figure 4.30 Effect of heating exposure on the ultimate slab strength for slabs E1, A1, B1, C1 and D1.

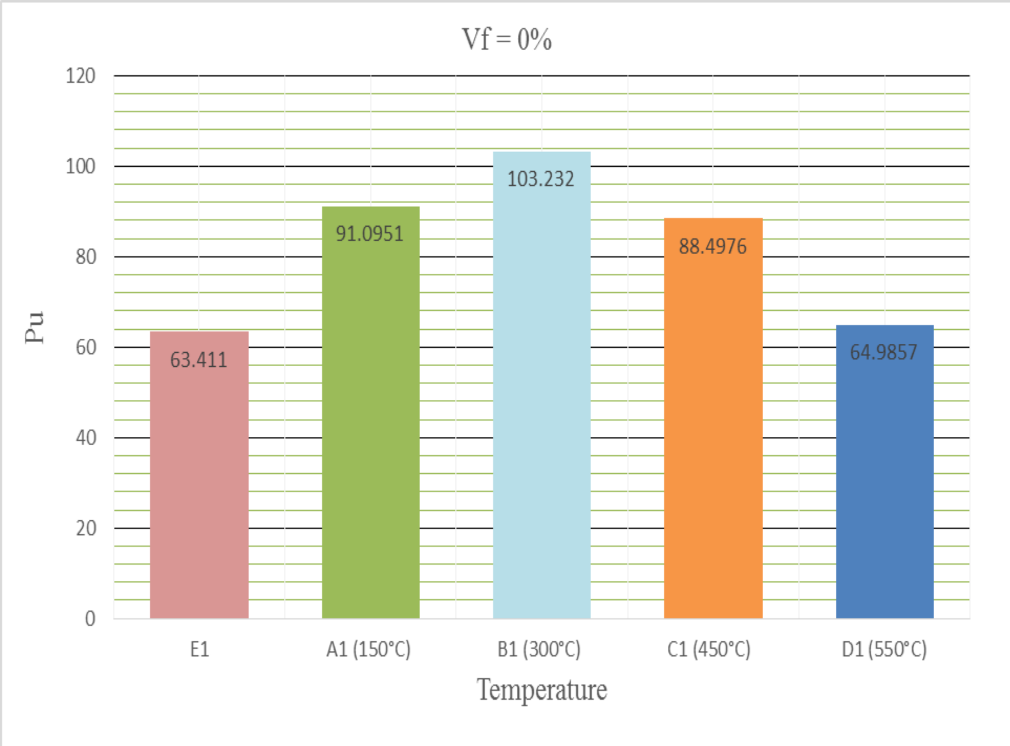

Figure 4.31 Effect of heating exposure on the ultimate slab strength for slabs E1, A1, B1, C1 and D1.

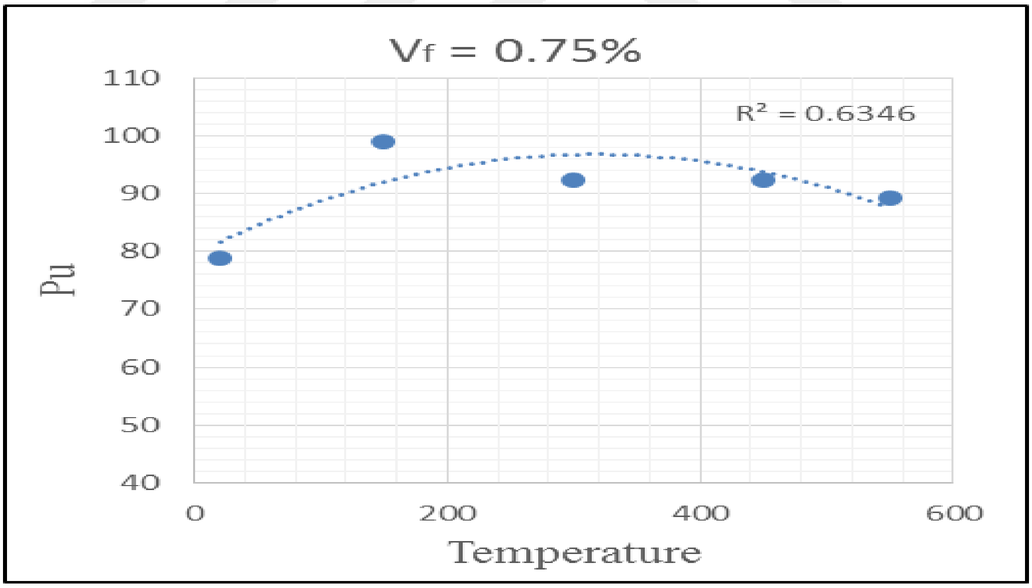

Figure 4.32 Effect of heating exposure on the ultimate slab strength for slabs E2, A2, B2, C2 and D2.

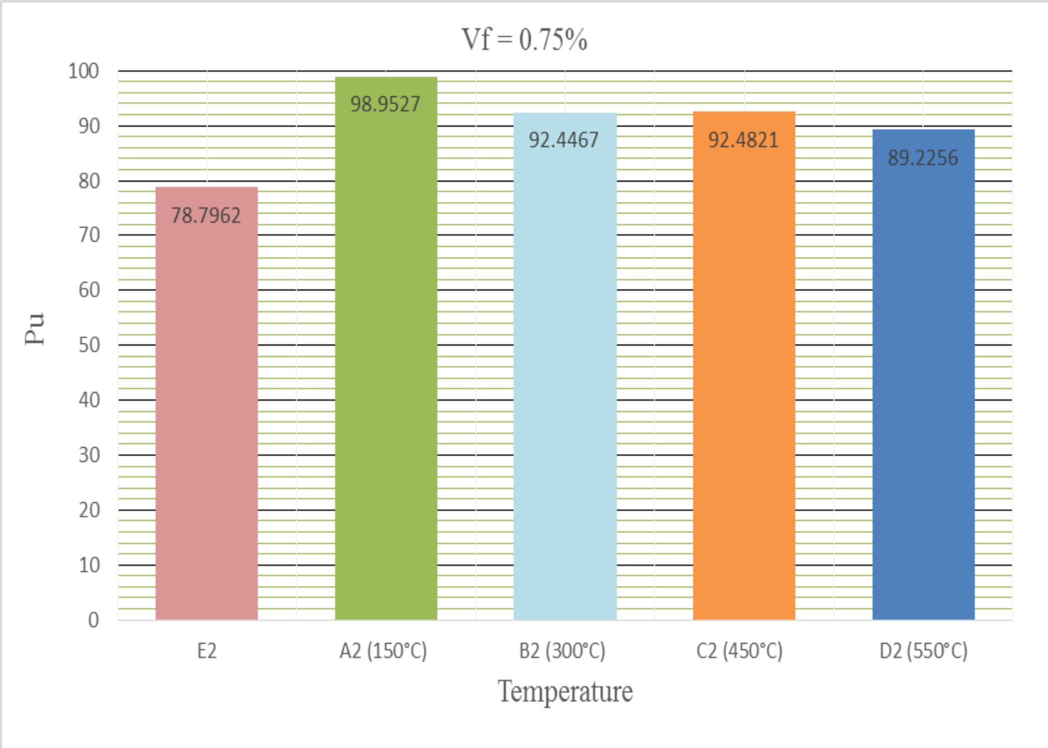

Figure 4.33 Effect of heating exposure on the ultimate slab strength for slabs E2, A2, B2, C2 and D2.

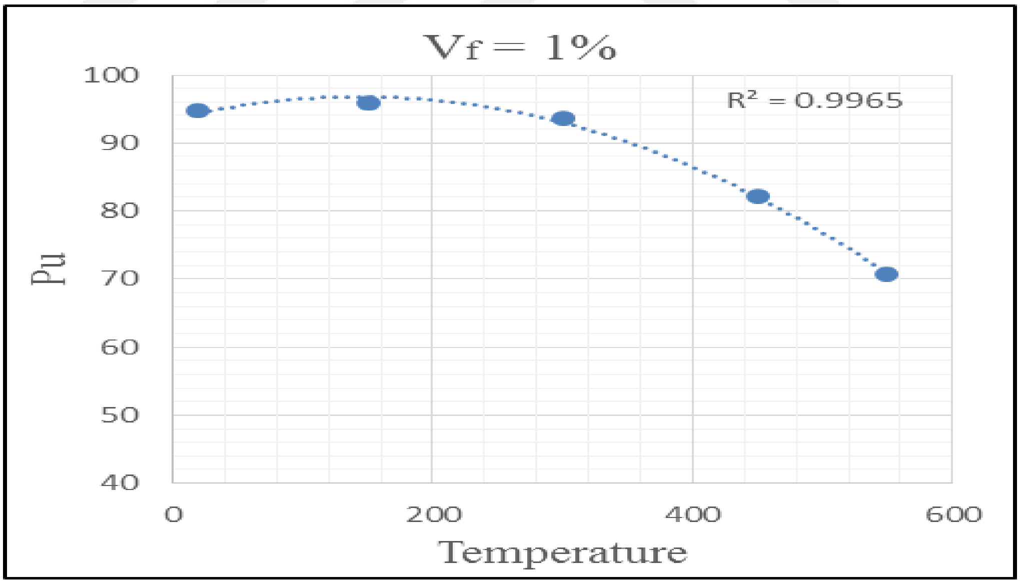

Figure 4.34 Effect of heating exposure on the ultimate slab strength for slabs E3, A3, B3, C3 and D3.

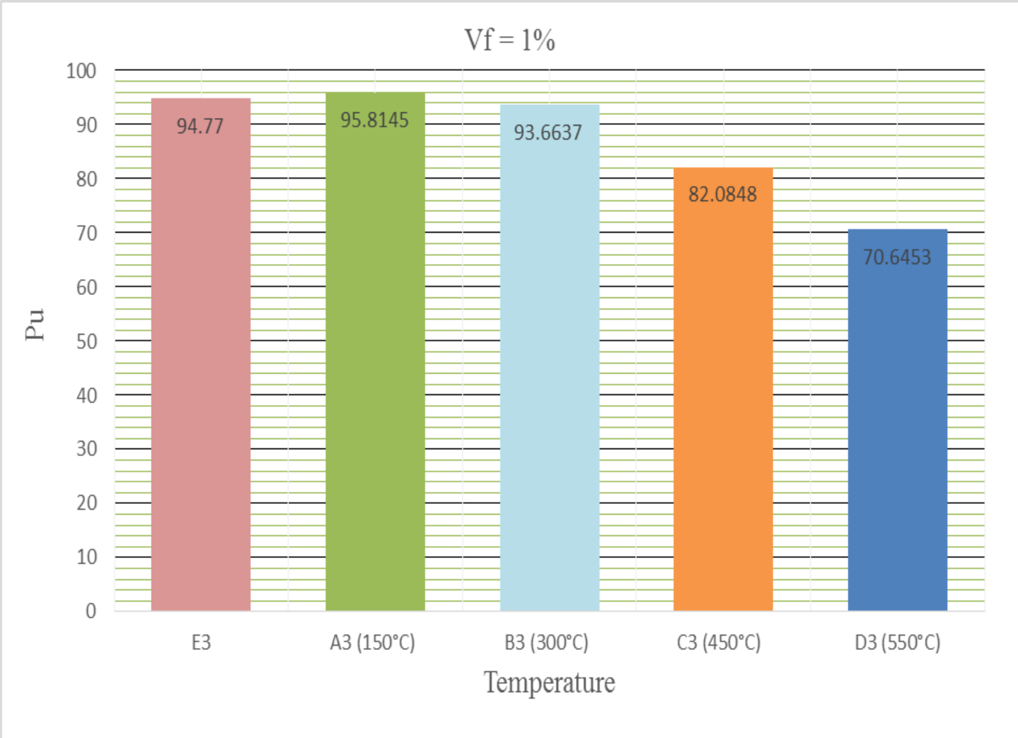

Figure 4.35 Effect of heating exposure on the ultimate slab strength for slabs E3, A3, B3, C3 and D3.

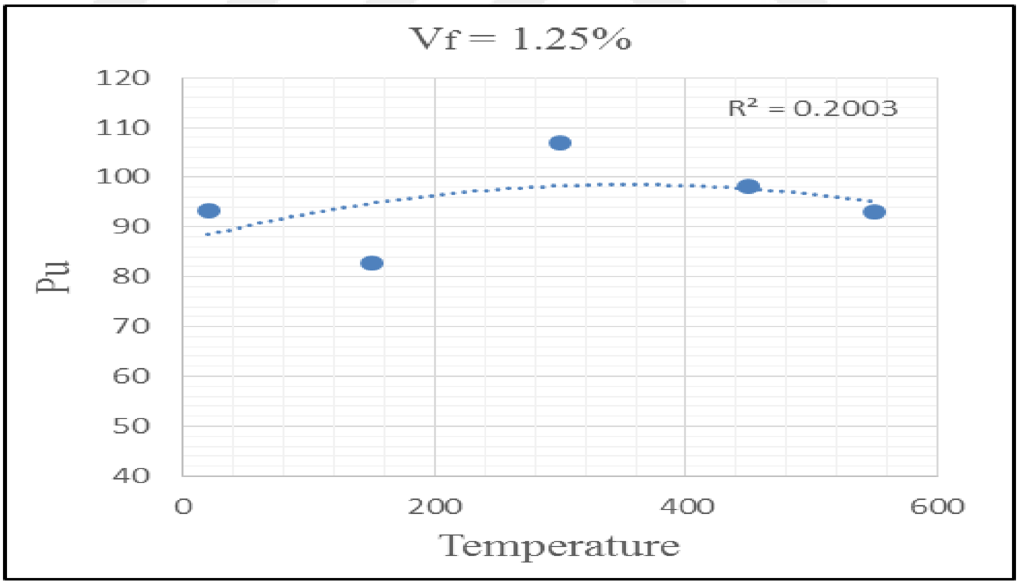

Figure 4.36 Effect of heating exposure on the ultimate slab strength for slabs E4, A4, B4, C4 and D4.

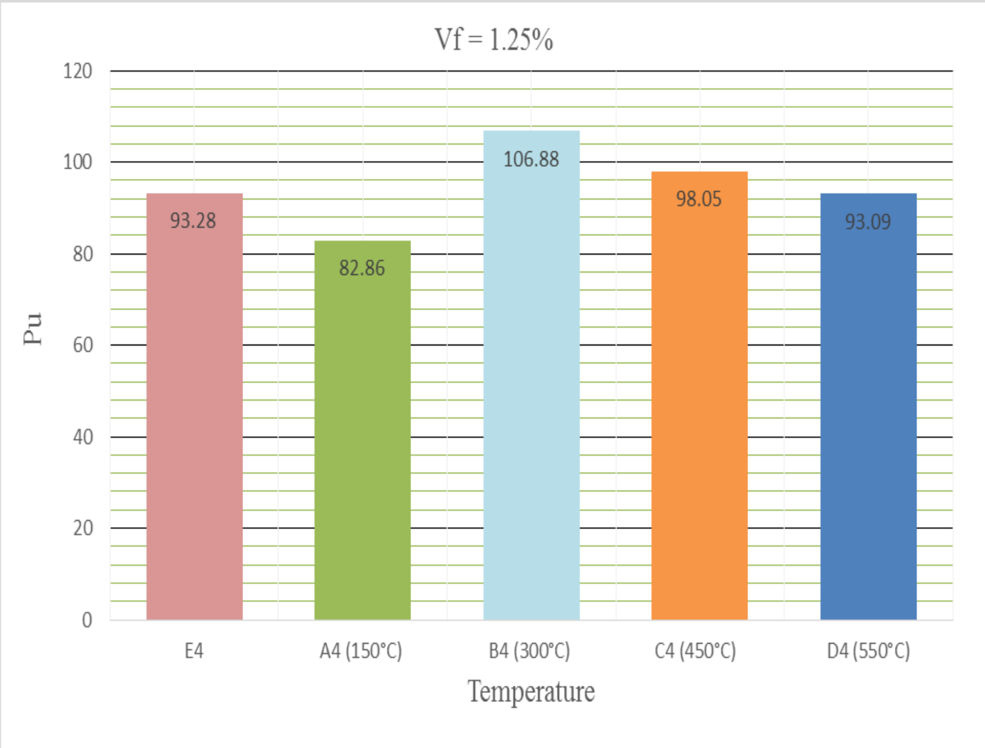

Figure 4.37 Effect of heating exposure on the ultimate slab strength for slabs E4, A4, B4, C4 and D4.

4.4.3 Effect of steel fiber percentage on slab tensile strength

The result shown in Table 4.9 clearly state that the addition of steel fiber enhanced the tensile strength, for Group E it enhanced the tensile strength for E2, E3 and E4 of specimen with 0.75%, 1%, and 1.25% by nearly (9%, 39% and 13%) respectively as shown in Figure 4.38.

For Group A it enhanced the tensile strength for A2, A3 and A4 of specimen with 0.75%, 1%, and 1.25% by nearly (50%, 40% and 30%) respectively as shown in Figure 4.39.

For Group B it enhanced the tensile strength for B2, B3 and B4 of specimen with 0.75%, 1%, and 1.25% by nearly (25%, 67% and 56%) respectively as shown in Figure 4.40.

For Group C it enhanced the tensile strength for C2, C3 and C4 of specimen with 0.75%, 1%, and 1.25% by nearly (73%, 63% and 102%) respectively as shown in Figure 4.41.

For Group D it enhanced the tensile strength for D2, D3 and D4 of specimen with 0.75%, 1%, and 1.25% by nearly (75%, 92% and 59%) respectively as shown in Figure 4.42.

Table 4.9 Experimental tensile strength result.

Spec.	Steel fiber V_f (%)	f_{ct}
E1	0	6.17
E2	0.75	6.76
E3	1	8.61
E4	1.25	7.00
A1	0	6.17
A2	0.75	9.21
A3	1	8.61
A4	1.25	7.97
B1	0	5.28
B2	0.75	6.55
B3	1	8.83
B4	1.25	8.26
C1	0	3.96
C2	0.75	6.87
C3	1	6.48
C4	1.25	8.03
D1	0	2.85
D2	0.75	5.02
D3	1	5.49
D4	1.25	4.53

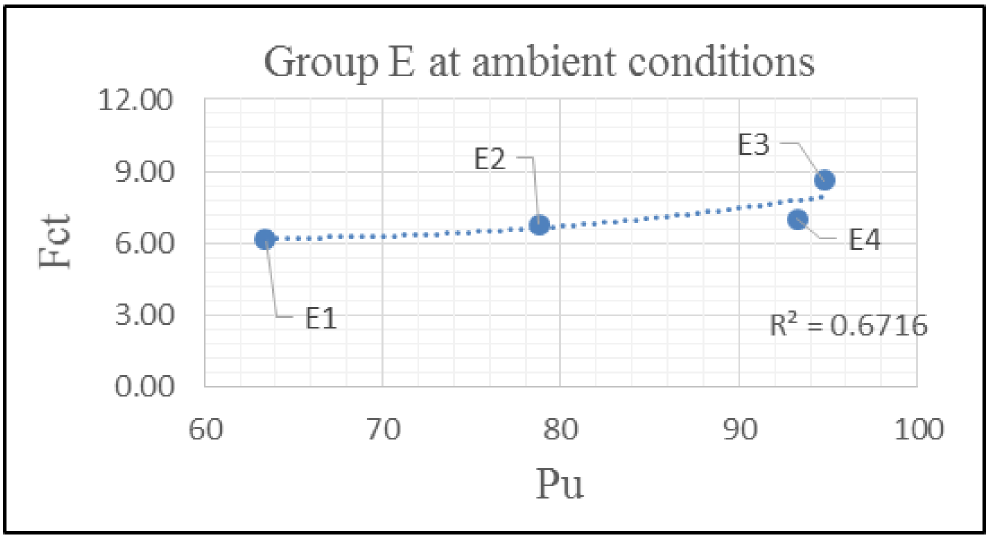

Figure 4.38 Effect of steel fiber percentages on the tensile strength for Group E.

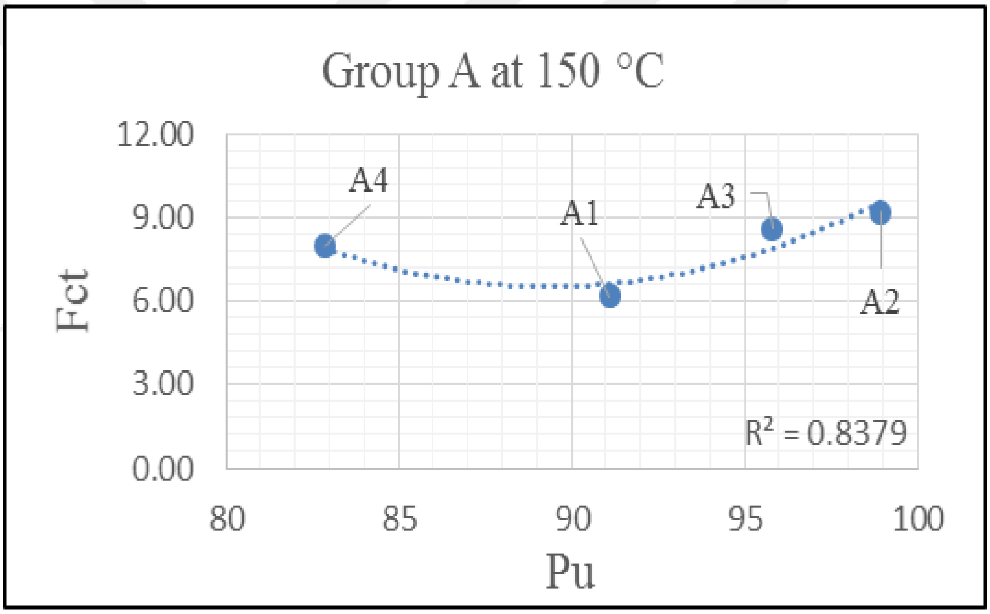

Figure 4.39 Effect of steel fiber percentages on the tensile strength for Group A.

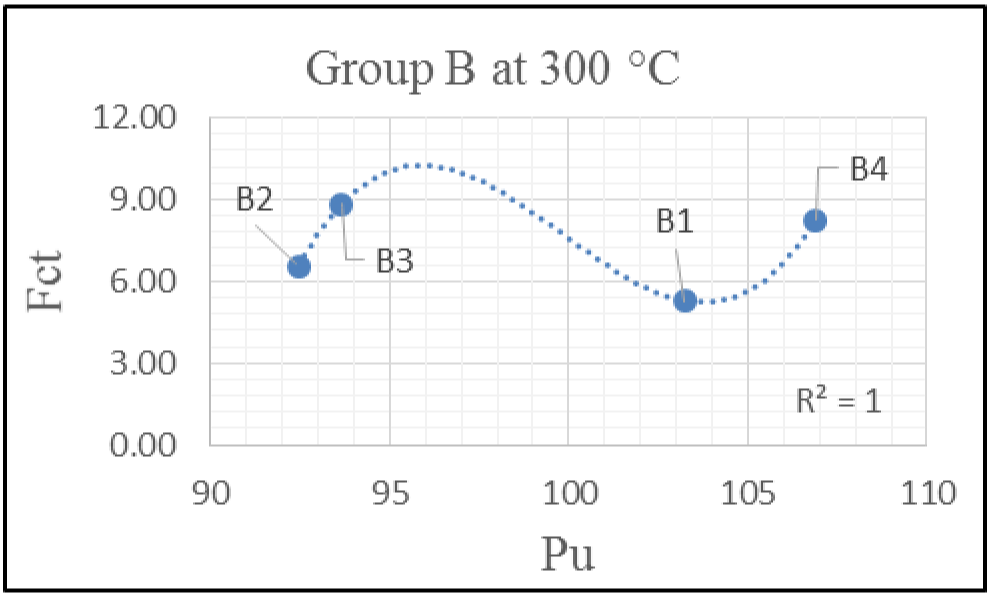

Figure 4.40 Effect of steel fiber percentages on the tensile strength for Group B.

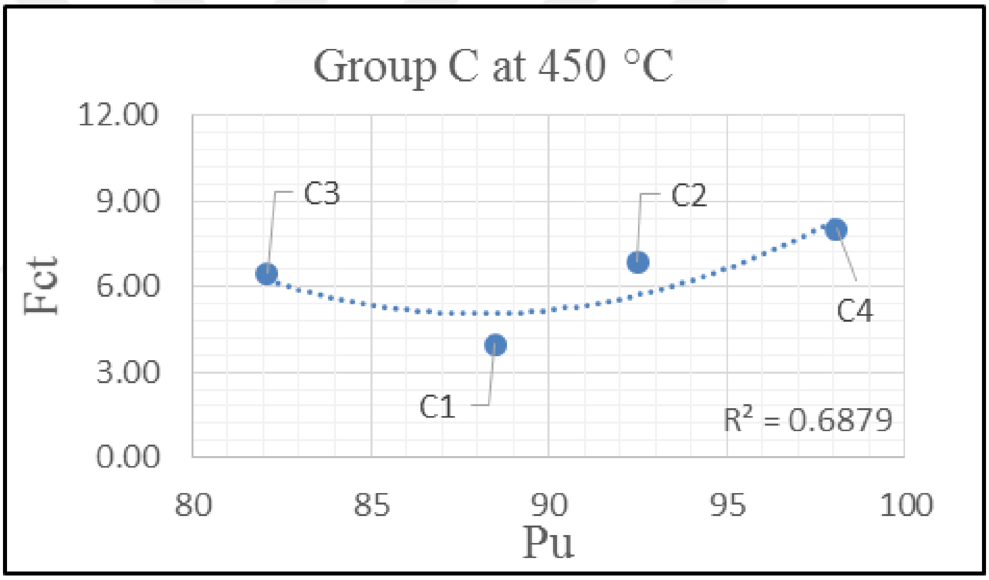

Figure 4.41 Effect of steel fiber percentages on the tensile strength for Group C.

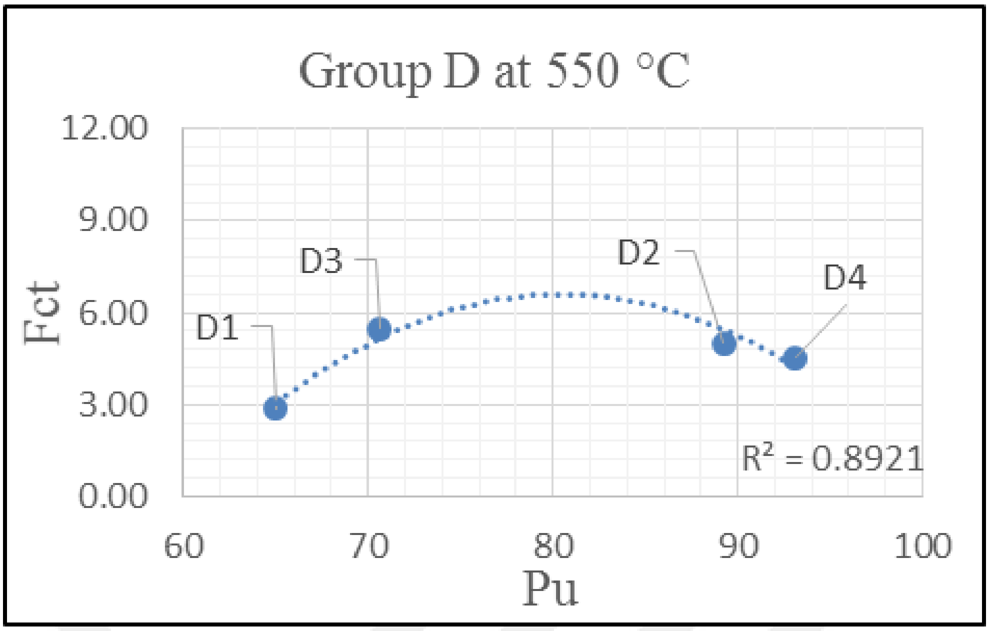

Figure 4.42 Effect of steel fiber percentages on the tensile strength for Group D.

4.4.4 Effect of heating exposure on slab tensile strength

Taking in consideration the effect of heat exposure on the tensile strength, the tensile resistance for the similar slabs consists of the same mixture in different temperatures is presented in Table 4.9.

As a comparison between the ambient condition and different temperature, for the slabs without the addition of steel fiber E1, A1, B1, C1 and D1 (ambient condition, 150°C 300°C, 450°C and 550°C) in sequence, it can be noticed that by elevating the temperature, the tensile strength was decreased for B1, C1 and D1by (nearly 16%, 55% and 116%) respectively, however for A1 remains constant as shown in Figure 4.43.

For the slabs with 0.75% addition of steel fiber E2, A2, B2, C2 and D2 (ambient condition, 150°C 300°C, 450°C and 550°C) in sequence, the tensile strength was improved for A2 and C2 by (nearly 36% and 1.5%) respectively, however the tensile strength was decreased for B2 and C2 by (nearly 3% and 35%) respectively as shown in Figure 4.44. It can be noticed in slabs with 1% addition of steel fiber E3, A3, B3, C3 and D3 (ambient condition, 150°C 300°C, 450°C and 550°C) in sequence, the tensile strength was improved for B3 by (nearly 2.5%), however it was decreased for C3 and D3 by nearly (32% and 56%) but remain constant for A3 as shown in Figure 4.45.

For the slabs with 1.25% addition of steel fiber E4, A4, B4, C4 and D4 (ambient condition, 150°C 300°C, 450°C and 550°C) in sequence, the tensile strength was improved for A4, B4 and C4 by (nearly 13%, 18% and 15%), however it was decreased for D4 by nearly 54.5% as shown in Figure 4.46.

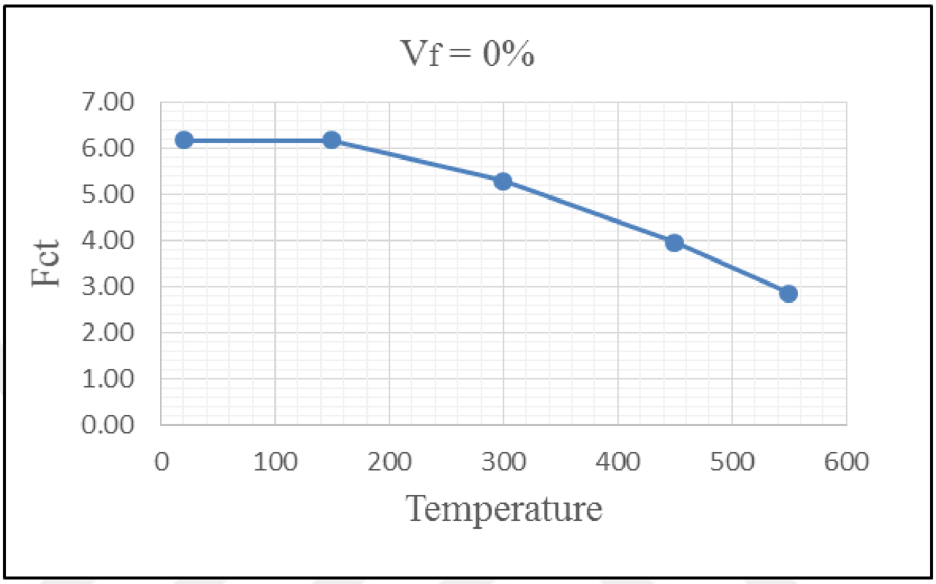

Figure 4.43 Effect of heating exposure on the tensile strength for slabs E1, A1, B1, C1 and D1.

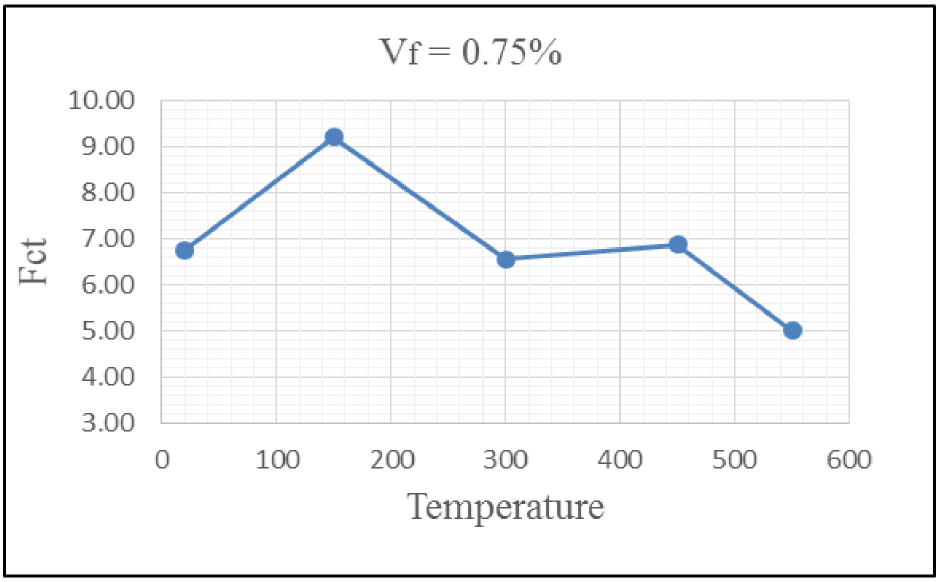

Figure 4.44 Effect of heating exposure on the tensile strength for slabs E2, A2, B2, C2 and D2.

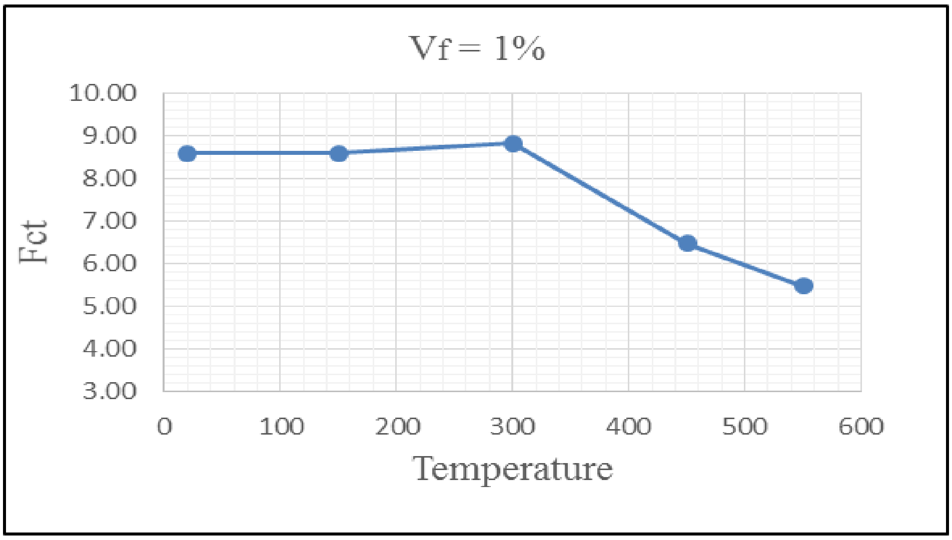

Figure 4.45 Effect of heating exposure on the tensile strength for slabs E3, A3, B3, C3 and D3.

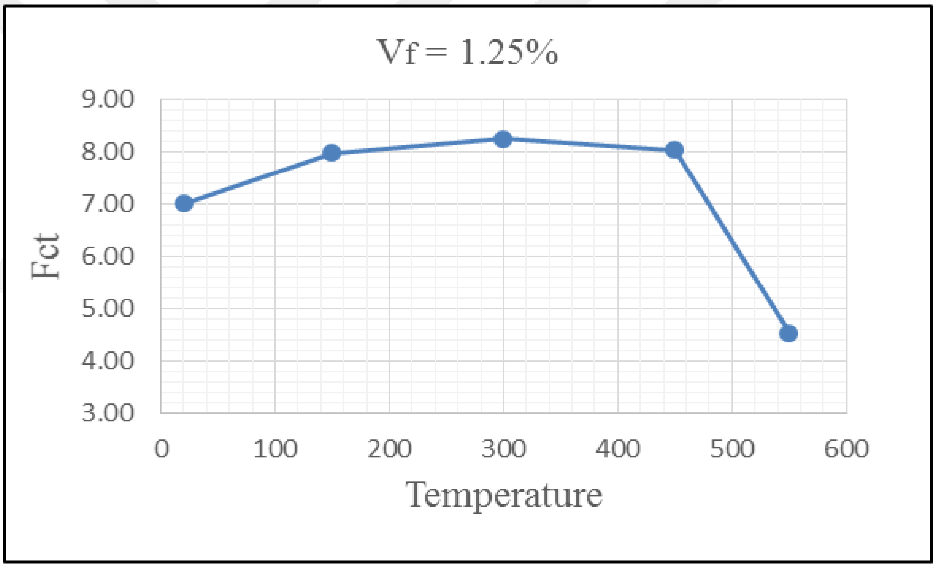

Figure 4.46 Effect of heating exposure on the tensile strength for slabs E4, A4, B4, C4 and D4.

4.5 Failure Mode

The observed details, such as the actual critical domains were measured, type of failures was categorized visually as shown in Table 4.10. For all slabs, the inclination of cracks with the horizontal axis were 17°-22°, which is agreed with (Gesund, 1994) and (Gardner, 1990). It is concluded that the inclusion of steel fiber has slightly effect on failure shape, which is agreed with the conclusion of (Gesund, 1994).

For Group E, In general, all specimens were failed because of punching shear effect with different punching shapes. The failure shape of the specimen E2 was the same as the E1 failed in punching shear with extensive spalling of tension concrete. Significantly, different behaviors were shown in E3, where the flexural horizontal cracks did not show it up, furthermore it can be noticed in specimen E4 that the steel fiber scatter the cracks which means it enhanced the ductility behavior. The diameter of main punching crack was less than the others, with hair crack located within the main cracks area. As shown in Figure 4.47.

For Group A, in general, all specimens were failed because of punching shear effect with different punching shapes, the shape of failure is changed between the slab with 0% percentage of steel fiber and the specimens that have steel fiber also the radius of failure circle is increased in slabs A2, A3 and A4 by the increase of fiber percentage 170, 180 and 195 respectively, furthermore it can be noticed that the steel fiber scatter the cracks which means it enhanced the ductility behaviour. As shown in Figure 4.48. From the visual observation of the cracks it can clearly be noticed that the flexural behavior is improved by adding and increasing the steel fiber percentage.

For Group B, all specimens exhibited a flexural failure with two specimens that exhibited both flexural and punching. In 300 °C exposure the ductility is improved and the type of failure is changed from punching to flexural. As shown in Figure 4.49.

For Group C, In general, all specimens were failed because of punching shear effect with different punching shapes, it can clearly be noticed that the flexural lines appear in all specimens, the specimen C1 without fibers failed in punching shear with extensive spalling of tension concrete, furthermore it can be noticed that the steel fiber scatter the cracks which means it enhanced the ductility behavior. As shown in Figure 4.50.

For Group D, In general, all specimens were failed because of punching shear effect with different punching shapes, the specimen D1 without fibers failed in punching shear with extensive spalling of tension concrete, furthermore it can be noticed that the steel fiber scatter the cracks which means it enhanced the ductility behaviour. As shown in Figure 4.51.

Table 4.10 Failure mode details.

Spec.	Steel fiber V_f (%)	Temperature °C	Failure[(1)] type	Punching shape	$r_{0,\ test}$[(2)] (mm)
E1	0	Room	P	circle	218
E2	0.75	Room	P	circle	188
E3	1	Room	P	square	131
E4	1.25	Room	P	circle	179
A1	0	150	P	ellipse	218
A2	0.75	150	P	circle	170
A3	1	150	P	circle	180
A4	1.25	150	P	circle	195
B1	0	300	Flex	-	-
B2	0.75	300	Flex + P	ellipse	170
B3	1	300	Flex + P	ellipse	85
B4	1.25	300	Flex	-	-
C1	0	450	P	ellipse	200
C2	0.75	450	P	circle	160
C3	1	450	P	circle	180
C4	1.25	450	P	ellipse	200
D1	0	550	P	circle	180
D2	0.75	550	P	square	180
D3	1	550	P	circle	190
D4	1.25	550	P	circle	200

(1) *P* refer to punching shear failure and, *F* refer to flexural failure.
(2) Radius of the critical punching crack taken as the longest size in ellipse and square.

E1

E2

E3

E4

Figure 4.47 Failure mode of Group E.

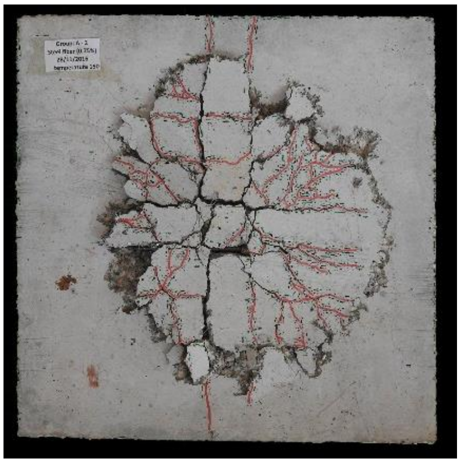

A1 A2

A3 A4

Figure 4.48 Failure mode of Group A.

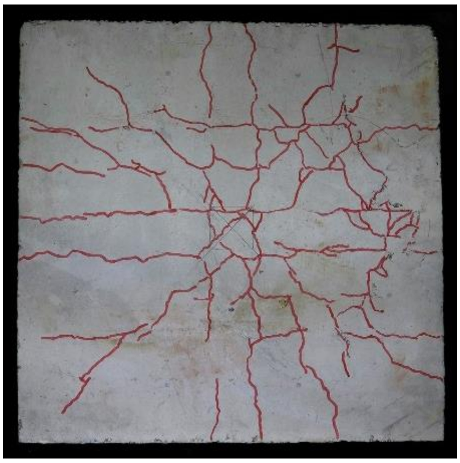

B1

B2

B3

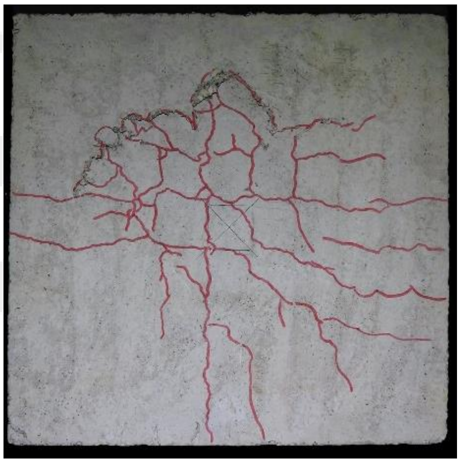

B4

Figure 4.49 Failure mode of Group B.

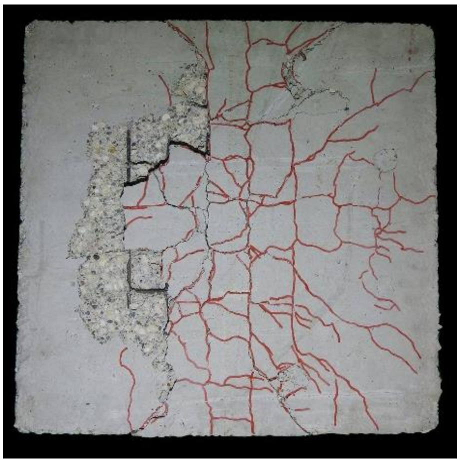

C1

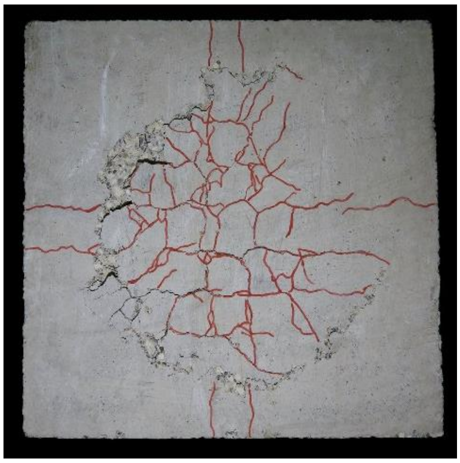

C2

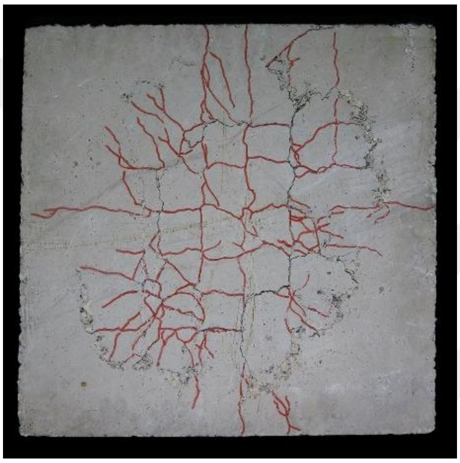

C3

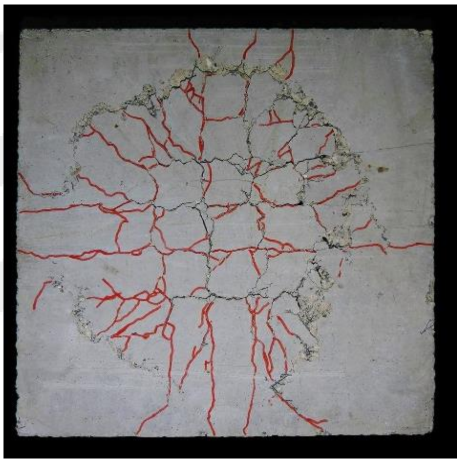

C4

Figure 4.50 Failure mode of Group C.

D1

D2

D3

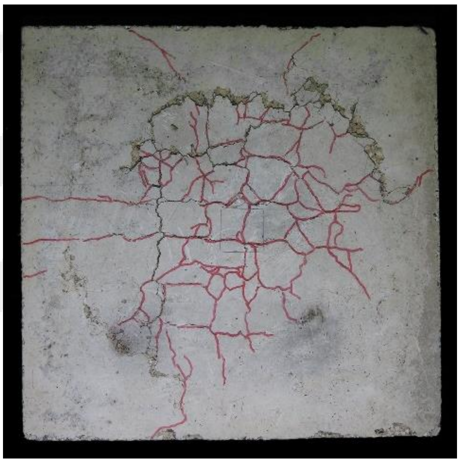

D4

Figure 4.51 Failure mode of Group D.

4.5.1 Failure mode according to Gesund

(Y. P, 1970) proposed the following equation for failure mode based on 200 tested slabs because they found out that ACI code is very conservative and under estimative of the shear.

The type of failure can be determined from the equation: $Q = \frac{\rho^2 f_y d^2}{b\mathrm{B}\sqrt{f'_c}} \times 10^4$

Where:

Q failure mode criterion parameter.

ρ reinforcement ratio.

B perimeter of the slab supported on one column

f_y yield stress of tension reinforcement.

d effective depth of the slab.

b perimeter of the column.

$\sqrt{f'_c}$ the square root of compressive strength.

If Q less than 2 then the failure is flexural.

If Q more than 2 and less than 4 then the failure is either.

If Q is more than 4 then the failure would be punching. The results are presented in Table 4.11.

Table 4.11 Failure modes.

Spec.	Steel fiber V_f (%)	Temperature °C	Q	Failure type
E1	0	Room	2.66	Either Failure
E2	0.75	Room	3.01	Either Failure
E3	1	Room	2.58	Either Failure
E4	1.25	Room	2.79	Either Failure
A1	0	150	2.70	Either Failure
A2	0.75	150	2.55	Either Failure
A3	1	150	2.55	Either Failure
A4	1.25	150	2.66	Either Failure
B1	0	300	2.99	Either Failure
B2	0.75	300	2.89	Either Failure
B3	1	300	2.67	Either Failure
B4	1.25	300	2.73	Either Failure
C1	0	450	3.66	Either Failure
C2	0.75	450	3.15	Either Failure
C3	1	450	3.13	Either Failure
C4	1.25	450	3.07	Either Failure
D1	0	550	4.39	punching
D2	0.75	550	3.43	Either Failure
D3	1	550	3.76	Either Failure
D4	1.25	550	3.93	Either Failure

4.6 ACI 318-14 Provisions

As it shown in Table 4.12, current work results exceeded the expectations by more than double the value expected in (American Concrete Institute 318-14, 2014) code.

Table 4.12 A comparison between current results and ACI.

Spec.	Steel fiber V_f (%)	V_{ACI}	Pu test (kN)	$Pu_{\ test}/V_{ACI}$
E1	0	36.49	63.41	1.73
E2	0.75	35.66	78.79	2.21
E3	1	38.93	94.77	2.43
E4	1.25	38.37	93.28	2.43
A1	0	39.74	91.09	2.29
A2	0.75	38.72	98.95	2.56
A3	1	Exceed code limitation	95.81	-
A4	1.25	40.28	82.86	2.06
B1	0	35.81	103.23	2.88
B2	0.75	37.09	92.44	2.49
B3	1	40.17	93.66	2.33
B4	1.25	39.23	106.882	2.72
C1	0	29.25	88.49	3.03
C2	0.75	34.04	92.48	2.72
C3	1	34.21	82.08	2.40
C4	1.25	34.89	98.05	2.81
D1	0	24.45	64.98	2.66
D2	0.75	31.29	89.22	2.85
D3	1	28.48	70.64	2.48
D4	1.25	27.27	93.09	3.41

Figures 4.52 to 4.56 show the values of punching shear capacity comparing with the values expected in ACI code for groups E, A, B, C and D in sequent, the long column represents the values of current work and the short column represents the values expected in ACI code.

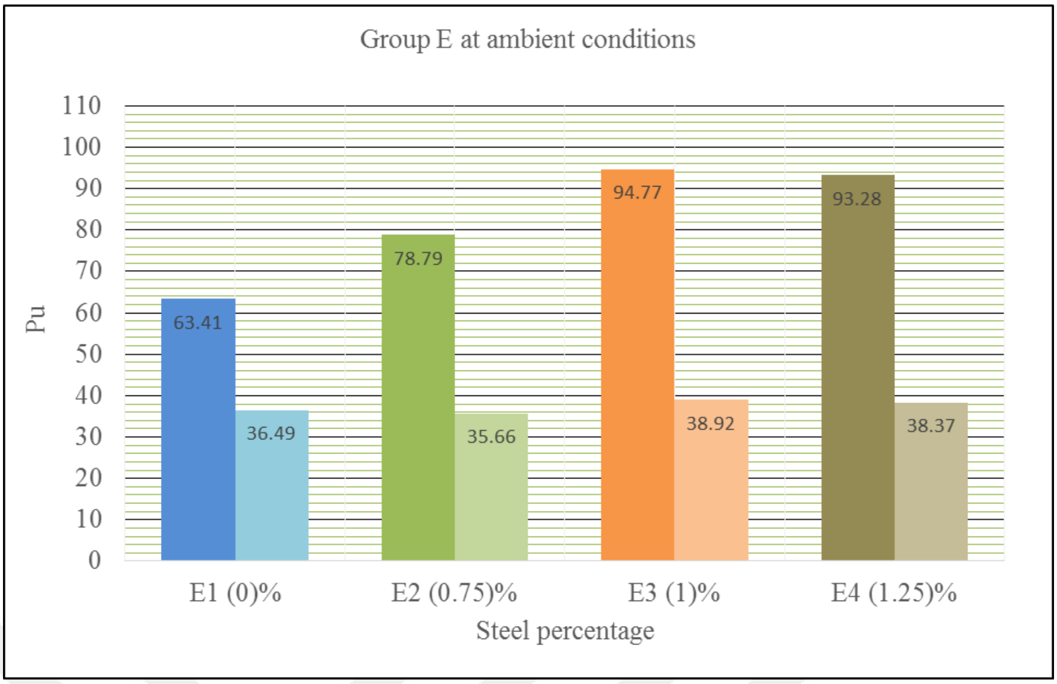

Figure 4.52 Current work results of Group E comparing with ACI expected results.

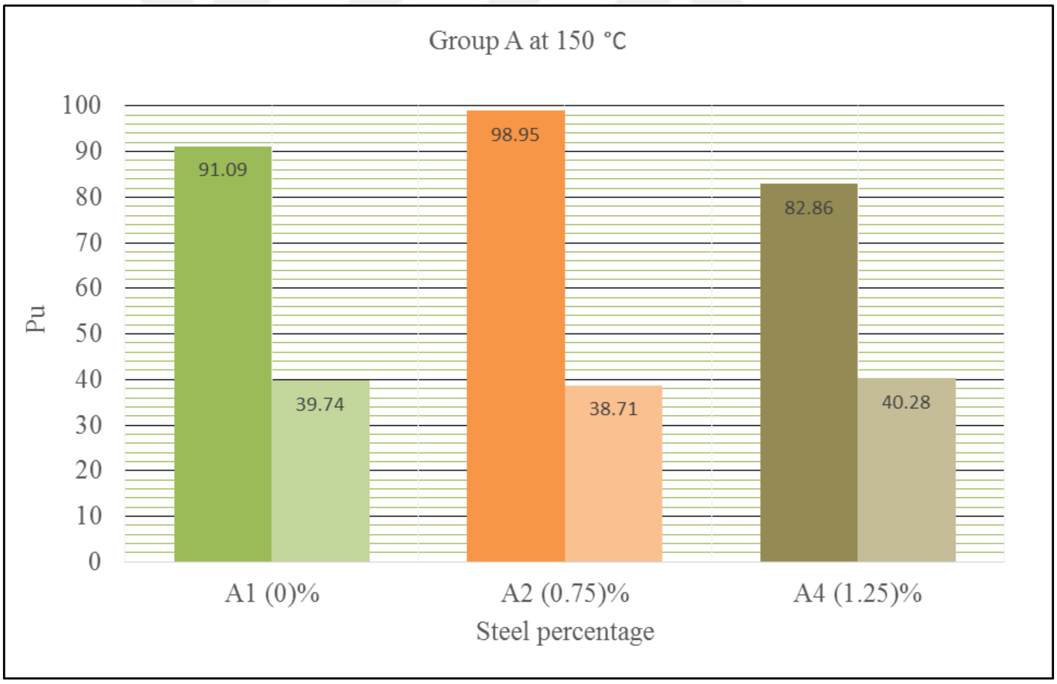

Figure 4.53 Current work results of Group A comparing with ACI expected results.

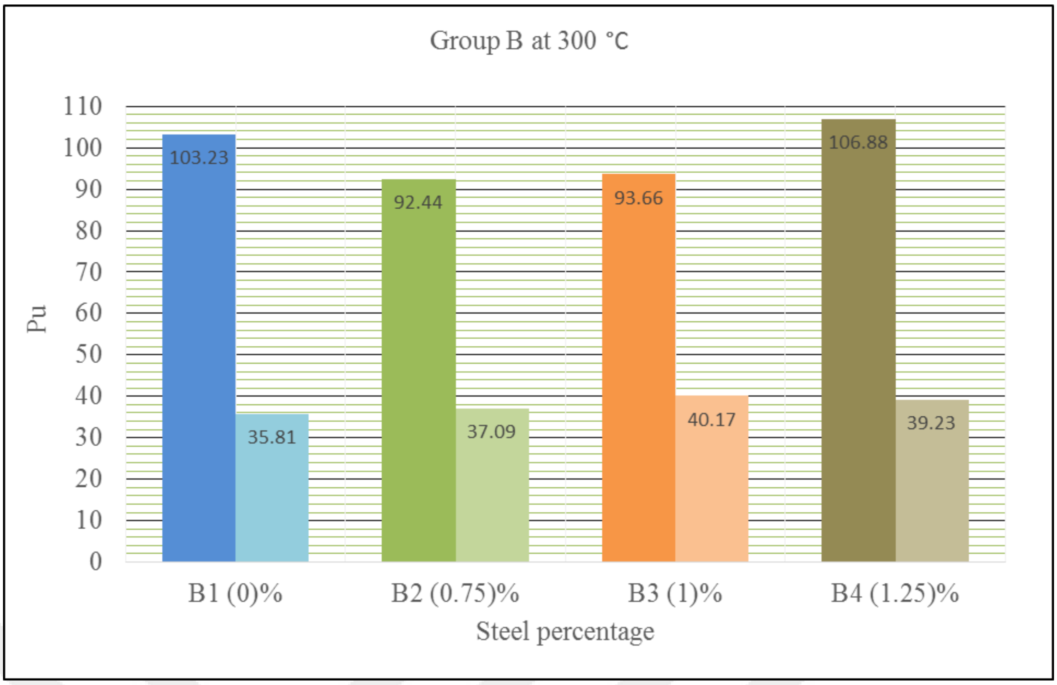

Figure 4.54 Current work results of Group B comparing with ACI expected results.

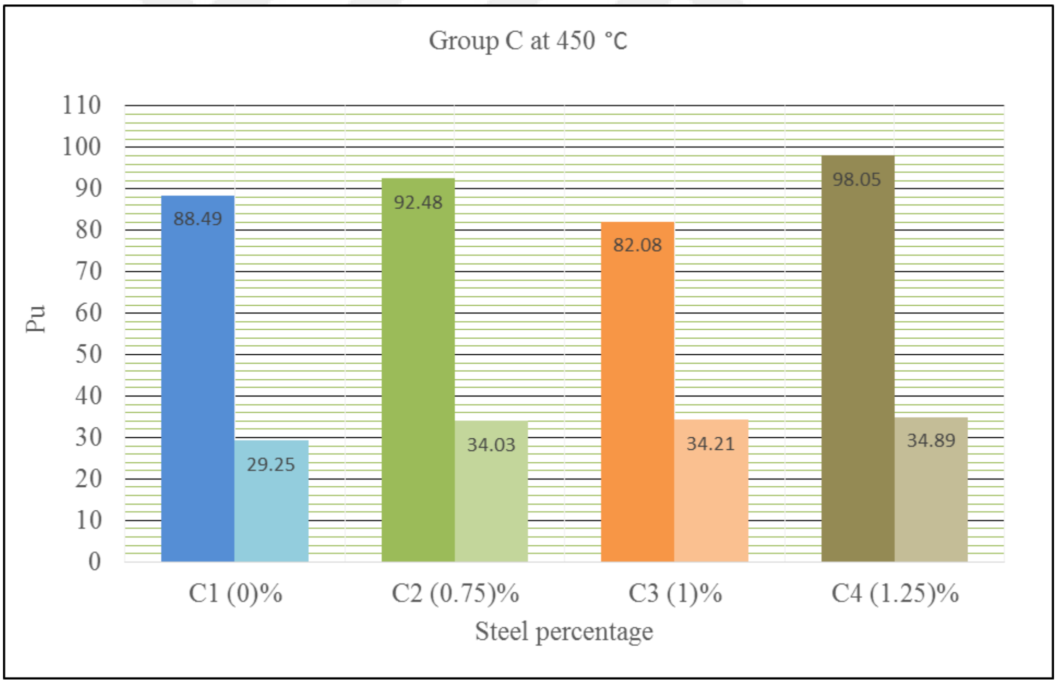

Figure 4.55 Current work results of Group C comparing with ACI expected results.

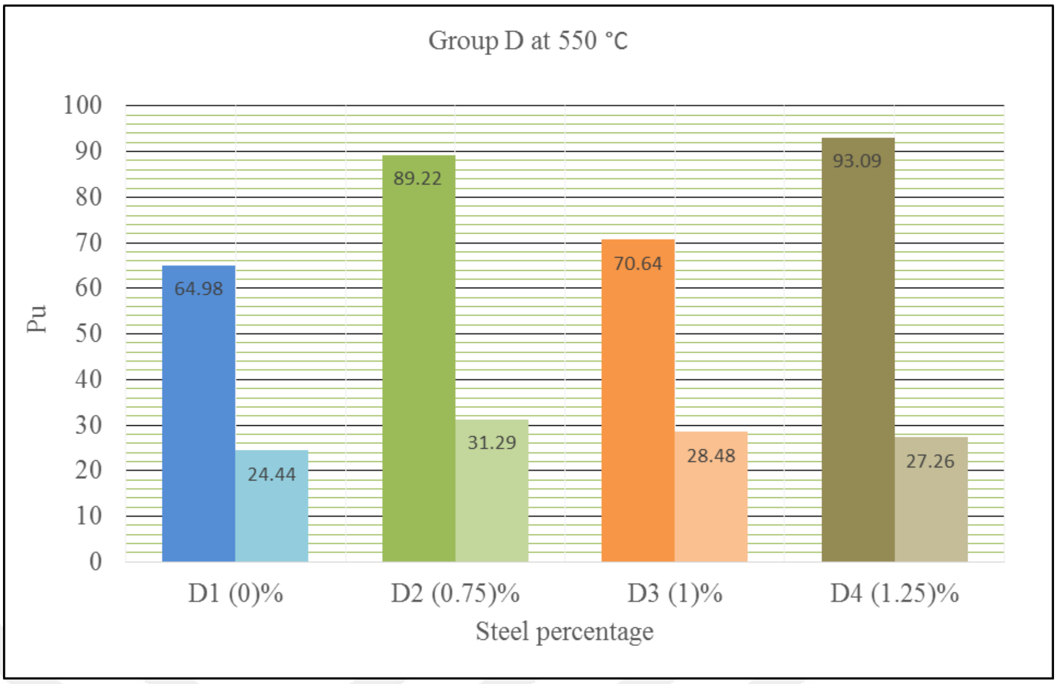

Figure 4.56 Current work results of Group D comparing with ACI expected results.

CHAPTER FIVE

CONCLUSIONS

5.1 Conclusions

The following conclusions are obtained from analyzing the results of current work:

1.Deflection values by taking in consideration the fiber percentages and the heat exposure comparing to the panels with 0% steel fiber at the same conditions:

•At ambient condition, the best deflection value is obtained from adding 0.75% of steel fiber.

- At 150 °C, in general adding fiber led to lower deflection values and the best deflection value is obtained from adding 1.25% of steel fiber.
- At 300 °C, in general adding fiber led to higher deflection values and the worst deflection value is obtained from adding 1.25% of steel fiber.
- At 450 °C, the best deflection value is obtained from adding 1% of steel fiber.
- At 550 °C, the best deflection value is obtained from adding 1% of steel fiber.

•Between the panels that consist of the same mix code in different heat exposure, for 0% of steel fiber specimen B1 at 300 °C gives the lowest deflection value, for 0.75% of steel fiber specimen E2 at ambient condition gives the lowest deflection value, for 1% of steel fiber specimen D3 at 550 °C gives the lowest deflection value, for 1.25% of steel fiber specimen A4 at 150 °C gives the lowest deflection value.

2.Exposing the panels to a high temperatures leads to increasing the mechanical properties of SFRC at 150 °C and 300 °C, in which the compressive strength are improved by almost 18% for (A1, A2 and A3) and almost 10% for A4, also it was improved by nearly 7% for (B2 and B3) and 4% for B4.

On the other hand it decreased almost 4% for B1. That improvement is less in tensile strength at the same temperatures. For heating exposure higher than 300 °C, all the mechanical properties of SFRC went down in low rate comparing with the plain concrete panels.

- Increasing the used amount of fine cementitious and aggregate materials, did not only increase the compressive and tensile strength but it also decrease the deterioration rates of concrete resistance under exposure to high temperatures. The best residual compressive and tensile strength at 550 °C were 63% and 78% respectively, compared to the associated specimens of plain concrete, this improvement has been obtained from SFRC that reinforced by low percentage of steel fibers ($V_f = 0.75$ %).

3. Most codes of practice available if not all are under estimation the punching shear capacity for concentric flat plate-column connections reinforced by steel fibers, in the present experimental work, the estimated punching strength in codes reached a maximum estimation of 41% of the obtained results in current experimental work at best case prediction.

- For Group E at ambient condition, the addition of steel fibers by percentage of 0.75, 1% and 1.25% in concrete significantly improved the ultimate slab strength for all specimens by nearly 24%, 49% and 47% respectively.

- For Group A at 150 °C, the addition of steel fibers in concrete significantly improved the ultimate slab strength of specimen with 0.75% and 1% (nearly 8% and 5%) respectively, however using 1.25 % of steel fiber, did not improve the behavior of the slab.

- For Group B at 300 °C, the addition of steel fibers in concrete significantly improved the ultimate slab strength of specimen with 1.25% (nearly 3%), on the contrary 0.75% and 1% of steel fiber, didn't improve the behavior of the slab.

- For Group C at 450 °C, using 0.75 % and 1.25% of steel fiber improved the ultimate slab strength by (nearly 4.5% and 11%) respectively, however using 1% of steel fiber, didn't improve the behavior of the slab.

- For Group D at 550 °C, the addition of steel fibers in concrete significantly improved the ultimate slab strength of specimen with 0.75%, 1% and 1.25% (nearly 37%, 8.7% and 43%) respectively.

- Between the panels that consist of the same mix code in different heat exposure, for 0% of steel fiber specimen B1 at 300 °C gives the highest punching shear strength value, for 0.75% of steel fiber specimen A2 at 150 °C gives the highest punching shear strength value, for 1% of steel fiber specimen A3 at 150 °C gives the highest punching shear strength value, for 1.25% of steel fiber specimen B4 at 300 °C gives the highest punching shear strength value.

4. There are no significant effects on failure shape due to using steel fibers, whereas the high temperature may affect.

5. In general than panels subjected to 150 °C and 300 °C heat exposure shows a significant improvement in mechanical properties and punching shear strength comparing with the panels at ambient conditions

.

REFERENCES

American Concrete Institute 318-14. (2014). *Building Code Requirements for Structural Concrete.* U.S.A.: American Concrete Institute.

Ashour, S. H. (1992). Shear behaviour of high-strength fiber reinforced concrete beams. *ACI Structural Journal. , 89*(2), 176–184.

ASTM C39. (1997). Standard test method for compressive strength of cylindrical concrete specimens. *Annual book of ASTM standards, 4*, 20-24.

ASTM C469. (2002). Standard test method for static modulus of elasticity and Poisson's ratio of concrete in compression. *Annual book of ASTM standards, 4*.

ASTM C496. (2004). Standard Test Method for Splitting Tensile Strength of Cylindrical Concrete Specimens. *ASTM International., 1*.

Banthia, N. M. (2008). Toughness Characterization of Fibre-Reinforced Concrete: Which Standard to Use? *Testing and Evaluation, 32*(2), 1-5.

Batson, G. B. (1972). Flexural fatigue strength of steel fiber reinforced concrete beams. *ACI Journal., 69*, 673–677.

Bayasi, Z. &. (2001). Steel fibres as crack arrestors in concrete. *Indian concrete journal, 75*(3), 215-222.

Bazant, Z., & Cao, Z. (1987, January-February). Size Effect in Punching Shear Failure of Slabs. *ACI Structural Journal, 84*(1), 44-53.

Chanh, N. (2005). *steel fiber reinforced concrete. Thesis. Faculty of Civil Engineering,* . Ho Chi Minh: University of Technology.

Chen YM, L. K. (1979). Numerical study on e€ffects of fiber orientation of a unidirectional elastic solid under impact. *Journal of Composite Materials* , 25.

Chen, S. (2004). Strength of steel fiber reinforced concrete ground slabs. *Structures and Buildings, 2*, 157.

CSA, A.-M. (1984). code for design of concrete structures for building. *canadian dtandard associatin, rexdale*, 281.

Gardner, N. J. (1990). Relationship of the Punching shear capacity of Reinforced Concrete Slab with Concrete Strength. *ACI Structural Journal, 87*(1), 66-71.

Gesund, A. S. (1994). Punching Shear Strength of Steel Fiber Reinforced Concrete Flat Plates. *ACI Structural Journal, 91*(3), 406-414.

Hannant, D. J. (2000). Cement-based composites. *University of Surrey-Gildford, UK.*

Hughes, B. P. (1976). Assessing the Workability of Steel Fiber Reinforced Concrete. *Magazine of Concrete Research, 28*(2), 157-161.

Johnston, C. &. (1991). Flexural fatigue performance of steel fiber reinforced concrete-influence of fiber content, aspect ratio and type. *ACI Materials Journal, 88*(4), 374–383.

Johnston, C. D. (1974). Steel fiber reinforced mortar and concrete: a review of mechanical properties. *Special Publication, 44*(1), 127-142.

Johnston, C. D. (1991). Flexural Fatigue Performance of Steel Fiber Reinforced Concrete--Influence of Fiber Content, Aspect Ratio, and Type. *Materials Journal, 88*(4), 374-383.

Katzer, J. (2006). Steel fibers and steel fiber reinforced concrete in civil engineering. *Pacific Journal of Science and Technology, 7*(1), 53-58.

Kwak, Y. E. (2002). Shear strength of steel fiber-reinforced concrete beams without stirrups. *ACI Structural Journal., 99*, S55:530-539.

Löfgren, I. (2005). *Fibre-reinforced Concrete for Industrial Construction-a fracture mechanics approach to material testing and structural analysis.* Chalmers University of Technology.

Muhammed, B. S.-N. (2012). Residual Punching Strength of NSC, HSC and LWC Panels Exposed to High Temperatures. *Journal of Engineering and Development, 16*(3), 1813-1822.

Narayanan, R., & Darwish, I.Y.S. (1987). Use of steel fibres as shear reinforcement. *ACI Structural Journal, 84*(3), 216–227.

Nataraja, M. C. (1999). Stress–strain curves for steel-fiber reinforced concrete under compression. *Cement and concrete composites, 21*(5), 383-390.

Orange, G. A. (1999). A new generation of UHP concrete: dual damage resistance and micro mechanical analysis, high performance fiber reinforced cement composites. *3rd RILEM International Conference on High Performance Fiber Reinforced Cement Composites.* Mainz, German 101–111.

part1, B. 8. (1985). Structural use of concrete part 1. *British standard institution and construction, london, 1*, 126.

Ramakrishnan, V. (1989). Flexural fatigue strength, endurance limit and impact strength of fibre reinforced refractory concrete. *International Conference on Recent Developments in Fiber Reinforced Cement and Concrete.*, (pp. 261-273).

Ramakrishnan, V. O. (1987). Flexural fatigue strength of steel fiber reinforced concrete, Fiber Reinforced Concrete – Properties and Applications. *ACI Special Publication, American Concrete Institute.*, 225–245.

Ramakrishnan, V. W. (1989). Flexural fatigue strength, endurance limit and impact strength of fiber reinforced concretes. . *Transportation Research Record.* , 1226:17–24.

Regan, p. E. (1981). *Behaviour of reinforced concrete flat slabs* . construction Inudstry Research and Information Association.

Šalna, R. &. (2007). The influence of shear span ratio on load capacity of fibre reinforced concrete elements with various steel fibre volumes. *Journal of Civil Engineering and Management, 13*(3), 209-215.

Sanyal, S. (2009). Fiber reinforced concrete: a new horizon in composite material. Business . *Canadian Chemical News.*

Shah, S. P. (march, 1981). Fiber Reinforced Concrete. *Concrete Construction, 26*(3), 261-266.

Sharma, A. K. (1986). Shear strength of steel fibres reinforced beams. *ACI Journal., 84*(4), 624–628.

Singh, S. P. (2003). Fatigue strength of steel fibre reinforced concrete in flexure. *Cement and Concrete Composite, 25*(7), 779-786.

smith, H. K. (2016). *PUNCHING SHEAR OF FLAT REINFORCED-CONCRETE SLABS UNDER FIRE CONDITIONS.* Edinburgh: Department of Civil Engineering University of Edinburgh.

Tan, K. H. (1994). Punching shear strength of steel fiber reinforced concrete slabs. *Journal of Materials in Civil Engineering, 6*(2), 240-253.

Tatro, S. (1987). Performance of steel fiber reinforced concrete using large aggregates. *Transportation Research Record.*, 1110:129–137.

Tepfers, R. (2010). Fiber-reinforced concretes with a high fiber volume fraction—a look in future. *Mechanics of Composite Materials, 46*(3), 323-330.

Y. P, K. a. (1970). Analysis of Punching Shear Fail-ures in Slabs. *International Association for Bridge and Structural Engineering, 30*(1), 41-60.

Yazıcı, Ş. İ. (2007). Effect of aspect ratio and volume fraction of steel fiber on the mechanical properties of SFRC. *Construction and Building Materials, 21*(6), 1250-1253.

Žiogas, V. &. (2005). Design and installation peculiarities of monolithic concrete floor. *Journal of Civil Engineering and Management, 11*(2), 153-162.